universität wien

MASTERARBEIT / MASTER'S THESIS

Titel der Masterarbeit / Title of the Master's Thesis

„Response of an Interferometer Mounted on an Elastic Quadratic Plate to Gravitational Waves“

verfasst von / submitted by

Thomas Spanner, BSc

angestrebter akademischer Grad / in partial fulfilment of the requirements for the degree of

Master of Science (MSc)

Wien, 2022 / Vienna, 2022

Studienkennzahl lt. Studienblatt / degree programme code as it appears on the student record sheet:	UA 066 876
Studienrichtung lt. Studienblatt / degree programme as it appears on the student record sheet:	Masterstudium Physik
Betreut von / Supervisor:	Univ.-Prof. Piotr T. Chrusciel, MSc PhD
Mitbetreut von / Co-Supervisor:	Dr. Stefan Palenta, B.Sc. M.Sc.

Abstract

LIGO uses kilometre long tunnels and freely suspended mirrors as a laser interferometer to detect gravitational waves. This thesis discusses the consequences of placing the interferometer on an elastic plate in a laboratory instead. The behaviour of the plate under the influence of a gravitational wave is described by the relativistic theory of elasticity as formulated by Beig and Schmidt [1]. For the limit of low gravitational wave frequencies a polynomial solution can be found. To solve the equations of motion for the deformation in general, a new spectral approach is developed. This considers the discontinuities at the boundaries, which appear when using a Fourier series to express non-periodic functions and taking their derivatives. The resulting series are approximated as finite sums and the resulting linear system of equation is solved numerically on a computer. Then the signal such an interferometer would measure is discussed and compared to the case of and interferometer with free mirrors. There are resonance-frequencies, corresponding to eigenmodes of the plate, for which the signal becomes very large.

Kurzfassung

LIGO nutzt kilometerlange Tunnel und frei aufgehängte Spiegel als Teil eines Interferometers um Gravitationswellen zu messen. Diese Masterarbeit untersucht, was passieren würde wenn das Laserinterferometer stattdessen auf einer elastischen Platte in einem Labor platziert wird. Das Verhalten der Platte unter dem Einfluss einer Gravitationswelle wird durch die relativistische Elastizitätstheorie beschrieben. Die hier verwendete Formulierung stammt von Beig und Schmidt [1]. Für den Grenzwert niedriger Gravitationswellenfrequenzen, kann eine Polynomiallösung gefunden werden. Um die Gleichungen für die Deformation im Allgemeinen zu lösen, wird ein neuer Fourier-Ansatz entwickelt. Dieser berücksichtigt die Unstetigkeiten an den Rändern, die auftreten, wenn eine Fourier-Reihe verwendet wird, um nichtperiodische Funktionen zu beschreiben und ihre Ableitungen zu bilden. Die auftretenden Reihen werden als endliche Summen genähert und das dabei entstehendne linearen Gleichungssystem wird numerisch am Computer gelöst. Dann wird das Signal, das ein solches Interferometer messen würde, berechnet und mit dem Interferometer mit freien Spiegeln verglichen. Es treten Resonanzen auf, bei denen das Signal sehr groß wird. Diese stimmen mit Eigenschwingungen der Platte überein.

Contents

Chapter 1

Introduction

This work builds upon the bachelor's thesis by Mario Hudelist [7]. Therein the equations of motion, describing an elastic body under the influence of gravitational waves (GWs), were derived by using a concrete matter model in the theory of relativistic elasticity. These were then used to solve the simple one-dimensional problem of a stick in a GW-background. This thesis aims to generalize this to a two-dimensional thin plate and then goes on to calculate the signal, an Michelson-Interferometer placed on the plate, would measure. The model considered here does not include any damping behaviour and we only search for the steady-state solution, when a continuous GW hits the plate.

In a first attempt to solve the problem, we discovered a set of eigenmodes, i.e. solutions for the in-plane vibrations of the plate without a gravitational wave. The next idea was to express the solution as a Fourier series, plug it into the equations, and solve for the Fourier coefficients. But for non-periodic functions, taking the derivative of the Fourier series doesn't result in the Fourier series of the derivative. To fix this, we go on to develop a modified spectral approach which is then used to find a solution. The resulting series are truncated, and the linear system of equations is then solved on the computer.

A brief outline of the structure is as follows: Chapter 2 briefly summarizes the theory of relativistic elasticity. Chapter 3 starts by summarizing the description of gravitational waves in TT-coordinates. Then it goes on to apply the formalism of relativistic elasticity to the 2D plate to formulate a boundary value problem(BVP) and presents a symmetry and polynomial solution for two special cases. In chapter 4 a set of solutions to the problem without GWs is found. Chapter 5 develops a spectral approach to deal with derivatives of Fourier Series of non-periodic functions. Then chapter 6 discusses solutions to the BVP and how to convert them to physical displacement fields. And finally, in chapter 7, the signal an interferometer mounted on the plate would measure is calculated.

1.1 Conventions

In this work the spacetime metric has signature (-,+,+,+). Uppercase latin indices belong to the body manifold and take values $A, B, ... = 1, 2, 3$. Greek indices belong to the spacetime and run from 0 to 3: $\mu, \nu, ... = 0, 1, 2, 3$. Lower case latin indices denote the spatial part of spacetime indices and run run from 1 to 3: $i, j, ... = 1, 2, 3$. The Einstein sum convention is used, i.e. repeated indices are summed over. Units are chosen in such a way that $c = 1$.

Chapter 2

Relativistic Elasticity

The Theory of Relativistic Elasticity as it is used in this work is due to Beig and Schmidt [1]. The developement of the theory in this chapter follows closely along the lines of [2] and [7]. For the historic development of the theory see [2], [13] or [1] and references therein.

First the general setup is explained: The configuration describes how a body lies in spacetime. Then a description of the particle number density follows. This is then used in a Lagrangian formalism from which the equations of motion can be obtained. Next, those are shown to be equivalent to the vanishing of the divergence of the energy-momentum tensor. Subsequently a connection to classical elasticity theory is built by introducing the Cauchy-stress(CS) tensor. Finally it is shown, that in the limit of small displacements and flat spacetime the equations of motion are equivalent to the classical wave equation for elastic waves in media.

2.1 Configuration

The Theory of Relativistic Elasticity describes the behaviour of elastic bodies in curved spacetime. For this two manifolds are used: The 4-dimensional orientable spacetime through which the body moves equipped with a metric (M, g) and coordinates x^μ and the 3-dimensional body manifold $\mathcal{B}$ with coordinates denoted by X^A, which can be thought of as representing the body at rest. The central object is the configuration

$$f^A : M' \to \mathcal{B} \tag{2.1}$$

which is a set of three smooth functions which assign to each point of spacetime the point ("particle") of the body it contains. The domain is restricted to $M' \subseteq M$, the part of spacetime through which the body moves. Writing the dependence on the spacetime coordinates in the following way $f^A(t, x^i)$ and keeping t constant, the f^A become smooth and invertible functions from the $t = const$ hypersurface in M' to $\mathcal{B}$. This, of course depends on the chosen coordinate system for M. Looking at a point X^A of the body and taking the inverse for all t, one finds the worldline of the particle residing at X^A. Since the f^A are scalar functions, the Lie derivative along any vector field ξ^μ, as well as the covariant derivative are just the partial derivative:

$$\mathcal{L}_\xi f^A = \xi^\mu \partial_\mu f^A, \qquad \nabla_\mu f^A = \partial_\mu f^A \tag{2.2}$$

This leads to the definition of the configuration gradient (also called deformation gradient)

$$\partial_\mu f^A = f^A{}_{,\mu} : T_pM \to T_{f^A(p)}\mathcal{B} \tag{2.3}$$

which maps vectors on M to vectors on $\mathcal{B}$ (or more precisely their corresponding tangent spaces). It locally describes the deformation of the body, i.e. how a vector connecting two nearby points of the body, is stretched or rotated. By the assumption that f^A is invertible on a suitable spatial hypersurface it follows that $\partial_\mu f^A$ has rank 3. Therefore, as it is a map from a 4D space to a 3D space, it has a null space of dimension 1. The element v^μ of this nullspace which satisfies

$$\partial_\mu f^A \; v^\mu = 0, \;\; v^\mu v_\mu = -1, \;\; v^\mu \text{ future-pointing} \tag{2.4}$$

is called the 4-velocity of a particle of the body. The motivation for the name comes from the interpretation of $v^\mu \partial_\mu f^A = 0$ as the directional derivative of f^A along the curve to which v^μ is the tangent vector. Since this directional derivative vanishes f^A is constant along that curve, or in other words, this curve is the worldline of the particle located at $X^A = f^A$. Next, one can define the strain(deformation)

$$B^{AB} := f^A{}_{,\mu} \; f^B{}_{,\nu} \; g^{\mu\nu}. \tag{2.5}$$

This is a symmetric matrix, but not a tensor on $\mathcal{B}$ because it depends on the spacetime coordinates. For a chosen coordinate system (t, x^i) it can be thought of as a one parameter family of tensors with parameter t. B^{AB} is also positive definite, i.e. $B^{AB}a_A a_B > 0$ for any (co)vector a_A on $\mathcal{B}$. To see this, the expression can be written as

$$B^{AB}a_A a_B = f^A{}_{,\mu} \; f^B{}_{,\nu} \; g^{\mu\nu} a_A a_B = (f^A{}_{,\mu} a_A)(f^B{}_{,\nu} a_B) \; g^{\mu\nu}. \tag{2.6}$$

$f^A{}_{,\mu} a_A$ are spacelike since they are orthogonal to the timelike vector v^μ:

$$v^\mu f^A{}_{,\mu} a_A = 0 \tag{2.7}$$

and therefore the expression (2.6) is positive. B^{AB} measures distances between points of the body as it currently lies in spacetime and hence it can be thought of as a metric on the body. Since $f^A{}_{,\mu}$ has rank 3 and $g_{\mu\nu}$ has a non-vanishing determinant, it follows that B^{AB} (as a product of matrices) has full rank and is therefore invertible. The inverse is called the Cauchy-Green deformation tensor C_{AB}. Since this is the inverse of a symmetric, positive definite matrix it is also symmetric and positive definite. One can define the corresponding spacetime tensor in two equivalent ways:

$$l_{\mu\nu} := g_{\mu\nu} + v_\mu v_\nu \equiv f^A{}_\mu f^B{}_\nu C_{AB}. \tag{2.8}$$

Proof. To check that both expressions are equivalent we show that their action on a complete set of basis vectors $\{v^\mu, f^{A\mu} = g^{\mu\nu} f^A{}_\nu\}$ of TM gives the same result. This can

be shown using the relations (2.4) defining v^μ:

$$\begin{aligned} v^\mu:\ (g_{\mu\nu}+v_\mu v_\nu)v^\mu &= v_\nu + (v^\mu v_\mu)v_\nu = v_\nu - v_\nu = 0 \\ f^A{}_\mu f^B{}_\nu C_{AB} v^\mu &= (f^A{}_\mu v^\mu) f^B{}_\nu C_{AB} = 0 \end{aligned}$$

$$\begin{aligned} f^{C\mu}:\ (g_{\mu\nu}+v_\mu v_\nu)f^{C\mu} &= (g_{\mu\nu}+v_\mu v_\nu)g^{\mu\alpha} f^C{}_\alpha = \delta^\alpha_\nu f^C{}_\alpha + v_\nu v^\alpha f^C{}_\alpha = f^C{}_\nu + 0 = f^C{}_\nu \\ f^A{}_\mu f^B{}_\nu C_{AB} f^{C\mu} &= f^A{}_\mu f^B{}_\nu C_{AB} g^{\mu\alpha} f^C{}_\alpha = (f^A{}_\mu f^C{}_\alpha g^{\mu\alpha}) f^B{}_\nu C_{AB} \\ &= B^{AC} C_{AB} f^B{}_\nu = \delta^C_B f^B{}_\nu = f^C{}_\nu \end{aligned}$$

In the last expression the definition of B^{AB}, as well as the fact that C_{AB} is its inverse, is used. Since the action on all basis vectors is the same it follows, that the two definitions are indeed equivalent. □

The tensor $l_{\mu\nu}$ acts on vectors orthogonal to v^μ (elements of the orthogonal complement $[v]^\perp$) as the metric. For such vectors it is equivalent to C_{AB} and hence a positive definite metric. Raising one index with the spacetime metric leads to a projection operator onto $[v]^\perp$

$$l^\mu{}_\nu = g^{\mu\lambda} l_{\lambda\nu} = \delta^\mu_\nu + v^\mu\ v_\nu \tag{2.9}$$

which annihilates v^μ

$$l^\mu{}_\nu v^\nu = \delta^\mu_\nu v^\nu + v^\mu\ v_\nu v^\nu = v^\mu - v^\mu = 0. \tag{2.10}$$

It can be easily checked, that $l^\mu{}_\nu$ is indeed a projection

$$l^\mu{}_\lambda l^\lambda{}_\nu = l^\mu{}_\lambda(\delta^\lambda_\nu + v^\lambda\ v_\nu) = l^\mu{}_\nu + 0 = l^\mu{}_\nu. \tag{2.11}$$

One can also find the inverse of $l_{\mu\nu}$ on $[v^\mu]^\perp$ by raising both indices with the spacetime metric:

$$l^{\mu\nu} = g^{\mu\alpha} g^{\nu\beta} l_{\alpha\beta}. \tag{2.12}$$

It's straightforward to check that this indeed is the inverse on $[v^\mu]^\perp$ i.e. $l^{\mu\nu} l_{\nu\alpha} = l^\mu_\alpha$ which is the identity on $[v^\mu]^\perp$. Now, B^{AB} can also be rewritten as

$$B^{AB} = f^A{}_{,\mu}\ f^B{}_{,\nu}\ l^{\mu\nu}, \tag{2.13}$$

which means, that $f^A{}_\mu$ is a one-to-one mapping between B^{AB} on $\mathcal{B}$ and $l^{\mu\nu}$ on $[v^\mu]^\perp$. Therefore $l^{\mu\nu}$ can be interpreted as the spacetime version of the deformation tensor. It is useful to calculate two derivatives here, which will be needed later:

$$\frac{\partial B^{AB}}{\partial g^{\mu\nu}} = \frac{\partial B^{AB}}{\partial l^{\mu\nu}} = f^A{}_\mu f^B{}_\nu \tag{2.14}$$

$$\begin{aligned} \frac{\partial B^{AB}}{\partial f^C{}_\lambda} &= \delta^A_C \delta^\lambda_\mu\ f^B{}_{,\nu}\ g^{\mu\nu} + f^A{}_{,\mu}\ \delta^B_C \delta^\lambda_\nu\ g^{\mu\nu} \\ &= \delta^A_C\ f^B{}_{,\nu}\ g^{\lambda\nu} + f^A{}_{,\mu}\ \delta^B_C\ g^{\mu\lambda} \\ &= 2\delta^{(A}_C f^{B)\lambda} \end{aligned} \tag{2.15}$$

2.2 Particle Number Density and Matter Flow

In this section we want to develop an expression for a vector J^μ describing the matter flow, and a scalar n describing the particle number density. We start with the assumption that there exists a volume form Ω_{ABC} on $\mathcal{B}$. As seen above, $f^A{}_\mu$ is an isomorphism between $[v^\mu]^\perp$ and $\mathcal{B}$, so we can use it to pull-back the volume form Ω from $\mathcal{B}$ to M via $N = f^*\Omega$:

$$N_{\mu\nu\rho} = f^A{}_\mu f^B{}_\nu f^C{}_\rho \Omega_{ABC}. \tag{2.16}$$

The Hodge operator $\star$ translates k-forms to (n-k) forms. So we can use it to define a vector J^μ (after raising the index) from the 3-form $N_{\mu\nu\rho}$ on the 4-dimensional spacetime: $J = - \star N$. Or in coordinates:

$$J^\mu = \frac{1}{3!}\epsilon^{\mu\nu\lambda\rho} N_{\nu\lambda\rho} = \frac{1}{3!}\epsilon^{\mu\nu\lambda\rho} f^A{}_\nu f^B{}_\lambda f^C{}_\rho \Omega_{ABC}. \tag{2.17}$$

This vector is orthogonal to the configuration gradient $f^A{}_{,\mu}$ which can be checked directly.

$$J^\mu f^D{}_\mu = \frac{\Omega_{ABC}}{3!}\epsilon^{\mu\nu\lambda\rho} f^A{}_\nu f^B{}_\lambda f^C{}_\rho f^D{}_\mu \tag{2.18}$$

The expression $\epsilon^{\mu\nu\lambda\rho} f^A{}_\nu f^B{}_\lambda f^C{}_\rho f^D{}_\mu$ is the determinant of a 4×4 matrix formed out of columns $f^A{}_\mu$. But $A, B, C, D = 1, 2, 3$ so there are at least two equal columns, and hence this determinant vanishes and $J^\mu f^A{}_\mu = 0$. As we also know that $v^\mu f^A{}_\mu = 0$ we can conclude that $J^\mu \propto v^\mu$. Next we want to show that J^μ is conserved, i.e. $\nabla_\mu J^\mu = 0$.

Proof.

$$\nabla_\mu J^\mu = \frac{1}{3!}\epsilon^{\mu\nu\lambda\rho} \nabla_\mu \left(f^A{}_\nu f^B{}_\lambda f^C{}_\rho \Omega_{ABC} \right) \tag{2.19}$$

The covariant derivative hitting the expression in the brackets using the product rule, has three terms containing $\nabla_\mu f^A{}_\nu$. But this is symmetric in $\mu\nu$ since covariant derivatives commute when acting on scalar functions:

$$\nabla_\mu f^A{}_\nu = \nabla_\mu \partial_\nu f^A = \nabla_\mu \nabla_\nu f^A = \nabla_\nu \nabla_\mu f^A = \nabla_\nu f^A{}_\mu. \tag{2.20}$$

When contracting with the totally anti-symmetric tensor all these terms vanish, and what remains is the fourth term, containing $\nabla_\mu \Omega_{ABC}$. The volume form is a function of the coordinates $X^D = f^D(x^\alpha)$ on the body manifold $\mathcal{B}$. So the chain-rule has to be used when taking the derivative with respect to the spacetime coordinates:

$$\nabla_\mu \Omega_{ABC}(X^D) = \partial_D \Omega_{ABC}(X^D) \nabla_\mu f^D. \tag{2.21}$$

This implies, when inserted into the expression for $\nabla_\mu J^\mu$, that

$$\nabla_\mu J^\mu \propto \epsilon^{\mu\nu\lambda\rho} f^A{}_\nu f^B{}_\lambda f^C{}_\rho f^D{}_\mu = 0 \tag{2.22}$$

as we have already seen that this is the determinant of a matrix with two identical columns, and hence vanishes. So the proof that J^μ is conserved is complete. □

Without loss of generality we can choose the orientation of Ω_{ABC} so that J^μ is future-pointing, and then we can write $J^\mu = nv^\mu$, with a scalar function $n > 0$, which represents the particle number density. To get an explicit formula for n we take the square:

$$\begin{aligned}
n^2 &= -J^\mu J_\mu \\
&= -\frac{1}{3!}\epsilon^{\mu\nu\lambda\rho}N_{\nu\lambda\rho}\frac{1}{3!}\epsilon_{\mu\alpha\beta\gamma}N^{\alpha\beta\gamma} \\
&= \frac{1}{3!}\delta^{[\nu}_{\alpha}\delta^{\lambda}_{\beta}\delta^{\rho]}_{\gamma}N_{\nu\lambda\rho}N^{\alpha\beta\gamma} && (\epsilon^{\mu\nu\lambda\rho}\epsilon_{\mu\alpha\beta\gamma} = -3!\ \delta^{[\nu}_{\alpha}\delta^{\lambda}_{\beta}\delta^{\rho]}_{\gamma}, \text{ cf. [3]}) \\
&= \frac{1}{3!}\delta^{\nu}_{\alpha}\delta^{\lambda}_{\beta}\delta^{\rho}_{\gamma}N_{[\nu\lambda\rho]}N^{\alpha\beta\gamma} && (\text{move anti-symmetrization down}) \\
&= \frac{1}{3!}N_{\nu\lambda\rho}N^{\nu\lambda\rho} && (N_{\nu\lambda\rho} \text{ is totally anti-symmetric}) \\
&= f^A{}_{\mu}f^B{}_{\nu}f^C{}_{\rho}\Omega_{ABC}g^{\mu\mu'}g^{\nu\nu'}g^{\rho\rho'}f^{A'}{}_{\mu'}f^{B'}{}_{\nu'}f^{C'}{}_{\rho'}\Omega_{A'B'C'} && (2.16) \\
&= \frac{1}{3!}B^{AA'}B^{BB'}B^{CC'}\Omega_{ABC}\Omega_{A'B'C'} && (2.5)
\end{aligned}$$

In a specific coordinate system the components of Ω can be written using the totally anti-symmetric symbol: $\Omega_{ABC} = \tilde{\epsilon}_{ABC}\Omega_{123} = \Omega(f^A(x^\mu))\tilde{\epsilon}_{ABC}$. Then we can use the formula for the determinant of a matrix:

$$\tilde{\epsilon}^{ABC}\det(B^{AB}) = \tilde{\epsilon}_{A'B'C'}B^{AA'}B^{BB'}B^{CC'}. \tag{2.23}$$

Inserting this back into the expression for n^2 we get

$$\frac{1}{3!}\Omega(f^A(x^\mu))^2\tilde{\epsilon}_{ABC}\tilde{\epsilon}^{ABC}\det(B^{AB}). \tag{2.24}$$

Now using the fact that $\tilde{\epsilon}_{ABC}\tilde{\epsilon}^{ABC} = 3!$ it follows for the particle number density

$$n = \Omega(f^A(x^\mu))\sqrt{\det(B^{AB})} = \frac{\Omega(f^A(x^\mu))}{\sqrt{\det(C_{AB})}} \tag{2.25}$$

where the relation for the determinant of the inverse matrix $\det(A^{-1}) = \det(A)^{-1}$ has been used. So the particle number density depends only on the configuration f^A and the strain B^{AB}:

$$n = n(f^A, B^{AB}). \tag{2.26}$$

2.3 Lagrangian formalism and Energy-Momentum Tensor

We want to derive the equations of motion from an action principle. The action in Relativistic Elasticity is given by

$$S[f^A] = \int_{M'} \rho\left(f^A(x^\mu), \partial_\mu f^A(x^\nu); g_{\mu\nu}\right)\sqrt{-\det g}\ d^4x \tag{2.27}$$

and so the Lagrangian reads $\mathcal{L} = \rho\left(f^A, \partial_\mu f^A; g_{\mu\nu}\right)\sqrt{-\det g}$. We use the notation $g = \det g$. Next, we calculate the derivatives appearing in the Euler-Lagrange equations

for this action:

$$\frac{\partial}{\partial x^\mu}\frac{\partial \mathcal{L}}{\partial {f^A}_\mu} = \frac{\partial}{\partial x^\mu}\left(\sqrt{-g}\frac{\partial \rho}{\partial {f^A}_\mu}\right) = \sqrt{-g}\nabla_\mu \frac{\partial \rho}{\partial {f^A}_\mu}. \tag{2.28}$$

Here the identity for the divergence of a vector $\nabla_\mu U^\mu = \frac{1}{\sqrt{-g}}\partial_\mu(\sqrt{-g}U_\mu)$ has been used. The other derivative is

$$\frac{\partial \mathcal{L}}{\partial f^A} = \sqrt{-g}\frac{\partial \rho}{\partial f^A}. \tag{2.29}$$

Putting this together the Euler-Lagrange equations $\frac{\partial}{\partial x^\mu}\frac{\partial \mathcal{L}}{\partial {f^A}_\mu} - \frac{\partial \mathcal{L}}{\partial f^A} = 0$ become (as the determinant of the metric is non-vanishing and can be cancelled out)

$$\mathcal{E}_A = \nabla_\mu \frac{\partial \rho}{\partial {f^A}_\mu} - \frac{\partial \rho}{\partial f^A} = 0. \tag{2.30}$$

The energy-momentum tensor can be derived by varying the action with respect to the metric (see e.g. [3]):

$$T_{\mu\nu} = -\frac{2}{\sqrt{-g}}\frac{\delta S}{\delta g^{\mu\nu}}. \tag{2.31}$$

Applying this to the Lagrangian $\mathcal{L} = \sqrt{-g}\rho$ leads to

$$-\frac{2}{\sqrt{-g}}\left(\frac{-1}{2\sqrt{-g}}\frac{\partial \det g}{\partial g^{\mu\nu}}\rho + \sqrt{-g}\frac{\partial \rho}{\partial g^{\mu\nu}}\right). \tag{2.32}$$

The formula $\frac{\partial \det(A)}{\partial A_{ij}} = \det(A)\left(A^{-1}\right)_{ji}$ is used to evaluate the derivative of the determinant (proof in Appendix of [2]). Following the sign convention used in [1] we choose the negative root and therefore the energy-momentum tensor takes the form

$$T_{\mu\nu} = -\rho g_{\mu\nu} + 2\frac{\partial \rho}{\partial g^{\mu\nu}}. \tag{2.33}$$

To find an expression for $\frac{\partial \rho}{\partial g^{\mu\nu}}$ we investigate the Lie Derivative of the total energy density. As ρ is assumed to transform as a scalar we can, on the one hand, evaluate the Lie Derivative directly:

$$\mathcal{L}_\xi \rho = \xi^\mu \partial_\mu \rho(f^A, \partial_\nu f^A; g^{\alpha\beta}) = \xi^\mu\left(\frac{\partial \rho}{\partial f^A}\partial_\mu f^A + \frac{\partial \rho}{\partial {f^A}_{,\alpha}}\partial_\mu {f^A}_{,\alpha} + \frac{\partial \rho}{\partial g^{\alpha\beta}}\partial_\mu g^{\alpha\beta}\right). \tag{2.34}$$

But on the other hand we can also use the chain rule for the Lie Derivative:

$$\begin{aligned}\mathcal{L}_\xi \rho &= \frac{\partial \rho}{\partial f^A}\mathcal{L}_\xi f^A + \frac{\partial \rho}{\partial {f^A}_{,\alpha}}\mathcal{L}_\xi {f^A}_{,\alpha} + \frac{\partial \rho}{\partial g^{\alpha\beta}}\mathcal{L}_\xi g^{\alpha\beta} \\ &= \frac{\partial \rho}{\partial f^A}\xi^\mu \partial_\mu f^A + \frac{\partial \rho}{\partial {f^A}_{,\alpha}}\left(\xi^\mu \partial_\mu {f^A}_{,\alpha} + {f^A}_{,\mu}\partial_\alpha \xi^\mu\right) \frac{\partial \rho}{\partial g^{\alpha\beta}}\left(\xi^\mu \partial_\mu g^{\alpha\beta} - g^{\mu\beta}\partial_\mu \xi^\alpha - g^{\alpha\mu}\partial_\mu \xi^\beta\right)\end{aligned}$$

Since this two expressions should give the same result, we can subtract them from each other and find

$$\left(\frac{\partial\rho}{\partial f^A{}_{,\mu}} f^A{}_{,\alpha} - 2\frac{\partial\rho}{\partial g^{\alpha\beta}} g^{\beta\mu}\right)\partial_\mu \xi^\alpha = 0 \tag{2.35}$$

after renaming dummy indices and using that $g^{\mu\nu}$ is symmetric. Since this is true for arbitrary ξ^α we obtain

$$g_{\mu\nu}\frac{\partial\rho}{\partial f^A{}_{,\mu}} f^A{}_{,\alpha} = 2\frac{\partial\rho}{\partial g^{\alpha\nu}} \tag{2.36}$$

where we have also multiplied by the metric $g_{\mu\nu}$. This can now be put back into the expression for the stress-energy tensor (2.33):

$$T_{\mu\nu} = -\rho g_{\mu\nu} + g_{\mu\alpha}\frac{\partial\rho}{\partial f^A{}_{,\alpha}} f^A{}_{,\nu} \tag{2.37}$$

The version with one index pulled up using the metric is

$$T^\mu{}_\nu = -\rho\delta^\mu_\nu + \frac{\partial\rho}{\partial f^A{}_{,\mu}} f^A{}_{,\nu}. \tag{2.38}$$

From the fact that energy is conserved, it follows that this tensor is divergence-free, i.e. $\nabla_\mu T^\mu{}_\nu$. This condition is equivalent to the Euler-Lagrange equations being satisfied $\mathcal{E}_A = 0$, which can be checked by calculating $\nabla_\mu T^\mu{}_\nu$ using the chain rule for the covariant derivative:

$$\begin{aligned}\nabla_\mu T^\mu{}_\nu &= -\delta^\mu_\nu \nabla_\mu \rho(f^A, f^A{}_{,\alpha}; g_{\alpha\beta}) + \nabla_\mu\left(\frac{\partial\rho}{\partial f^A{}_{,\mu}} f^A{}_{,\nu}\right) \\ &= -\frac{\partial\rho}{\partial f^A}\nabla_\nu f^A - \frac{\partial\rho}{\partial f^A{}_{,\alpha}}\nabla_\nu f^A{}_{,\alpha} - \frac{\partial\rho}{\partial g^{\alpha\beta}}\nabla_\nu g^{\alpha\beta} + \left(\nabla_\mu\frac{\partial\rho}{\partial f^A{}_{,\mu}}\right) f^A{}_{,\nu} + \frac{\partial\rho}{\partial f^A{}_{,\mu}}\nabla_\mu f^A{}_{,\nu}\end{aligned}$$

The term containing the covariant derivative of the metric vanishes, since the Levi-Civita connection is metric compatible. Moreover the second and the last term cancel each other, since we have already seen that $f^A{}_{;\mu\nu} = f^A{}_{;\nu\mu}$, the covariant derivative is symmetric when acting on a scalar function. Then what remains is

$$\left(\frac{\partial\rho}{\partial f^A} - \nabla_\mu\frac{\partial\rho}{\partial f^A{}_{,\mu}}\right) f^A{}_{,\nu} = \mathcal{E}_A f^A{}_{,\nu} = 0 \tag{2.39}$$

so that the Euler-Lagrange equations and the vanishing of the divergence of the EM-tensor are indeed equivalent.

2.3.1 Stored Energy Function

In this section we look closer at the dependence of the energy density on its arguments $\rho = \rho(f^A(x^\mu), \partial_\mu f^A(x^\nu); g_{\mu\nu})$. First notice, that the contraction of the derivative with respect to the metric components, with the four-velocity v^μ vanishes.

$$\frac{\partial\rho}{\partial g^{\mu\nu}} v^\mu = \frac{1}{2} g_{\alpha\nu}\frac{\partial\rho}{\partial f^A{}_{,\alpha}} f^A{}_{,\mu} v^\mu = 0 \tag{2.40}$$

The relation (2.36) has been used for the first equality. The second equality follows because the four-velocity is, by definition (2.4), orthogonal to the configuration gradient. Now we add a term $av^\mu v^\nu$ to the metric and see how $\rho = \rho(f^A(x^\mu), \partial_\mu f^A(x^\nu); g^{\mu\nu} + av^\mu v^\nu)$ changes with the parameter a:

$$\frac{d\rho}{da} = \frac{\partial \rho}{\partial g^{\mu\nu}} v^\mu v^\nu = 0. \tag{2.41}$$

That means ρ is independent of a and we can equate the cases $a = 0$ and $a = 1$

$$\rho(f^A, \partial_\mu f^A; g^{\mu\nu}) = \rho(f^A, \partial_\mu f^A; g^{\mu\nu} + v^\mu v^\nu) = \rho(f^A, \partial_\mu f^A; l^{\mu\nu}) \tag{2.42}$$

so that we find that the dependence of the energy density on $g^{\mu\nu}$ can be turned into a dependence on $l^{\mu\nu}$. But relation (2.13) tells us that $l^{\mu\nu}$ contains the same information as the deformation B^{AB} so that

$$\rho = \sigma \left(f^A, \partial_\mu f^A; B^{AB}(f^C{}_{,\mu}, g^{\alpha\beta}) \right) \tag{2.43}$$

where σ has been used to indicate that the dependence on the deformation is different than the dependence on the metric. Next we look at the dependence on the configuration gradient by using the total derivative:

$$\begin{aligned} \frac{\partial \rho}{\partial f^A{}_{,\nu}} f^A{}_{,\mu} = \frac{d\sigma}{df^A{}_{,\nu}} f^A{}_{,\mu} &= \left(\frac{\partial \sigma}{\partial f^A{}_{,\nu}} + \frac{\partial \sigma}{\partial B^{CD}} \frac{\partial B^{CD}}{\partial f^A{}_{,\nu}} \right) f^A{}_{,\mu} \\ &= \frac{\partial \sigma}{\partial f^A{}_{,\nu}} f^A{}_{,\mu} + \frac{\partial \sigma}{\partial B^{CD}} 2\delta^{(C}_A f^{D)\nu} f^A{}_{,\mu} \qquad \text{(use equation (2.15))} \\ &= \frac{\partial \sigma}{\partial f^A{}_{,\nu}} f^A{}_{,\mu} + \frac{\partial \sigma}{\partial B^{CD}} 2 f^{D\nu} f^C{}_{,\mu} \end{aligned}$$

But we also have relation (2.36) so that we can write:

$$\frac{\partial \rho}{\partial f^A{}_{,\nu}} f^A{}_{,\mu} = 2 \frac{\partial \rho}{\partial g^{\mu\beta}} g^{\beta\nu} = 2 \frac{\partial \sigma}{\partial B^{CD}} \frac{\partial B^{CD}}{\partial g^{\mu\beta}} g^{\beta\nu} = 2 \frac{\partial \sigma}{\partial B^{CD}} f^C{}_{,\mu} f^D{}_{,\beta} g^{\beta\nu} \tag{2.44}$$

where in the final equality relation (2.14) has been used. Subtracting these two expressions from each other one obtains

$$\frac{\partial \sigma}{\partial f^A{}_{,\nu}} f^A{}_{,\mu} = 0 \tag{2.45}$$

and, since $f^A{}_{,\mu}$ has full rank, this is only true if

$$\frac{\partial \sigma}{\partial f^A{}_{,\nu}} = 0 \tag{2.46}$$

which means that σ doesn't depend on the deformation gradient explicitly, and hence the total energy density can be written as

$$\rho = \rho(f^A, B^{AB}). \tag{2.47}$$

As we have seen in equation (2.26) the particle number density has the same arguments and therefore we can write the energy density as a product

$$\rho = nw \tag{2.48}$$

defining the energy per particle $w = w(f^A, B^{AB})$, also called stored energy function. A relation between stresses and strains can be derived from w (as we will see in the next section) so that the stored energy function contains the same information as the equation of state.

2.4 Cauchy Stress Tensor

In equation (2.37) we have seen an expression for the energy-momentum tensor:

$$T_{\mu\nu} = -\rho g_{\mu\nu} + g_{\mu\alpha}\frac{\partial \rho}{\partial f^A{}_{,\alpha}} f^A{}_{,\nu}. \tag{2.49}$$

We can contract it with the four-velocity v^μ to find

$$T_{\mu\nu}v^\nu = -\rho g_{\mu\nu}v^\nu + g_{\mu\alpha}\frac{\partial \rho}{\partial f^A{}_{,\alpha}}(f^A{}_{,\nu}v^\nu) = \rho v_\mu + 0 = \rho v_\mu. \tag{2.50}$$

Using this we can rewrite $T_{\mu\nu}$ as the sum of a part along v^μ and a part 'orthogonal' to v^μ, which we call the Cauchy-stress tensor $\sigma_{\mu\nu}$:

$$T_{\mu\nu} = \rho v_\mu v_\nu - \sigma_{\mu\nu}. \tag{2.51}$$

The Cauchy-stress tensor has to satisfy $\sigma_{\mu\nu}v^\nu = 0$ and is symmetric (since $T_{\mu\nu}$ also was symmetric). To find an explicit expression we use relation (2.8) to rewrite (2.33)

$$T_{\mu\nu} = -\rho(l_{\mu\nu} - v_\mu v_\nu) + 2\frac{\partial \rho}{\partial g^{\mu\nu}} \tag{2.52}$$

and read off

$$\sigma_{\mu\nu} = \rho l_{\mu\nu} - 2\frac{\partial \rho}{\partial g^{\mu\nu}}. \tag{2.53}$$

For an interpretation we write the energy-momentum tensor in coordinates of the rest frame of the particles, i.e. $v^\mu = \partial_t$:

$$T_{\mu\nu} = \begin{pmatrix} \rho & 0 & 0 & 0 \\ 0 & & & \\ 0 & & -\sigma_{ij} & \\ 0 & & & \end{pmatrix}. \tag{2.54}$$

This leads to think of ρ as the total energy density and σ_{ij} as the internal stresses exerted on a volume element by its surroundings. To get an expression for the Cauchy-stress

tensor in terms of the stored energy function we evaluate the derivative in (2.53) using (2.48):

$$\frac{\partial \rho}{\partial g^{\mu\nu}} = \frac{\partial \rho}{\partial l^{\mu\nu}} = \frac{\partial (nw)}{\partial l^{\mu\nu}} = \frac{\partial n}{\partial l^{\mu\nu}} w + n \frac{\partial w}{\partial l^{\mu\nu}}. \tag{2.55}$$

The first equality holds because of equation (2.42). For the derivative of n we use equation (2.25), $n = \Omega(f^A)\sqrt{\det(B^{AB})}$.

$$\begin{aligned}
\frac{\partial n}{\partial l^{\mu\nu}} &= \frac{\Omega}{2\sqrt{\det(B^{AB})}} \frac{\partial \det(B^{AB})}{\partial l^{\mu\nu}} \\
&= \frac{\Omega^2}{2n} \frac{\partial \det(B^{AB})}{\partial B^{CD}} \frac{\partial B^{CD}}{\partial l^{\mu\nu}} \\
&= \frac{\Omega^2}{2n} \det(B^{AB}) C_{CD} f^C{}_\mu f^D{}_\nu && \text{(used eq. (2.14))} \\
&= \frac{n}{2} l_{\mu\nu} && \text{(eq. (2.8))}
\end{aligned}$$

Now this can be plugged back into the previous relation to find:

$$\frac{\partial \rho}{\partial g^{\mu\nu}} = \frac{n}{2} l_{\mu\nu} w + n \frac{\partial w}{\partial l^{\mu\nu}} = \frac{\rho}{2} l_{\mu\nu} + n \frac{\partial w}{\partial l^{\mu\nu}}. \tag{2.56}$$

With this the Cauchy-stress tensor (2.53) becomes

$$\sigma_{\mu\nu} = \rho l_{\mu\nu} - 2\left(\frac{\rho}{2} l_{\mu\nu} + n \frac{\partial w}{\partial l^{\mu\nu}}\right) = 2n \frac{\partial w}{\partial l^{\mu\nu}}. \tag{2.57}$$

Knowing this relation between stresses ($\sigma_{\mu\nu}$) and strain ($l^{\mu\nu}$) is equivalent to knowing the equation of state.

2.5 Classical Wave Equation for Small Displacements

In this section we want to derive the equations of motion for small displacements, and compare it to the classical wave equation for elastic waves in media found in textbooks of classical Elasticity Theory, e.g. [8]. We start with the assumption that in equilibrium the coordinates of both manifolds (body and spacetime) coincide and the particles of the body are at rest:

$$f^A(x^\mu) = x^A, \qquad v^\mu = (1, 0, 0, 0). \tag{2.58}$$

Now we add a small displacement $\epsilon u^A, \epsilon \ll 1$, from equilibrium

$$f^A(x^\mu) = x^A - \epsilon u^A(x^\mu). \tag{2.59}$$

This also adds a small spatial velocity to the four-velocity of the particles

$$v^\mu = (1, \epsilon \vec{w}). \tag{2.60}$$

Now we can check the orthogonality condition $v^\mu \partial_\mu f^A = 0$:

$$0 \overset{!}{=} v^\mu(\delta^A_\mu - \epsilon\partial_\mu u^A) \tag{2.61}$$
$$= \epsilon w^A - \epsilon v^0 \partial_t u^A - \epsilon v^i \partial_i u^A \tag{2.62}$$
$$= \epsilon w^A - \epsilon \partial_t u^A - \epsilon^2 w^i \partial_i u^A \tag{2.63}$$

Ignoring the $O(\epsilon^2)$ term this leads to

$$w^A = \partial_t u^A \tag{2.64}$$

and hence the four-velocity becomes

$$v^\mu = (1, \epsilon\partial_t u^i) \tag{2.65}$$

which is very intuitive since we would classically expect, that the velocity is the time-derivative of the displacement. We have seen, that the equations of motion can be derived from the condition that the energy-momentum Tensor

$$T^{\mu\nu} = \rho v^\mu v^\nu - \sigma^{\mu\nu} \tag{2.66}$$

is divergence-free. We use an linear approximation in ϵ for the Cauchy-stress tensor. The constant term is set to zero because there are no stresses when the deformation vanishes.

$$\sigma^{\mu\nu} = \epsilon s^{\mu\nu} \tag{2.67}$$

Next we look at $\rho = nw$ and expand both n and w in orders of ϵ.

$$n = n_0 + \epsilon n_1 \tag{2.68}$$
$$w = m_0 + \epsilon^2 e \tag{2.69}$$
$$\rho_0 := n_0 m_0 \tag{2.70}$$

In analogy to Hook's law, the linear term for w vanishes, which represents the fact that stored energy function has a minimum in equilibrium (without deformation, i.e. $\epsilon = 0$). Then e can be interpreted as some parameter similar to a spring constant per atom. m_0 is the rest mass and ρ_0 the rest energy density. With this we can now calculate the divergence of the EM tensor:

$$\nabla_\mu T^{\mu\nu} = \nabla_\mu(nwv^\mu v^\nu) - \nabla_\mu \sigma^{\mu\nu} \tag{2.71}$$
$$= \nabla_\mu(nv^\mu) w v^\nu + n v^\mu \nabla_\mu(w v^\nu) - \nabla_\mu \sigma^{\mu\nu} \tag{2.72}$$

The first term now vanishes because of the continuity equation (2.22) as $J^\mu = nv^\mu$. As we are considering the classical case here, the spacetime metric becomes the Minkowski metric of flat spacetime $g_{\mu\nu} = \eta_{\mu\nu}$, which also means that the covariant derivatives can be replaced by partials $\nabla_\mu \to \partial_\mu$. With this, the divergence of the EM-tensor becomes

$$\partial_\mu T^{\mu\nu} = n v^\mu \partial_\mu (w v^\nu) - \partial_\mu \sigma^{\mu\nu}. \tag{2.73}$$

These are four equations, one for each value of ν. The time component and spatial components are considered separately, as the Cauchy-stress tensor has only spatial components. This can be seen as follows:

$$v^\mu \sigma_{\mu\nu} = v^0 \sigma_{0\nu} + v^i \sigma_{i\nu} = \sigma_{0\nu} + \epsilon \partial_t u^i \epsilon s_{i\nu} \tag{2.74}$$

as $\sigma_{\mu\nu}$ is introduced in (2.51) as the part of $T_{\mu\nu}$ which is orthogonal to v^μ we have $v^\mu \sigma_{\mu\nu} = 0$ and hence the expression above must vanish. But since the last term is $O(\epsilon^2)$ one obtains

$$\sigma_{0\nu} = 0 \tag{2.75}$$

so that the Cauchy-stress tensor has only spatial components. As a consequence the divergence of $\sigma^{\mu\nu}$ in (2.73) can be restricted to spatial indices

$$\partial_\mu T^{\mu\nu} = n v^\mu \partial_\mu (w v^\nu) - \partial_i \sigma^{i\nu}. \tag{2.76}$$

We first consider the time component $\nu = 0$ where only the first term remains as the time-component of the Cauchy-stress tensor in the last term vanishes:

$$\partial_\mu T^{\mu 0} = n v^\mu \partial_\mu (w v^0) = n v^\mu \partial_\mu (m_0 + \epsilon^2 e) = \epsilon^2 n v^\mu \partial_\mu e = O(\epsilon^2). \tag{2.77}$$

As we are working only up to order ϵ^2 this is satisfied and we get no new condition. The other components with $\nu = j = 1, 2, 3$ are more interesting.

$$\begin{aligned} \partial_\mu T^{\mu j} &= n v^\mu \partial_\mu (w v^j) - \partial_i \sigma^{ij} \\ &= n v^\mu \partial_\mu ((m_0 + \epsilon^2 e) \epsilon \partial_t u^j) - \partial_i \sigma^{ij} \\ &= (n_0 + \epsilon n_1) \partial_t (m_0 \epsilon \partial_t u^j) + n \epsilon \partial_t u^i \partial_i (m_0 \epsilon \partial_t u^j) - \partial_i \sigma^{ij} \\ &= \epsilon n_0 m_0 \partial_t^2 u^j - \partial_i \sigma^{ij} \\ &= \epsilon \rho_0 \partial_t^2 u^j - \partial_i \sigma^{ij} = 0 \end{aligned} \tag{2.78}$$

This is the desired equation of motion for the displacement u^i. To turn it into the classical wave equation we need to get an explicit expression for the Cauchy-stress tensor. For this we introduce the Saint Venant-Kirchhoff model of a hyperelastic isotropic material with the Cauchy-stress tensor

$$\sigma_{ij} = \lambda E \delta_{ij} + 2\mu E_{ij} \tag{2.79}$$

and the Green-strain tensor

$$E_{ij} = \tfrac{1}{2}(C_{ij} - \gamma_{ij}) \tag{2.80}$$

which describes the deformation relative to a reference deformation γ_{ij} in the rest frame, and its trace $E = E^k_k$. Here we have $\gamma_{ij} = \delta_{ij}$. C_{ij} is the Cauchy-Green deformation tensor from section 2.1, where it was denoted C_{AB}. We can find an explicit expression in terms of the deformation u^i by remembering, that it is the inverse of B^{AB}.

$$\begin{aligned} B^{AB} &= \partial_\mu f^A \partial_\nu f^B \eta^{\mu\nu} \\ &= (\delta^A_\mu - \epsilon \partial_\mu u^A)(\delta^B_\nu - \epsilon \partial_\nu u^B) \eta^{\mu\nu} \\ &= \eta^{AB} - \epsilon(\eta^{A\nu} \partial_\nu u^B + \eta^{\mu B} \partial_\mu u^A) + O(\epsilon^2) \\ &= \delta^{AB} - \epsilon(\partial^A u^B + \partial^B u^A) + O(\epsilon^2) \end{aligned} \tag{2.81}$$

It is easy to check, that the inverse up to order $O(\epsilon^2)$ is given by

$$C_{AB} = \delta_{AB} + \epsilon(\partial_A u_B + \partial_B u_A). \tag{2.82}$$

Putting this back into the Green-strain tensor one obtains

$$E_{AB} = \tfrac{1}{2}\epsilon(\partial_A u_B + \partial_B u_A) \tag{2.83}$$

with trace

$$E = E^k_k = \epsilon \partial_k u^k. \tag{2.84}$$

Finally this leads to the Cauchy-stress tensor in the following form:

$$\sigma_{ij} = \epsilon[\lambda \partial_k u^k \delta_{ij} + \mu(\partial_i u_j + \partial_j u_i)]. \tag{2.85}$$

As we saw in equation (2.78) the equations of motion contain the divergence of σ^{ij} (indices raised with the Minkowski metric) which can now calculated to be

$$\begin{aligned} \partial_i \sigma^{ij} &= \epsilon[\lambda \partial_i \partial_k u^k \delta^{ij} + \mu(\partial_i \partial^i u^j + \partial_i \partial^j u^i)] \\ &= \epsilon[(\lambda + \mu)\partial^j \partial_i u^i + \mu \Delta u^j] \end{aligned}$$

so that finally the equations of motion read

$$\epsilon[\rho_0 \partial_t^2 u^j - (\lambda + \mu)\partial^j \partial_i u^i - \mu \Delta u^j] = 0. \tag{2.86}$$

The part in the brackets is indeed equivalent to the wave equation of classical elasticity theory.

Chapter 3

Setup of Plate and Gravitational Wave

In the previous chapter we derived the equations of motion of an elastic body in the case of small displacements. Then we used the Minkowski metric to retrieve the classical limit. In this chapter we want to consider how the equations of motion change, when we use a metric describing a gravitational wave background.

Then we also look at the boundary conditions for a free quadratic plate of length L lying in the x-y plane. We look at the concrete case where the gravitational wave travels in z-direction, so it hits the plate at a right angle.

Next, two simplifications are discussed. First that the time dependence can be separated off, so that the problem can be considered stationary. And second, that we can restrict the size of the plate to a length of $L = 1m$, because all other cases can be obtained by a simple scaling argument.

For the two special case of pure plus-polarization and pure cross-polarization the boundary value problem exhibits a symmetry. These are discussed in sections 3.6 and 3.7. The final two sections describe a polynomial solution for these two special cases, in the limit of small frequencies.

3.1 Gravitatonal Waves and TT-Coordinates

Gravitational Waves belong to the most interesting phenomena predicted by Einstein's General Theory of Relativity. First predicted by Einstein himself in 1916, they were long considered to have too weak effects to ever be measurable. The long history of how scientists struggled to overcome the odds and measure them is related elsewhere, for instance in [4]. Suffice it to say that it culminated in the first detection of GWs, created by the merger of a binary black hole in 2015 by LIGO. The Nobel Prize in Physics 2017 was awarded for this achievement.

Far from the source, GWs are weak and therefore can be described using linearized gravity. The metric has the form

$$g_{\mu\nu} = \eta_{\mu\nu} + \epsilon h_{\mu\nu} \tag{3.1}$$

consisting of the Minkowski metric of flat spacetime $\eta_{\mu\nu}$ plus some perturbation $\epsilon h_{\mu\nu}$ with $\epsilon \lll 1$. Typical values for ϵ are 10^{-20}. Terms of order $O(\epsilon^2)$ and smaller are ignored from now on. The inverse is then given by

$$g^{\mu\nu} = \eta^{\mu\nu} - \epsilon h^{\mu\nu}. \tag{3.2}$$

It is convenient to work in the TT gauge, which is adapted to the gravitational wave such that free particles remain at fixed coordinates.

The metric perturbation satisfies the linearized Einstein equations and has the form $h_{\mu\nu} = \Re(A_{\mu\nu}e^{ik_\mu x^\mu})$ with constants $A_{\mu\nu}$, which in general can be complex. The wave vector k_μ is null $k_\mu k^\mu = 0$ and for a wave traveling in z-Direction looks like

$$k_\mu = (\omega, 0, 0, \omega) \tag{3.3}$$

where ω is the (angular) frequency of the gravitational wave. Moreover in the TT(transverse traceless)-gauge it holds that

$$A_{\mu\nu}k^\nu = 0, \quad A^\mu_\mu = 0 \tag{3.4}$$

so that

$$h_{ij} = \begin{pmatrix} h_+ & h_\times & 0 \\ h_\times & -h_+ & 0 \\ 0 & 0 & 0 \end{pmatrix} \tag{3.5}$$

with $h_+ = A_+ \cos(\omega(t-z))$ and $h_\times = A_\times \cos(\omega(t-z)+\gamma)$ where A_+ and $A_\times$ are real constants and give the relative amplitudes of the two polarizations. The time origin can be chosen such that A_{11} is real. In case of complex $A_{12} = A_\times e^{i\gamma}$, the phase shift between the two polarizations is given by γ. The proof that gauge transformations which bring the metric into this form exists can be found in many textbooks of GR (e.g. [5], [3] or [11])

3.2 Equations of Motion for a Quadratic Plate

In section 2.5 we have seen that the general equations of motion in the case of small displacements are related to the vanishing of the energy-momentum tensor $\nabla_\mu T^{\mu\nu} = 0$. Moreover we saw that for the case of flat spacetime this turns into the classical equations for elastic waves in media (2.86). To describe the behaviour of an elastic plate in a gravitational wave background this approach has to be slightly adjusted. This and the next section is again based on the procedure in [7].

Instead of the Minkowski metric we now use the linearized metric from section 3.1. The perturbation of the metric is of order $O(\epsilon)$ and so are its derivatives. The Christoffel Symbols in the covariant Derivative contain first derivatives of the metric so they are also of order $O(\epsilon)$. In the divergence of the EM-tensor (2.71) the covariant derivative acts only on quantities which are themselves of order $O(\epsilon)$ so that it differs from the partial only by terms of $O(\epsilon^2)$. Therefore we can again replace the covariant Derivative by partials.

The second difference lies in the Cauchy-stress tensor. In contrast to before, where we inserted the Minkowski metric in equation (2.81), we now use the spacetime metric $g_{\mu\nu}$, so that the strain B^{AB} becomes

$$\begin{aligned} B^{AB} &= \partial_\mu f^A \partial_\nu f^B g^{\mu\nu} \\ &= (\delta^A_\mu - \epsilon\partial_\mu u^A)(\delta^B_\nu - \epsilon\partial_\nu u^B)(\eta^{\mu\nu} - \epsilon h^{\mu\nu}) \\ &= \eta^{AB} - \epsilon\left(\eta^{A\nu}\partial_\nu u^B + \eta^{\mu B}\partial_\mu u^A + h^{AB}\right) + O(\epsilon^2) \\ &= \delta^{AB} - \epsilon\left(\partial^A u^B + \partial^B u^A + h^{AB}\right) + O(\epsilon^2). \end{aligned} \tag{3.6}$$

The inverse of this (up to terms of order $O(\epsilon^2)$) is given by

$$C_{AB} = \delta_{AB} + \epsilon \left(\partial_A u_B + \partial_B u_A + h_{AB}\right) \tag{3.7}$$

which can then be inserted into the expression for the Cauchy-stress tensor, for which one obtains

$$\sigma_{ij} = \epsilon[\lambda \partial_k u^k \delta_{ij} + \mu(\partial_i u_j + \partial_j u_i + h_{ij})]. \tag{3.8}$$

In the equations of motion only the divergence of the CS-tensor $\partial_i \sigma^{ij}$ appears. The new term in this expression is $\partial_i h^{ij}$. But this vanishes in the TT-gauge because of the transversality condition. Therefore the equations of motion are unchanged:

$$\partial_t^2 u^j - \frac{\lambda + \mu}{\rho_0} \partial^j \partial_i u^i - \frac{\mu}{\rho_0} \Delta u^j = 0 \tag{3.9}$$

We consider a quadratic plate lying in the x-y plane centered at the origin, i.e. $(x, y) \in \left[-\frac{L}{2}, \frac{L}{2}\right] \times \left[-\frac{L}{2}, \frac{L}{2}\right] =: P$. The plate is assumed to be thin so that the deformation is independent of the z-direction, i.e. $u^i = u^i(x, y)$. Moreover, only the in-plane deformations are considered, i.e. $u^z \equiv 0$. Then the indices can be restricted to the values $i, j... = 1, 2$ or $i, j... = x, y$.

3.3 Boundary Conditions

To arrive at a well-posed boundary value problem we need, in addition to the equations of motion (3.9), boundary conditions. These prescribe the forces F_i acting on the body, and are given by the contraction of the outward pointing normal vector with the Cauchy-stress tensor $\sigma_{ij} n^j = F_i$. We consider a free plate, with no forces acting on it, i.e. $\sigma_{ij} n^j = 0$ at the boundary ∂P. The boundary can be split into two parts (see Figure 3.1):

- The 'right' and 'left' boundary ∂P_x where $x = \pm \frac{L}{2}$ and the normal vector is given by $\vec{n} = (\pm 1, 0)$. Hence the boundary condition there is $\sigma_{1j} = \sigma_{xj} = 0$.
- The 'top' and 'bottom' boundary ∂P_y where $y = \pm \frac{L}{2}$ and the normal vector is given by $\vec{n} = (0, \pm 1)$. Hence the boundary condition there is $\sigma_{2j} = \sigma_{yj} = 0$.

In general, one would also need to consider the forces acting on the $z = const.$ surfaces. There the normal vector is $n^i = (0, 0, 1)$, such that $\sigma_{ij} n^j = \sigma_{i3}$. Looking at the expression for the CS-tensor (3.8) one can see, that the off-diagonal components vanish $\sigma_{13} = \sigma_{23} = 0$. This is, because the deformation depends only on the coordinates in the plane, and has vanishing z-component. Moreover, the GW has $h_{i3} = 0$. Then $F_3^{(z)} = \epsilon\lambda \, \nabla \cdot \vec{u}$ is the force needed to keep the plate flat, which can be calculated once we have solved the PDE and satisfied the two boundary conditions above. But it is not itself part of the BVP. [1]

[1] An alternative approach for thin plates is to set σ_{zz} to zero instead. Then u^z would be determined by the other two components. In that case the longitudinal wave speed would need to be modified, see [8].

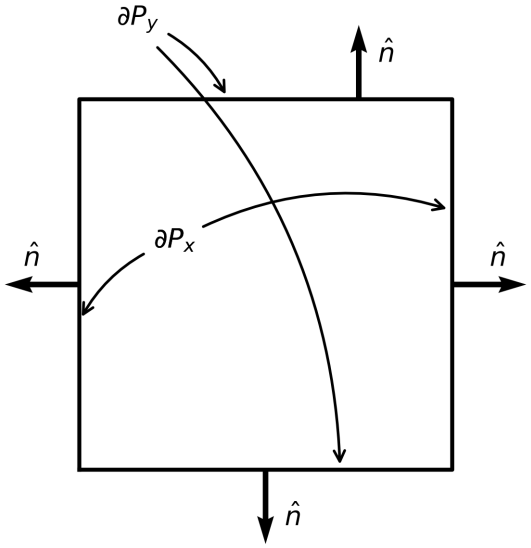

Figure 3.1: Illustration of the boundary, which splits into two parts ∂P_x and ∂P_y, and the outward-pointing normal vectors.

It turns out to be convenient to rewrite the boundary conditions in the following form:

$$\begin{aligned} \sigma_{xx}|_{\partial P_x} = 0 \implies & (2\mu+\lambda)\partial_x u^x + \lambda \partial_y u^y = -\mu h_+ \\ \sigma_{yy}|_{\partial P_y} = 0 \implies & (2\mu+\lambda)\partial_y u^y + \lambda \partial_x u^x = \mu h_+ \\ \sigma_{xy}|_{\partial P} = 0 \implies & \partial_x u^y + \partial_y u^x = -h_\times \end{aligned} \tag{3.10}$$

where we denote $h_+ = h_{11} = -h_{22}$ and $h_\times = h_{12} = h_{21}$. It is interesting to note, that the gravitational wave enters only through the boundary conditions and doesn't appear in the equations of motion. But, one has to keep in mind that this is coordinate dependent.

3.4 Separation of Time-Dependence

In analogy to a Harmonic oscillator, driven by a periodic force, we assume that the plate is driven by the GW, and oscillates with its frequency ω. Therefore we make the ansatz $u^i = \cos(\omega t)\ \varphi^i(x,y)$. Plugging this into the equation (3.9) yields an equation only for $\varphi^i(x,y)$:

$$\omega^2 \varphi^i + \frac{\mu}{\rho_0}\Delta\varphi^i + \frac{\mu+\lambda}{\rho_0}\partial^i\partial_k\varphi^k = 0. \tag{3.11}$$

Remark: *It is sufficient to solve the BVP for both pure polarization cases, i.e. once with $A_\times = 0$ and once with $A_+ = 0$. Since the equations and boundary conditions are linear, the general solution is then a superposition of these two solutions. In case of a complex A_{12} the cross-polarization picks up a phase-factor γ, i.e. $\cos(\omega t + \gamma)$.*

The same factor can also be split off from the boundary conditions. They can then be written as three equations:

$$\begin{aligned} \sigma_{xx}|_{\partial P_x} = 0 \implies & (2\mu+\lambda)\partial_x\varphi^x|_{\partial P_x} + \lambda\partial_y\varphi^y|_{\partial P_x} = -\mu A_+ \\ \sigma_{yy}|_{\partial P_y} = 0 \implies & (2\mu+\lambda)\partial_y\varphi^y|_{\partial P_y} + \lambda\partial_x\varphi^x|_{\partial P_y} = \mu A_+ \\ \sigma_{xy}|_{\partial P} = 0 \implies & \partial_x\varphi^y|_{\partial P} + \partial_y\varphi^x|_{\partial P} = -A_\times \end{aligned} \tag{3.12}$$

Remark: *Is it justified to write the time-dependence as* $\cos(\omega t)$*, i.e. shouldn't be there a phase shift* α *relative to the gravitational wave so that the time-dependence looks like* $\cos(\omega t - \alpha)$*? There are two answers to this:*

- *For the one-dimensional harmonic oscillator the phase shift depends on the damping factor. In particular, there is no phase shift when there is no damping. As there is no damping in our model, we expect that there is no phase shift. This analogy is confirmed by the second argument.*

- *We consider the complex valued function* $\bar{u}^i$ *and take* $u^i = \Re(\bar{u}^i)$ *the physical solution to be only the real part. The separation ansatz then looks like this:* $\bar{u}^i = e^{i(\omega t-\alpha)}\bar{\varphi}^i$ *with a phase-shift* α*. But the phase factor* $e^{-i\alpha}$ *can also be included in the complex spatial part so that we have* $\bar{u}^i = e^{i\omega t}\bar{\varphi}^i$*. With this modified ansatz we get the same equation* (3.11)*. Since there are no factors i in the equation and it is linear, it is satisfied by the real and imaginary parts on their own. Looking at the boundary conditions* (3.10) *we see that* $e^{i\omega t}$ *can be factored out of the Cauchy-stress tensor* (3.8)*.* A_{ij} *is purely real, so that only the real part feels the influence of the gravitational wave. The imaginary part satisfies the boundary conditions for eigenmodes and hence it exists only for very specific GW-frequencies, namely the eigenfrequencies so that the solution is in general again real and hence there is no phase shift. This would change if damping is implemented.*

3.5 Scaling behaviour with L

In this section we argue that it is enough to solve equation (3.11) for $L = 1$ and arbitrary ω because the solution for all other L can be deduced from this. It is convenient to introduce 'scaled' coordinates $\bar{x}^i = \frac{x^i}{L}$ which implies for the derivatives $\partial_{x^i} = \frac{1}{L}\partial_{\bar{x}^i}$. Using this (and also dividing by ω^2) equation (3.11) becomes

$$\varphi^i + \frac{c_2^2}{\omega^2 L^2}\Delta\varphi^i + \frac{c_3^2}{\omega^2 L^2}\partial^i\partial_k\varphi^k = 0 \tag{3.13}$$

with the constants $c_1^2 = \frac{2\mu+\lambda}{\rho_0}, c_2^2 = \frac{\mu}{\rho_0}$ and $c_3^2 = c_1^2 - c_2^2 = \frac{\mu+\lambda}{\rho_0}$. In an abuse of notation we denote the new coordinates again by x^i (without the bar). Moreover, we define the normalized wave-speeds $\bar{c}_i = \frac{c_i}{\omega L}$ so that the PDE turns into

$$\varphi^i + \bar{c}_2^2\Delta\varphi^i + \bar{c}_3^2\partial^i\partial_k\varphi^k = 0. \tag{3.14}$$

Using the new coordinates in the boundary conditions and multiplying by a factor of L one obtains from equation (3.12)

$$\begin{aligned}(2\mu+\lambda)\partial_x\varphi^x|_{\partial P_x}+\lambda\partial_y\varphi^y|_{\partial P_x}&=-\mu LA_+\\(2\mu+\lambda)\partial_y\varphi^y|_{\partial P_y}+\lambda\partial_x\varphi^x|_{\partial P_y}&=\mu LA_+\\\partial_x\varphi^y|_{\partial P}+\partial_y\varphi^x|_{\partial P}&=-LA_\times\end{aligned}\tag{3.15}$$

where only the right hand side has changed. Now we assume that we have the solution to this BVP for some ω and L. Then we can scale the length by some factor a to aL and at the same time change the frequency to $\frac{\omega}{a}$. Since only the product ωL appears in (3.14) this doesn't change the solution. Moreover, the PDE is linear so that we can multiply the solution by the constant a and still have a solution. If one then puts $a\varphi^i$ into the left side of the boundary conditions (3.15) (which are also linear) one obtains a times the old right hand side, which is exactly what is needed to solve the new BVP.

3.6 Symmetry for pure plus-polarized Gravitational Wave

For the two special cases of pure plus or pure cross polarization the boundary value problem exhibits certain symmetries which we explore in this and the next section. Assuming that the problem is well-posed and hence the solution is unique (see [13]), this also leads to a symmetry in the solution. The PDE (3.11) can be rewritten in matrix form with the help of the differential operator $\mathcal{D}$

$$\mathcal{D}:=\begin{pmatrix}\omega^2+c_1^2\partial_x^2 & c_2^2\partial_y^2+c_3^2\partial_x\partial_y\\ \partial_x^2+c_3^2\partial_x\partial_y & \omega^2+c_1^2\partial_y^2\end{pmatrix}\tag{3.16}$$

as $\mathcal{D}\vec{\varphi}(x,y)=0$. There are two sets of boundary conditions in equation (3.12), namely $\sigma_{ij}n^j$ vanishing on the ∂_{P_x} boundary and $\sigma_{ij}n^j$ vanishing on the ∂_{P_y} boundary. Writing them in Matrix form gives:

$$\mathcal{B}_1\vec{\varphi}(x,y)|_{\partial P_x}:=\begin{pmatrix}(2\mu+\lambda)\partial_x & \lambda\partial_y\\ \partial_y & \partial_x\end{pmatrix}\vec{\varphi}(x,y)|_{\partial P_x}=\begin{pmatrix}-\mu A_+\\ -A_\times\end{pmatrix}=:\mathcal{C}_1\tag{3.17}$$

$$\mathcal{B}_2\vec{\varphi}(x,y)|_{\partial P_y}:=\begin{pmatrix}\partial_y & \partial_x\\ \lambda\partial_x & (2\mu+\lambda)\partial_y\end{pmatrix}\vec{\varphi}(x,y)|_{\partial P_y}=\begin{pmatrix}-A_\times\\ \mu A_+\end{pmatrix}=:\mathcal{C}_2\tag{3.18}$$

where the matrices $\mathcal{B}_1$ and $\mathcal{B}_2$ as well as the vectors $\mathcal{C}_1$ and $\mathcal{C}_2$ have been introduced. The symmetry transformation for the plus-polarization case (i.e. $A_\times=0$), which we investigate here, is given by the matrix

$$\mathcal{S}_+:=\begin{pmatrix}0 & -1\\ -1 & 0\end{pmatrix}.\tag{3.19}$$

First we look at the action of the symmetry transformation on the differential operator:

$$\mathcal{S}_+\mathcal{D}\mathcal{S}_+^T=\begin{pmatrix}\omega^2+c_1^2\partial_y^2 & \partial_x^2+c_3^2\partial_x\partial_y\\ c_2^2\partial_y^2+c_3^2\partial_x\partial_y & \omega^2+c_1^2\partial_x^2\end{pmatrix}\tag{3.20}$$

This looks again very similar to the original operator, except that the names of the x- and y variables have been exchanged. The unknown function turns, under this symmetry transformation, into

$$\mathcal{S}_+\vec{\varphi}(x,y) = \begin{pmatrix} -\varphi^y(x,y) \\ -\varphi^x(x,y) \end{pmatrix}. \tag{3.21}$$

We now define a new vector $\vec{\varphi}\,'(x,y) = -\vec{\varphi}(y,x)$ to deal with the renaming of variables. The boundary conditions transform as follows:

$$\mathcal{S}_+\mathcal{B}_1\mathcal{S}_+^T = \begin{pmatrix} \partial_x & \partial_y \\ \lambda\partial_y & (2\mu+\lambda)\partial_x \end{pmatrix} \tag{3.22}$$

$$\mathcal{S}_+\mathcal{B}_2\mathcal{S}_+^T = \begin{pmatrix} (2\mu+\lambda)\partial_y & \lambda\partial_x \\ \partial_x & \partial_y \end{pmatrix} \tag{3.23}$$

$$\mathcal{S}_+\mathcal{C}_1 = \begin{pmatrix} 0 \\ \mu A_+ \end{pmatrix} = \mathcal{C}_2 \qquad\qquad \mathcal{S}_+\mathcal{C}_2 = \begin{pmatrix} -\mu A_+ \\ 0 \end{pmatrix} = \mathcal{C}_1 \tag{3.24}$$

So under multiplication by $\mathcal{S}_+$ the boundary value problem gets transformed into itself(inserting $\mathcal{S}_+^T\mathcal{S}_+ = \mathcal{S}_+^2 = I$):

$$\begin{aligned} \mathcal{D}\vec{\varphi} = 0 &\longrightarrow \mathcal{S}_+\mathcal{D}\mathcal{S}_+^T\mathcal{S}_+\vec{\varphi} = \mathcal{D}\vec{\varphi}\,' = 0 \\ \mathcal{B}_1\vec{\varphi} = \mathcal{C}_1 &\longrightarrow \mathcal{S}_+\mathcal{B}_1\mathcal{S}_+^T\mathcal{S}_+\vec{\varphi} = \mathcal{S}_+\mathcal{C}_1 \iff \mathcal{B}_2\vec{\varphi}\,' = \mathcal{C}_2 \\ \mathcal{B}_2\vec{\varphi} = \mathcal{C}_2 &\longrightarrow \mathcal{S}_+\mathcal{B}_2\mathcal{S}_+^T\mathcal{S}_+\vec{\varphi}\,' = \mathcal{S}_+\mathcal{C}_2 \iff \mathcal{B}_1\vec{\varphi}\,' = \mathcal{C}_1 \end{aligned}$$

So we have a solution $\vec{\varphi}$ and a solution $\vec{\varphi}\,'$ to the same problem. But since the solution is unique this means that $\vec{\varphi} = \vec{\varphi}\,'$ and in particular

$$\varphi^y(x,y) = -\varphi^x(y,x). \tag{3.25}$$

To see why this is true, think of the plate at times $t = 0$ and half a period later at $t = \frac{T}{2}$. Because the plate is quadratic, someone looking at the plate from the x-direction at $t = 0$ should see the same behaviour as someone looking from the y-direction at $t = \frac{T}{2}$. The effect of the GW relative to the observer is the same in both cases so the response of the plate should be the same as well. The minus sign comes from the factor of $\cos(\frac{\omega T}{2}) = -1$ in front of φ.

Now assume the x-component of the PDE (3.11) is satisfied:

$$\omega^2\varphi^x(x,y) + c_1^2\partial_1^2\varphi^x(x,y) + c_2^2\partial_2^2\varphi^x(x,y) + c_3^2\partial_1\partial_2\varphi^y(x,y) = 0. \tag{3.26}$$

Then the other component of the equation is

$$\omega^2\varphi^y(x,y) + c_2^2\partial_1^2\varphi^y(x,y) + c_1^2\partial_2^2\varphi^y(x,y) + c_3^2\partial_1\partial_2\varphi^x)(x,y). \tag{3.27}$$

The partial derivatives can be related to the other component:

$$\partial_1\varphi^y(x,y) = -\partial_2\varphi^x(y,x) \qquad \partial_1^2\varphi^y(x,y) = -\partial_2^2\varphi^x(y,x) \tag{3.28}$$

$$\partial_2\varphi^y(x,y) = -\partial_1\varphi^x(y,x) \qquad \partial_2^2\varphi^y(x,y) = -\partial_1^2\varphi^x(y,x) \tag{3.29}$$

$$\partial_1\partial_2\varphi^x(x,y) = -\partial_2\partial_1\varphi^y(y,x). \tag{3.30}$$

Using this, (3.27) becomes

$$-\left[\omega^2\varphi^x(y,x) + c_2^2\partial_2^2\varphi^x(y,x) + c_1^2\partial_1^2\varphi^x(y,x) + \partial_2\partial_1\varphi^y(y,x)\right] = 0 \tag{3.31}$$

which is satisfied automatically if (3.26) is already satisfied. What's confusing about the symmetry is, that the role of x and y is exchanged. The way to think about this is that we have a function

$$\varphi^i : \mathbb{R}^2 \to \mathbb{R} \tag{3.32}$$

which takes two arguments and returns a number. What we call these arguments doesn't really matter. If we take the derivative with respect to one of the arguments $\partial_i\phi^j$ we again have a function with two arguments, and the name of these has no influence on the derivatives.

One can also use this to simplify the boundary conditions.

$$\begin{aligned}\sigma_{xx}|_{\partial P_x} &= \epsilon[(2\mu+\lambda)\partial_1\varphi^x(\pm\tfrac{1}{2},y) + \lambda\partial_2\varphi^y(\pm\tfrac{1}{2},y) + \mu A_+] \\ &= \epsilon[(2\mu+\lambda)\partial_1\varphi^x(\pm\tfrac{1}{2},y) - \lambda\partial_1\varphi^x(y,\pm\tfrac{1}{2}) + \mu A_+] = 0\end{aligned}$$

$$\begin{aligned}\sigma_{yy}|_{\partial P_y} &= \epsilon[(2\mu+\lambda)\partial_2\varphi^y(x,\pm\tfrac{1}{2}) + \lambda\partial_1\varphi^x(x,\pm\tfrac{1}{2}) - \mu A_+] \\ &= \epsilon[-(2\mu+\lambda)\partial_1\varphi^x(\pm\tfrac{1}{2},x) + \lambda\partial_1\varphi^x(x,\pm\tfrac{1}{2}) - \mu A_+] = 0\end{aligned}$$

These two expressions are the same (up to a minus sign), only in the first case the argument is called y, while in the second it's called x. So, if the condition that σ_{xx} vanishes on ∂P_x is fulfilled, then automatically also the condition that σ_{yy} vanishes on ∂P_y is satisfied. The condition of σ_{xy} vanishing on the whole boundary can be simplified similarly (and for now we keep the $A_\times$ term):

$$\begin{aligned}\sigma_{xy}|_{\partial P} &= \epsilon\mu[\partial_1\varphi^y(x,y) + \partial_2\varphi^x(x,y) + A_\times)] \\ &= \epsilon\mu[-\partial_2\varphi^x(y,x) + \partial_2\varphi^x(x,y) + A_\times)] = 0.\end{aligned}$$

This can be evaluated once at $x = \pm\frac{1}{2}$ and once at $y = \pm\frac{1}{2}$:

$$\begin{aligned}\sigma_{xy}(\pm\tfrac{1}{2},y) &= \epsilon\mu[-\partial_2\varphi^x(y,\pm\tfrac{1}{2}) + \partial_2\varphi^x(\pm\tfrac{1}{2},y) + A_\times)] = 0 \\ \sigma_{xy}(x,\pm\tfrac{1}{2}) &= \epsilon\mu[-\partial_2\varphi^x(\pm\tfrac{1}{2},x) + \partial_2\varphi^x(x,\pm\tfrac{1}{2}) + A_\times)] = 0.\end{aligned}$$

When these two cases are added to each other (with the same argument, $x = y$) the $\partial_2\varphi^x$ terms cancel and what remains is $2\epsilon\mu A_\times = 0$. This confirms that this symmetry only describes the case for pure plus-polarization, i.e. $A_\times = 0$. This boundary condition then becomes very simple:

$$\partial_2\varphi^x(\pm\tfrac{1}{2},s) = \partial_2\varphi^x(s,\pm\tfrac{1}{2}) \tag{3.33}$$

The partial derivative in y-Direction is symmetric in its arguments on the boundary.

Summary:
BVP before:

$$\mathcal{D}\vec{\varphi}(x,y) = 0, \quad \mathcal{B}_1\vec{\varphi}(x,y) = \mathcal{C}_1, \quad \mathcal{B}_2\vec{\varphi}(x,y) = \mathcal{C}_2 \tag{3.34}$$

Apply Symmetry $\mathcal{S}_+$ and rename x and y into each other.

$$\mathcal{S}_+ := \begin{pmatrix} 0 & -1 \\ -1 & 0 \end{pmatrix}, \qquad \vec{\varphi}\,'(x,y) = -\vec{\varphi}(y,x) \tag{3.35}$$

BVP after:

$$\mathcal{D}\vec{\varphi}\,'(x,y) = 0, \quad \mathcal{B}_1\vec{\varphi}\,'(x,y) = \mathcal{C}_1, \quad \mathcal{B}_2\vec{\varphi}\,'(x,y) = \mathcal{C}_2 \tag{3.36}$$

Due to the uniqueness of the solution $\vec{\varphi}\,'(x,y) = \vec{\varphi}(x,y)$ and

$$\varphi^y(x,y) = -\varphi^x(y,x). \tag{3.37}$$

So that the whole BVP is satisfied when

$$\omega^2\varphi^x(x,y) + c_1^2\partial_1^2\varphi^x(x,y) + c_2^2\partial_2^2\varphi^x(x,y) - c_3^2\partial_1\partial_2\varphi^x(y,x) = 0. \tag{3.38}$$

$$(2\mu+\lambda)\partial_1\varphi^x(\pm\tfrac{1}{2},y) - \lambda\partial_1\varphi^x(y,\pm\tfrac{1}{2}) + \mu A_+ = 0 \tag{3.39}$$

$$\partial_2\varphi^x(\pm\tfrac{1}{2},s) = \partial_2\varphi^x(s,\pm\tfrac{1}{2}) \tag{3.40}$$

are solved.

This symmetry is used in section 3.8 to find a solution for the low frequency limit. For the general analysis in the following chapters it is not useful, because it describes only special cases, and the simplifications it would bring, are not enough to do the whole analysis twice.

3.7 Symmetry for purely cross-Polarized Gravitational Wave

In the case with a purely cross-polarized Gravitational Wave the symmetry looks similar, except for the missing minus sign in front:

$$\mathcal{S}_\times := \begin{pmatrix} 0 & 1 \\ 1 & 0 \end{pmatrix}. \tag{3.41}$$

The matrices $\mathcal{D}, \mathcal{B}_1$ and $\mathcal{B}_2$ transform in the same way as before, since the two factors of -1 cancel each other. Only the transformed vectors look different:

$$\vec{\varphi}\,'(x,y) = \mathcal{S}_\times\vec{\varphi}(y,x) = \begin{pmatrix} \varphi^y(y,x) \\ \varphi^x(y,x) \end{pmatrix} \tag{3.42}$$

$$\mathcal{S}_\times \mathcal{C}_1 = \begin{pmatrix} -A_\times \\ 0 \end{pmatrix} = \mathcal{C}_2 \qquad \mathcal{S}_\times \mathcal{C}_2 = \begin{pmatrix} 0 \\ -A_\times \end{pmatrix} = \mathcal{C}_1 \tag{3.43}$$

By the same argument as before (BVP gets transformed into itself and uniqueness of solution) we again have $\vec{\varphi} = \vec{\varphi}'$ and hence

$$\varphi^y(x,y) = \varphi^x(y,x). \tag{3.44}$$

3.8 Small frequency limit for plus-Polarization

Based on the Symmetry of the previous section and the assumption that $\varepsilon := \frac{\omega L}{c_1}$ is small, we want to find a approximate solution in form of a polynomial up to third degree. It is important to note that this ε is different from the ϵ used to describe the strength of the gravitational wave.

For an interpretation of ε we notice that $T_c = \frac{L}{c_1}$ is the time it takes a sound wave traveling with speed c_1 to cross the plate. Then we express ω in terms of the gravitational wave period $\omega = \frac{2\pi}{T_{GW}}$ so that epsilon becomes $\epsilon = 2\pi \frac{T_c}{T_{GW}}$ the ratio of these two time intervals and we call it period-ratio. Thus, the approximation applies as long as the crossing time is small compared to the gravitation wave period. This can be the case for a) small frequencies, b) large plates or c) very stiff materials, i.e. large c_1.

We want the solution to be accurate to second order in the period-ratio so we ignore terms $O(\varepsilon^3)$ and higher. The guess for the solution is

$$\varphi^x(x,y) = -Ax + Bxy^2 + Cx^3 \tag{3.45}$$

where A, B and C are constants to be determined by the BVP. By using the symmetry the other component is then given by

$$\varphi^y(x,y) = Ay - Bx^2y - Cy^3. \tag{3.46}$$

The PDE given in a convenient form for this problem reads(when using the normalized coordinates such that $x, y \in [-\frac{1}{2}, \frac{1}{2}]$)

$$\tfrac{\omega^2 L^2}{c_1^2}\varphi^x(x,y) + \partial_1^2\varphi^x(x,y) + \tfrac{c_2^2}{c_1^2}\partial_2^2\varphi^x(x,y) - \tfrac{c_3^2}{c_1^2}\partial_1\partial_2\varphi^x(y,x) = 0. \tag{3.47}$$

To get the boundary conditions in terms of the same constants we divide them by ρ and use that $\frac{\lambda}{\rho} = c_1^2 - 2c_2^2$. The condition $\sigma_{xx}(\pm\frac{1}{2}, y) = 0$ then reads

$$c_1^2\partial_1\varphi^x(\pm\tfrac{1}{2}, y) + (c_1^2 - 2c_2^2)\partial_2\varphi^y(\pm\tfrac{1}{2}, y) = \tag{3.48}$$

$$= c_1^2(-A + By^2 + \tfrac{3}{4}C) + (c_1^2 - 2c_2^2)(A - \tfrac{1}{4}B - 3Cy^2) = -Lc_2^2A_+. \tag{3.49}$$

Equating the coefficients in front of powers of y we find the following:

$$
\begin{aligned}
y^2: \quad & c_1^2 B - 3C(c_1^2 - 2c_2^2) = 0 && \Longrightarrow \boxed{B = 3(1 - 2\tfrac{c_2^2}{c_1^2})C} \\
y^0: \quad & -2c_2^2 A + \tfrac{3}{4} C c_1^2 - (c_1^2 - 2c_2^2)\tfrac{1}{4} B = -L c_2^2 A_+ \\
& -2c_2^2 A + \frac{3}{4} C c_1^2 \left(1 - (1 - 2\tfrac{c_2^2}{c_1^2})^2\right) = -L c_2^2 A_+ \\
& -A + \frac{3}{8} C \tfrac{c_1^2}{c_2^2} \left(4\tfrac{c_2^2}{c_1^2} - 4\tfrac{c_2^4}{c_1^4}\right) = -\tfrac{L}{2} A_+ \\
& \boxed{A = \tfrac{L}{2} A_+ + \tfrac{3}{2} C \left(1 - \tfrac{c_2^2}{c_1^2}\right)}
\end{aligned}
$$

The other boundary condition $\sigma_{xy}|_{\partial P} = 0$ is satisfied because

$$\sigma_{xy}(x, y) = \epsilon\mu \left(\partial_x \varphi^y + \partial_y \varphi^x + A_\times\right) = \epsilon\mu \left(-2Bxy + 2Bxy + 0\right) = 0. \tag{3.50}$$

Now we go back to PDE (3.47) to find the last missing constant C:

$$\varepsilon^2[-Ax + Bxy^2 + Cx^3] + 6Cx + \tfrac{c_2^2}{c_1^2} 2Bx - \tfrac{c_3^2}{c_1^2} 2Bx = 0. \tag{3.51}$$

Again we compare the coefficients:

$$
\begin{aligned}
x^3: \quad & \varepsilon^2 C = 0 && \Longrightarrow \boxed{C \leq O(\varepsilon)} \\
xy^2: \quad & \varepsilon^2 B = 0 && \Longrightarrow \boxed{B \leq O(\varepsilon)} \\
x: \quad & -A\varepsilon^2 + 6C + 2B\tfrac{c_2^2 - c_3^2}{c_1^2} = 0 \\
& -\tfrac{L}{2} A_+ \varepsilon^2 + \tfrac{3}{2} \varepsilon^2 C \left(1 - \tfrac{c_2^2}{c_1^2}\right) + 6C + 6C(1 - 2\tfrac{c_2^2}{c_1^2})\tfrac{2c_2^2 - c_1^2}{c_1^2} = 0 \\
& 6C \left(1 - (1 - 4\tfrac{c_2^2}{c_1^2} + 4\tfrac{c_2^4}{c_1^4})\right) = \tfrac{L}{2} A_+ \qquad (C\varepsilon^2 \leq O(\varepsilon^3)) \\
& \boxed{C = \tfrac{L}{48} A_+ \varepsilon^2 \tfrac{c_1^2}{c_2^2} \tfrac{c_1^2}{c_3^2}}
\end{aligned}
$$

A_+ is only the relative amplitude for the polarization of the GW so it is $O(1)$. L is the dimension of the plate which we also expect to be of $O(1)$. The same goes for the ratio of the wave speeds. Therefore $C = O(\varepsilon^2)$ and the condition $C \leq O(\varepsilon)$ are both satisfied. B is related to C by $B = 3(1 - 2\frac{c_2^2}{c_1^2})C$. The factor between them is (in absolute value) less than 3 so $B \leq O(\varepsilon)$ is also satisfied.

One can now insert all the constants into equation (3.45) to obtain the final form

$$\varphi^x(x, y) = \tfrac{L}{2} A_+ \left(-x + \tfrac{1}{24} \varepsilon^2 \tfrac{c_1^2}{c_2^2} \tfrac{c_1^2}{c_3^2} \left[-\tfrac{3}{2} x \left(1 - \tfrac{c_2^2}{c_1^2}\right) + 3\left(1 - 2\tfrac{c_2^2}{c_1^2}\right) xy^2 + x^3\right]\right). \tag{3.52}$$

It is very intuitive, that the solution is proportional to the amplitude of the GW A_+. Also the linear dependence on L seems reasonable, the larger the plate, the larger the deformation. This also agrees with the scaling behaviour from section 3.5. The dominating term is the linear behaviour $-\frac{L}{2} A_+ x$, and then there is a small correction term of order $O(\epsilon^2)$.

3.9 Small frequency limit for cross-Polarization

After being successful in finding a polynomial solution for the limit of a small period-ratio ε in the case of pure plus-polarization, we tried to do the same for a cross-polarized wave. After a computer assisted exhaustive search for polynomials up to order 5 in x and y we didn't find any solution accurate up to third order in the period ration $O(\varepsilon^3)$.

There is only a very simple solution accurate up to order $O(\varepsilon^2)$:

$$\varphi^x = -\tfrac{A_\times}{2} y \tag{3.53}$$

$$\varphi^y = -\tfrac{A_\times}{2} x \tag{3.54}$$

Chapter 4

Bulk Solutions and Eigenmodes

This chapter starts by trying to solve the BVP (3.11) and (3.12) using a finite sum of exponential factors. This yields two sets of solutions, p-waves and s-waves, to the PDE. It turns out that these can't be used to satisfy the boundary conditions, which leads to a modified spectral method as discussed in chapter 5.

In the case where there is no gravitational wave, one of the solutions can satisfy the boundary conditions and this leads to s-wave eigenmodes, which will be described in the last section of this chapter.

4.1 Bulk Solutions

The idea here is to write $\vec{\varphi}$ as a product of an amplitude vector and an exponential:

$$\varphi^j(x,y) = \vec{a}e^{i\vec{k}\cdot\vec{x}}. \tag{4.1}$$

For now, there are no restrictions on $\vec{a}$ or $\vec{k}$. Plugging this ansatz into (3.11) and this leads to an algebraic relation for $\vec{a}$:

$$\left(k^2\frac{\mu}{\rho_0} - \omega^2\right)a^j + \frac{\mu+\lambda}{\rho_0}k^j k_l a^l = 0 \tag{4.2}$$

where $k = |\vec{k}|$. This can also be expressed in matrix form:

$$B\vec{a} = \begin{pmatrix} (k^2\frac{\mu}{\rho_0} - \omega^2) + \frac{\mu+\lambda}{\rho_0}k_x^2 & \frac{\mu+\lambda}{\rho_0}k_x k_y \\ \frac{\mu+\lambda}{\rho_0}k_x k_y & (k^2\frac{\mu}{\rho_0} - \omega^2) + \frac{\mu+\lambda}{\rho_0}k_y^2 \end{pmatrix}\begin{pmatrix} a^x \\ a^y \end{pmatrix} = 0 \tag{4.3}$$

Since we want a solution which is not the trivial one $\vec{a} = 0$, we require that the determinant of B vanishes. There are two values of k, and the corresponding 0-Eigenvectors of B, for which this is the case :

- p-waves: $\omega = c_1\kappa$ with $c_1^2 = \frac{2\mu+\lambda}{\rho_0}$. Here the wave vector is called $\vec{\kappa}$ to distinguish it from the second case. The matrix then simplifies to

  $$\frac{\mu+\lambda}{\rho_0}\begin{pmatrix} -\kappa_y^2 & \kappa_x\kappa_y \\ \kappa_x\kappa_y & -\kappa_x^2 \end{pmatrix}\begin{pmatrix} a^x \\ a^y \end{pmatrix} = 0$$

  and is solved by vectors $\vec{a}$ which are co-linear with $\vec{\kappa}$. This means that the oscillations are in the direction of propagation of the wave.

- s-waves: $\omega = c_2 k$ with $c_2^2 = \frac{\mu}{\rho_0}$. In this case we call the amplitude b^i instead of a^i to easier distinguish between the two cases. Here the matrix becomes

$$\frac{\mu+\lambda}{\rho_0}\begin{pmatrix} k_x^2 & k_x k_y \\ k_x k_y & k_y^2 \end{pmatrix}\begin{pmatrix} b^x \\ b^y \end{pmatrix} = 0$$

  and is solved when $\vec{b}\cdot\vec{k} = 0$, so $\vec{b}$ is normal to $\vec{k}$. The oscillations are then orthogonal to the direction of propagation of the wave.

These two sets form solutions to the PDE, before considering the boundary (hence the name bulk solutions). For a given gravitational wave frequency, the magnitude of the wave vector is now restricted to possible values, given by either one of the two dispersion relations. The direction of the wave vector, is still free to choose. One could imagine that the general solution can be written as a "ring integral" over all possible directions. As it is not clear how to deal with such an integral, we consider finite combinations of s-wave and p-wave terms.

When one inserts these two into the boundary conditions (3.12), one quickly discovers that they cannot be used to give the correct right hand side. The left hand side can be made either zero, by choosing the $\vec{k}$-vectors so that the cosines and sines have a zero on the boundary, or there remains some dependence on the position on the boundary. But there is no way to get a nonzero constant value. This is explained further in section 4.3. But first we look closer at the two types of waves and investigate their relation to the Helmholtz Decomposition.

4.2 Relation to the Helmholtz Decomposition

According to a weak formulation of Helmholtz's theorem, any square-integrable vector-field $\vec{u}$ can be decomposed into a divergence-free (transverse) part $\nabla\cdot\vec{u}_T = 0$ and a curl-free (longitudinal) part $\nabla\times\vec{u}_L = 0$, see [6]. Moreover, the curl-free part may be written as the gradient of a scalar field q and the divergence-free part as the curl of a vector field $\vec{A}$:

$$\vec{u} = \vec{u}_L + \vec{u}_T = \nabla q + \nabla\times\vec{A}. \tag{4.4}$$

By imposing boundary conditions on q and $\vec{A}$ the decomposition can be made unique. Otherwise it is possible to add/subtract the gradient $\nabla\psi$ of a harmonic function $\Delta\psi = 0$ to the longitudinal/transverse part without changing the vector field, while still preserving their properties.

This decomposition can be used to rewrite the PDE (3.9).

$$-\partial_t^2(u_L^i + u_T^i) + \frac{\mu}{\rho_0}\Delta(u_L^i + u_T^i) + \frac{\mu+\lambda}{\rho_0}\partial^i\partial_k(u_L^k + u_T^k) = 0 \tag{4.5}$$

Now we can use the properties of u_L and u_T. Since u_T is divergence-free in the last term $\partial_k u_T^k$ vanishes. Moreover we write $u_L^i = \partial^i\phi$ and commute the partial derivatives as follows:

$$\frac{\mu}{\rho}\partial_k\partial^k\partial^i\phi + \frac{\mu+\lambda}{\rho}\partial^i\partial_k\partial^k\phi = \frac{2\mu+\lambda}{\rho}\partial_k\partial^k u_L^i = c_1^2\partial_k\partial^k u_L^i \tag{4.6}$$

Introducing the wave speeds $c_1^2 = \frac{2\mu+\lambda}{\rho}$ for p-waves and $c_2^2 = \frac{\mu}{\rho}$ for s-waves the equation splits into the sum of two wave equations:

$$\left[-\partial_t^2 u_T^i + c_2^2 \Delta u_T^i\right] + \left[-\partial_t^2 u_L^i + c_1^2 \Delta u_L^i\right] = 0. \tag{4.7}$$

Solutions to the wave equation have the form $\cos(\omega t)\vec{a}e^{i\vec{k}\cdot\vec{x}}$ with $\omega^2 = c_i^2 k^2$. Applying the conditions of vanishing divergence and curl respectively, we recover the same conditions we found in the previous section:

- p-wave: $\omega = c_1\kappa$

  $$(\nabla \times u_L^i)_z = \partial_x u_L^y - \partial_y u_L^x = i\cos(\omega t)e^{i\vec{\kappa}\cdot\vec{x}}(\kappa_x a^y - \kappa_y a^x) = 0$$

  This is satisfied if $\vec{a}$ is collinear with $\vec{\kappa}$.

- s-wave: $\omega = c_2 k$

  $$\partial_i u_T^i = \partial_i \cos(\omega t)\vec{b}e^{i\vec{k}\cdot\vec{x}} = ik_i b^i u_T^i = 0$$

  So u_T being divergence-free is equivalent to $\vec{k}\cdot\vec{b} = 0$.

So p waves are curl-free while s-waves are divergence-free and hence volume preserving.

4.3 Solutions without GW: Eigenmodes

Without a GW ($h_{ij} = 0$), the differential equations we want to solve stay the same, but the boundary conditions change to

$$\begin{aligned} \sigma_{xx}|_{\partial P_x} &= \epsilon[(2\mu+\lambda)\partial_x u^x + \lambda\partial_y u^y] &&= 0 \\ \sigma_{yy}|_{\partial P_y} &= \epsilon[(2\mu+\lambda)\partial_y u^y + \lambda\partial_x u^x] &&= 0 \\ \sigma_{xy}|_{\partial P} &= \epsilon\mu[\partial_x u^y + \partial_y u^x)] &&= 0 \end{aligned} \tag{4.8}$$

We can again separate off the time dependence $u^i(t,x,y) = \cos(\omega t)\varphi^i(x,y)$, though now ω is no longer the frequency of the GW. Instead it is connected to k or κ through the dispersion relations $\omega = c_1\kappa$ or $\omega = c_2 k$. These belong to p-waves and s-waves respectively and are considered separately in the following sections. The idea here is, that we choose the wave vector $\vec{k}$ or $\vec{\kappa}$ freely, so as to satisfy the boundary conditions, instead of it being restricted by the GW.

4.3.1 s-wave Eigenmodes

Here the solutions to the PDE have the form $\vec{b}_{\vec{k}}\, e^{i\vec{k}\cdot\vec{x}}$ with the condition that $\vec{b}_{\vec{k}}\cdot\vec{k} = 0$. This also means that $\vec{\varphi}$ is divergence-free. To make the solution real, we combine it with the wave traveling in the opposite direction $\vec{b}_{-\vec{k}}\, e^{-i\vec{k}\cdot\vec{x}}$ and write the result as

$$\varphi^i = b^i(A\cos(\vec{k}\cdot\vec{x}) + B\sin(\vec{k}\cdot\vec{x})). \tag{4.9}$$

Thereby the k-space can be restricted to the right half-plane $k_x \geq 0$. The vector $\vec{k}$ and the constants A and B are otherwise free to choose. The direction of $\vec{b}$ is fixed by the condition $\vec{b} \cdot \vec{k} = 0$ and its length is included in the constants A and B, i.e. $\vec{b} = (k_y, -k_x)$. With the help of trigonometric identities the cosines and sines can be written as products:

$$\cos(\vec{k} \cdot \vec{x}) = \cos(k_x x)\cos(k_y y) - \sin(k_x x)\sin(k_y y)$$

$$\sin(\vec{k} \cdot \vec{x}) = \sin(k_x x)\cos(k_y y) + \cos(k_x x)\sin(k_y y).$$

It might be the case that a combination of more such solutions is needed to satisfy the boundary conditions. For the separation of the time dependence to still work they all need to have the same magnitude of $\vec{k}$ (and therefore also ω), while the direction is still free. Which $\vec{k}$-vectors should we combine? Looking at one boundary, e.g. $x = \frac{L}{2}$, we have a linear combination of $\cos(k_y y)$ and $\sin(k_y y)$ which has to vanish. The only other $\vec{k}$ which can help to cancel these terms are the ones with the same k_y. The same follows for k_x from the condition on the boundary $y = \frac{L}{2}$. So only two $\vec{k}$ vectors can be combined helpfully:

$$\vec{k}_1 = (k_x, k_y) \text{ and } \vec{k}_2 = (k_x, -k_y). \tag{4.10}$$

Putting this all together φ^i can be written as

$$\vec{\varphi} = \begin{pmatrix} k_y \\ -k_x \end{pmatrix} \left(\tilde{A}\cos(\vec{k}_1 \cdot \vec{x}) + \tilde{B}\sin(\vec{k}_1 \cdot \vec{x}) \right) + \begin{pmatrix} k_y \\ k_x \end{pmatrix} \left(\tilde{C}\cos(\vec{k}_2 \cdot \vec{x}) + \tilde{D}\sin(\vec{k}_2 \cdot \vec{x}) \right) \tag{4.11}$$

and then, using trigonometric formulas and the notation $\cos(k_x x) = c_x$ and similar, this becomes

$$\begin{aligned} \varphi_x &= k_y \left(A c_x c_y + B s_x s_y + C s_x c_y + D c_x s_y \right) \\ \varphi_y &= k_x \left(B c_x c_y + A s_x s_y - D s_x c_y - C c_x s_y \right). \end{aligned} \tag{4.12}$$

Since $\vec{\varphi}$ is divergence free, the boundary conditions reduce to

$$\begin{aligned} \sigma_{xx}|_{\partial P_x} &= \epsilon 2\mu \partial_x u^x &&= 0 \\ \sigma_{yy}|_{\partial P_y} &= \epsilon 2\mu \partial_y u^y &&= 0 \\ \sigma_{xy}|_{\partial P} &= \epsilon\mu[\partial_x u^y + \partial_y u^x] &&= 0. \end{aligned} \tag{4.13}$$

Evaluating the first condition with the help of Mathematica for ∂P_x at $(\pm\frac{L}{2}, \pm y)$ and adding the four terms with different sign combinations $(++++,\ +++-,\ ++-+,\ +--+,\ +---)$ gives four simpler, necessary but not sufficient conditions:

$$8Ck_x k_y \mu \cos\left(\frac{k_x L}{2}\right)\cos\left(k_y y\right) = 0 \tag{4.14}$$

$$8Bk_x k_y \mu \cos\left(\frac{k_x L}{2}\right)\sin\left(k_y y\right) = 0 \tag{4.15}$$

$$8Ak_xk_y\mu \sin\left(\frac{k_xL}{2}\right)\cos\left(k_y y\right) = 0 \tag{4.16}$$

$$8Dk_xk_y\mu \sin\left(\frac{k_xL}{2}\right)\sin\left(k_y y\right) = 0. \tag{4.17}$$

Doing something similiar with the other conditions/boundaries and trying to solve them all, results in two possible eigenmode solutions:

$$\begin{aligned} A = B = C = 0, \quad k_x = k_y = \frac{2\pi}{L}n \\ A = B = D = 0, \quad k_x = k_y = \frac{\pi}{L}(2n+1). \end{aligned} \tag{4.18}$$

Therefore the whole solution $\vec{u}$ can be written as:

'Quadratic' s-wave Eigenmodes:

- For n even:

$$\begin{aligned} u^x = \quad & \cos(\omega t)\ \cos(\frac{\pi}{L}nx)\ \sin(\frac{\pi}{L}ny) \\ u^y = - \quad & \cos(\omega t)\ \sin(\frac{\pi}{L}nx)\ \cos(\frac{\pi}{L}ny). \end{aligned} \tag{4.19}$$

- For n odd:

$$\begin{aligned} u^x = - \quad & \cos(\omega t)\ \sin(\frac{\pi}{L}nx)\ \cos(\frac{\pi}{L}ny) \\ u^y = \quad & \cos(\omega t)\ \cos(\frac{\pi}{L}nx)\ \sin(\frac{\pi}{L}ny). \end{aligned} \tag{4.20}$$

Figure 4.1 shows the eigenmodes for $n = 1$ and $n = 2$. What's special about these is, that the corners always stay fixed.

4.3.2 p-wave Eigenmodes

Here we follow a similar procedure as we did above for the s-wave eigenmodes. The difference is, that the solutions now have the form $\vec{a}_{\vec{\kappa}}\ e^{i\vec{\kappa}\cdot\vec{x}}$ with $\vec{a}_{\vec{\kappa}} || \vec{\kappa}$. Hence the solution can be written as

$$\vec{\varphi} = \begin{pmatrix} \kappa_x \\ \kappa_y \end{pmatrix}\left(\tilde{A}\cos(\vec{\kappa}_1\cdot\vec{\kappa}) + \tilde{B}\sin(\vec{\kappa}_1\cdot\vec{x})\right) + \begin{pmatrix} \kappa_x \\ -\kappa_y \end{pmatrix}\left(\tilde{C}\cos(\vec{\kappa}_2\cdot\vec{x}) + \tilde{D}\sin(\vec{\kappa}_2\cdot\vec{x})\right)$$

or

$$\begin{aligned} \varphi_x &= \kappa_x\left(Ac_xc_y + Bs_xs_y + Cs_xc_y + Dc_xs_y\right) \\ \varphi_y &= \kappa_y\left(-Bc_xc_y - As_xs_y + Ds_xc_y + Cc_xs_y\right). \end{aligned} \tag{4.21}$$

Here the boundary conditions don't simplify (since the divergence doesn't vanish) but can again be combined to simpler, necessary but not sufficient conditions as above. But when one tries to solve them all, the only remaining solution is $\varphi_x = \varphi_y = 0$. This would suggest, that there can't be any pure p-wave eigenmodes.

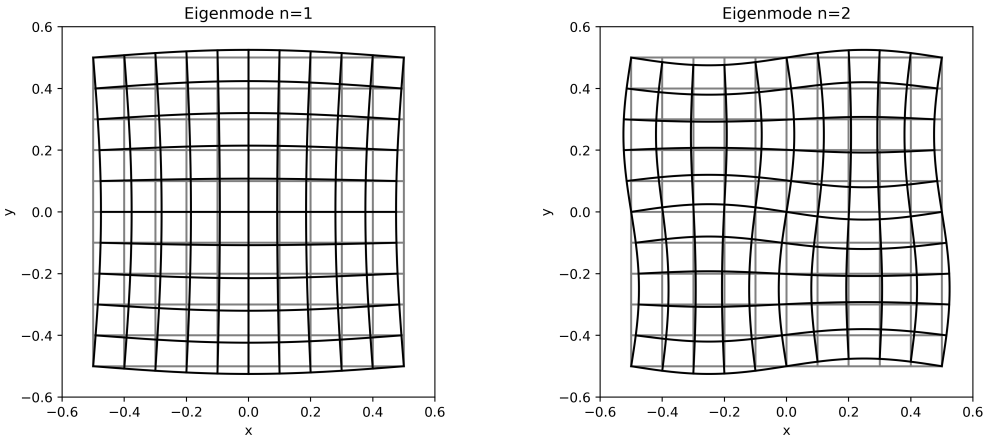

Figure 4.1: Grid plots of the first two eigenmodes. The grey lines represent the undisturbed plate, the black lines the deformed one. The deformation is not to scale.

4.3.3 Mixed Eigenmodes

So far we saw that there are s-wave eigenmodes, but no pure p-wave eigenmodes. The next logical step is to ask whether a finite combination of both gives a solution. The answer lies in the following theorem.

Theorem: Consider solutions $\vec{\varphi}$ made up of the building blocks $\vec{b}_{\vec{k}}\ e^{i\vec{k}\cdot\vec{x}}$, $\vec{b}_{\vec{k}} \cdot \vec{k} = 0$ (s-waves) and $\vec{a}_{\vec{\kappa}}\ e^{i\vec{\kappa}\cdot\vec{x}}$,$\vec{a}_{\vec{\kappa}} || \vec{\kappa}$ (p-waves). The magnitude of the wave vectors is given by the dispersion relations $\omega = c_1\kappa$ and $\omega = c_2 k$ while the direction is still free to choose. Then there exists no finite sum of such terms which satisfies the boundary conditions (4.8), except for pure s-wave eigenmodes (4.3.1).

Before proving this statement a comment about why it is enough to consider only one frequency ω, i.e. the spatial part of solutions $\vec{u} = \cos(\omega t)\vec{\varphi}$ with one fixed ω: Assume that the spatial part of two such solutions $\vec{\varphi}_1$ and $\vec{\varphi}_2$ together satisfies the boundary conditions at one time. Because they have different time dependence, they change differently so that at other times they can't cancel each other out anymore. Therefore, each one separately has to satisfy the boundary conditions. But then we are back to the case, where we consider only one frequency ω.

Proof. First note, that since $c_1 > c_2$ the relation $\kappa < k$ for the magnitudes of the wave vectors holds. Since we do not want a pure s-wave solution, $\vec{\varphi}$ contains at least one p-wave term $\vec{a}_{\vec{\kappa}}\ e^{i\vec{\kappa}\cdot\vec{x}}$. In the previous section (equation (4.21)) we saw, that the most general such term looks as follows

$$\begin{aligned} \varphi_x &= \kappa_x \left(A c_x c_y + B s_x s_y + C s_x c_y + D c_x s_y\right) \\ \varphi_y &= \kappa_y \left(-B c_x c_y - A s_x s_y + D s_x c_y + C c_x s_y\right) \end{aligned} \tag{4.22}$$

for some constants A, B, C, D. This leads to a σ_{xx} component, evaluated at the $x = \frac{1}{2}$ boundary which has the following form

$$\sigma_{xx}\left(\frac{L}{2}, y\right) = E\cos(\kappa_y y) + F\sin(\kappa_y y) \tag{4.23}$$

with some constants E and F. It doesn't satisfy the boundary condition on its own, so we need to add a s-wave term with the same y-component $k_y = \kappa_y$. But the k_x component of the s-wave is then given by

$$k_x = \pm\sqrt{\left(\frac{\omega}{c_2}\right)^2 - k_y^2}. \tag{4.24}$$

As $\vec{k}$ is longer than $\vec{\kappa}$ there is no other possible p-wave with the same κ_x component, so that this term has to satisfy the boundary conditions on ∂P_y on its own, in particular:

$$\sigma_{yy}\left(x, \frac{L}{2}\right) \pm \sigma_{yy}\left(x, -\frac{L}{2}\right) = 0. \tag{4.25}$$

The general form of such a s-wave then looks like (4.12) and if we insert the resulting CS-tensor in the above relation two necessary conditions follow:

$$\begin{aligned} 4k_x k_y \mu \cos\left(\frac{k_y L}{2}\right)\left(A\sin\left(k_x x\right) - C\cos\left(k_x x\right)\right) &= 0 \\ 4k_x k_y \mu \sin\left(\frac{k_y L}{2}\right)\left(D\sin\left(k_x x\right) - B\cos\left(k_x x\right)\right) &= 0. \end{aligned}$$

This has to be true for all x. Since $\vec{k}$ is already fixed, only the constants A, B, C and D can be used to satisfy these conditions. But in general the only possibility to do this is $A = B = C = D = 0$. Therefore there is no s-wave and we are back at a pure p-wave. But we already saw in the previous section that this doesn't satisfy the boundary conditions. □

This concludes our investigation of eigenmode-solutions. In terms of finite sums there are only the quadratic s-wave eigenmodes (4.3.1). To find more eigenmodes the whole Fourier-Series would need to be used.

Chapter 5

Delta Corrected Spectral Method

So far, we found out that the PDE (3.9) is solved by s-waves and p-waves. In section 4.3 we found one set of solutions which solved the boundary conditions for the case without a gravitational wave, i.e. the right side of (3.15) vanishes. That was only possible, because ω is not dictated by the GW and hence $\vec{k}$ can be chosen such, that a cosine or sine has a zero at the boundary. But there is no way to do this with a constant value on the right side of (3.15), i.e. with GW.

This leads to the idea to write the solution as a Fourier series. But in general the solution won't be periodic on the plate. Taking the derivative of a Fourier series of a function, which is not periodic is problematic, especially at the boundary. This is explained further in this chapter. First in the one-dimensional case, where it is easier to grasp and visualize what is going on. Then it is generalized to two dimensions and applied to the elastic plate.

5.1 Illustration of the Problem in 1D

We want to solve (3.14), which in 1D reduces to

$$\varphi + \bar{c}_1^2 \partial_x^2 \varphi = 0. \tag{5.1}$$

and we want to solve it on $\left[-\frac{1}{2}, \frac{1}{2}\right]$. We call the constant $\alpha^2 = \bar{c}_1^2 = \frac{c_1^2}{L^2\omega^2}$. Notice, that this is the inverse of the period-ratio appearing in section 3.8. The equation now looks like a simple harmonic oscillator for which we know the solution:

$$\varphi(x) = A\ \cos(\tfrac{x}{\alpha}) + B\ \sin(\tfrac{x}{\alpha}). \tag{5.2}$$

Moreover, the boundary conditions now fix the value of the derivative at the boundary

$$\sigma_{xx}|_{x=\pm\frac{1}{2}} = 0 \implies \varphi'|_{x=\pm\frac{1}{2}} = -\frac{A_+ L c_2^2}{c_1^2} = -\beta \tag{5.3}$$

which defines the constant $\beta = \frac{A_+ L c_2^2}{c_1^2}$. From this follows the solution for the boundary value problem (cf. [7])

$$\varphi(x) = -\alpha\ \beta\ \sec(\tfrac{1}{2\alpha})\ \sin(\tfrac{x}{\alpha}). \tag{5.4}$$

But we want to learn something about how to solve the problem using Fourier series so we make the ansatz for the Fourier series, of φ:

$$F[\varphi](x) = \sum_{n=0}^{\infty} a_n \ \cos(2\pi n x) + \sum_{n=1}^{\infty} b_n \ \sin(2\pi n x) \tag{5.5}$$

with the Fourier coefficients given by the integrals

$$\begin{aligned} a_0 &= \int_{-\frac{1}{2}}^{\frac{1}{2}} dx \ \varphi(x) \\ a_n &= 2\int_{-\frac{1}{2}}^{\frac{1}{2}} dx \ \varphi(x) \ \cos(2\pi n x) \\ b_n &= 2\int_{-\frac{1}{2}}^{\frac{1}{2}} dx \ \varphi(x) \ \sin(2\pi n x) \end{aligned} \tag{5.6}$$

Ideally we would just substitute this ansatz into the equation we want to solve, calculating the derivatives of the series term by term, and then require the coefficients of the sine and cosine series to vanish. But the solution is not necessarily periodic on $[-\frac{1}{2}, \frac{1}{2}]$, so the Fourier series represents the periodic continuation of the function, see Figure 5.1. The periodic continuation in general has a jump at the boundary. At such points the Fourier series $F[\varphi]$ takes the average of both one-sided limits, which correspond to the values of the original function. The size of the jump is denoted by $d_0 = \varphi(\frac{1}{2}) - \varphi(-\frac{1}{2})$. Then the correct function values can be recovered by the following relation:

$$\varphi(x) = \begin{cases} F[\varphi](x) & x \in (-\frac{1}{2}, \frac{1}{2}) \\ F[\varphi](\frac{1}{2}) \pm \frac{d_0}{2} & x = \pm\frac{1}{2} \end{cases} \tag{5.7}$$

The first derivative is again not necessarily periodic, and therefore has a jump $d_1 = \varphi'(\frac{1}{2}) - \varphi'(-\frac{1}{2})$ at the boundary. It would be nice if the derivative of the Fourier series corresponds to the Fourier series of the derivative: $\partial_x F[\varphi] \stackrel{?}{=} F[\varphi']$. But we saw that the Fourier series has a jump of size d_0. When taking the derivative of a jump one obtains a delta function, i.e. there is a delta function in $\partial_x F[\varphi]$. To cancel this unwanted behaviour we add another delta function multiplied by the jump size d_0 and expect to get the correct Fourier series:

$$F[\varphi'] = \partial_x F[\varphi] + d_0 F[\delta(x - \tfrac{1}{2})]. \tag{5.8}$$

To recover the values of $\varphi'(x)$ we need a similar relation as above:

$$\varphi'(x) = \begin{cases} F[\varphi'](x) & x \in (-\frac{1}{2}, \frac{1}{2}) \\ F[\varphi'](\frac{1}{2}) \pm \frac{d_1}{2} & x = \pm\frac{1}{2} \end{cases}. \tag{5.9}$$

This procedure can be iterated again to gain expressions for the second derivative. The jump which appears there is denoted by $d_2 = \varphi''(\frac{1}{2}) - \varphi''(-\frac{1}{2})$. To correct the derivative of the Fourier series we again add a delta term

$$F[\varphi''] = \partial_x F[\varphi'] + d_1 F[\delta(x - \tfrac{1}{2})] \tag{5.10}$$

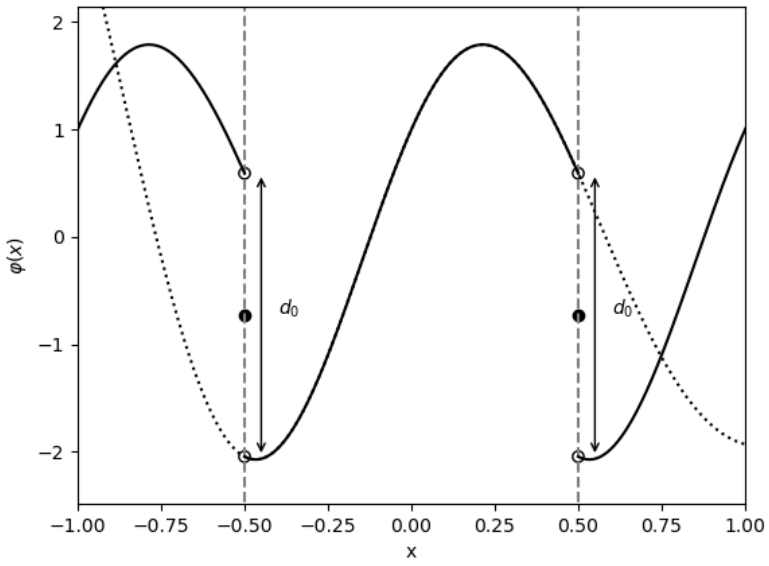

Figure 5.1: Periodic continuation (black) and original function (dotted)

which is equivalent to

$$F[\varphi''] = \partial_x^2 F[\varphi] + d_0 F[\delta'(x - \tfrac{1}{2})] + d_1 F[\delta(x - \tfrac{1}{2})] \tag{5.11}$$

and the original function values are given by

$$\varphi''(x) = \begin{cases} F[\varphi''](x) & x \in (-\frac{1}{2}, \frac{1}{2}) \\ F[\varphi''](\frac{1}{2}) \pm \frac{d_2}{2} & x = \pm\frac{1}{2} \end{cases}. \tag{5.12}$$

Before doing explicit calculations, we need the Fourier series for $\delta(x - \frac{1}{2})$ and $\delta'(x - \frac{1}{2})$ which are listed for reference below. They can be computed by using the integrals(5.6).

$$F[\delta(x - \tfrac{1}{2})] = 1 + 2\sum_{n=1}^{\infty}(-1)^n \ \cos(2\pi n x) \tag{5.13}$$

$$F[\delta'(x - \tfrac{1}{2})] = -4\pi \sum_{n=1}^{\infty} n(-1)^n \ \sin(2\pi n x) = \partial_x F[\delta(x - \tfrac{1}{2})] \tag{5.14}$$

Plugging this into the equation (5.1) results in

$$\begin{aligned} 0 &= F[\varphi] + \alpha^2 F[f''] + \alpha^2 d_0 \delta'(x - \tfrac{1}{2}) + \alpha^2 d_1 \delta(x - \tfrac{1}{2}) = \\ &= (a_0 + \alpha^2 d_1) + \sum_{n=1}^{\infty}(a_n - a_n \alpha^2 4\pi^2 n^2 + 2\alpha^2 d_1 (-1)^n)\cos(2\pi n x) + \\ &\quad + \sum_{n=1}^{\infty}(b_n - b_n \alpha^2 4\pi^2 n^2 - \alpha^2 d_0 4\pi n (-1)^n)\sin(2\pi n x) \end{aligned} \tag{5.15}$$

The vanishing of all Fourier coefficients implies

$$\begin{aligned} a_0 &= -\alpha^2 d_1 \\ a_n &= \frac{-2\alpha^2 d_1 (-1)^n}{1-\alpha^2 4\pi^2 n^2} = \frac{2a_0(-1)^n}{1-\alpha^2 4\pi^2 n^2} \\ b_n &= \frac{d_0 \alpha^2 4\pi n (-1)^n}{1-\alpha^2 4\pi^2 n^2} \end{aligned} \tag{5.16}$$

So the Fourier series of the solution becomes:

$$F[\varphi] = a_0 \left(1 + 2\sum_{n=1}^{\infty} \frac{(-1)^n}{1-\alpha^2 4\pi^2 n^2} \cos(2\pi n x)\right) + d_0 4\pi\alpha^2 \sum_{n=1}^{\infty} \frac{(-1)^n n}{1-\alpha^2 4\pi^2 n^2} \sin(2\pi n x).$$

If we expand the known solution (5.2) in Fourier series, this gives the same result (up to some constants). The needed Fourier series of cosine and sine are listed below:

$$F[\cos(\tfrac{x}{\alpha})] = 2\alpha \ \sin(\tfrac{1}{2\alpha}) \left(1 + 2\sum_{n=1}^{\infty} \frac{(-1)^n}{1-\alpha^2 4\pi^2 n^2} \cos(2\pi n x)\right) \tag{5.17}$$

$$F[\sin(\tfrac{x}{\alpha})] = 8\pi\alpha^2 \ \sin(\tfrac{1}{2\alpha}) \sum_{n=1}^{\infty} \frac{(-1)^n n}{1-\alpha^2 4\pi^2 n^2} \sin(2\pi n x) \tag{5.18}$$

What remains is to solve the boundary conditions and thereby determine the constants d_0 and d_1. For this we need the derivative of $F[f]$:

$$\partial_x F[\varphi] = \alpha^2 d_1 4\pi \sum_{n=1}^{\infty} \frac{(-1)^n n}{1-\alpha^2 4\pi^2 n^2} \sin(2\pi n x) + d_0 \ 8\pi^2\alpha^2 \sum_{n=1}^{\infty} \frac{(-1)^n n^2}{1-\alpha^2 4\pi^2 n^2} \cos(2\pi n x)$$

Here again the correction term has to be used

$$\begin{aligned} F[\varphi'] &= \partial_x F[\varphi] + d_0 F[\delta(x-\frac{1}{2})] \\ &= \alpha^2 d_1 4\pi \sum_{n=1}^{\infty} \frac{(-1)^n n}{1-\alpha^2 4\pi^2 n^2} \sin(2\pi n x) \\ &\qquad + d_0 \left(1 + 2\sum_{n=1}^{\infty} \left[\frac{n^2 4\pi^2\alpha^2}{1-\alpha^2 4\pi^2 n^2} + 1\right] (-1)^n \cos(2\pi n x)\right) \\ &= \alpha^2 d_1 4\pi \sum_{n=1}^{\infty} \frac{(-1)^n n}{1-\alpha^2 4\pi^2 n^2} \sin(2\pi n x) + d_0 \left(1 + 2\sum_{n=1}^{\infty} \frac{(-1)^n}{1-\alpha^2 4\pi^2 n^2} \cos(2\pi n x)\right). \end{aligned}$$

Then we also need to consider the jumps at the boundary (5.1):

$$F[\varphi'](\pm\tfrac{1}{2}) \pm \frac{d_1}{2} = -\beta \tag{5.19}$$

The Fourier series evaluated at both boundary points gives the same value. Subtracting the expression for $x = \frac{1}{2}$ from the one for $x = -\frac{1}{2}$ gives

$$d_1 = 0 \tag{5.20}$$

Then the rest can be solved for d_0:

$$d_0 = -\beta \left(1 + 2 \sum_{n=1}^{\infty} \frac{1}{1 - \alpha^2 4\pi^2 n^2} \right)^{-1} \tag{5.21}$$

Using the expression for the Fourier series of $\cos(\frac{x}{\alpha})$ at $x = \frac{1}{2}$ we can even evaluate the series:

$$d_0 = -\beta 2\alpha \frac{\sin(\frac{1}{2\alpha})}{\cos(\frac{1}{2\alpha})} \tag{5.22}$$

Then the final solution becomes

$$F[\varphi] = -\beta 8\pi\alpha^3 \frac{\sin(\frac{1}{2\alpha})}{\cos(\frac{1}{2\alpha})} \sum_{n=1}^{\infty} \frac{(-1)^n n}{1 - \alpha^2 4\pi^2 n^2} \sin(2\pi n x) \tag{5.23}$$

and comparing it with the Fourier series of $\sin(\frac{x}{\alpha})$

$$\varphi(x) = -\beta\alpha \sec(\tfrac{1}{2\alpha}) \sin(\tfrac{x}{\alpha}) \tag{5.24}$$

which is the same result as found in (5.4).

5.2 Finite vs. Infinite Sums

In section 4.1 we found two possible solutions to the PDE (3.11): p-waves $\vec{a}\, e^{i\vec{\kappa}\cdot\vec{x}}$ with $\kappa = \frac{\omega}{c_1}$ and $\vec{a} || \vec{\kappa}$ or s-waves $\vec{b}\, e^{i\vec{k}\cdot\vec{x}}$ with $k = \frac{\omega}{c_2}$ and $\vec{a} \cdot \vec{k} = 0$. We tried to find a finite linear combination of such terms(with the same ω), which together satisfies the boundary conditions. This was successful in the case without a gravitational wave and lead to the 'quadratic' eigenmodes (see Section 4.3.1) but does not yield any solution to the case with a gravitational wave.
It still might be possible to sum terms, which on their own don't solve the PDE, but their sum does. That this is possible can be seen for the one dimensional case in equation (5.23). The $\sin(2\pi n x)$ terms are no solutions for the given frequency ω, but the whole series is. It should be noted however, that this is only possible with an infinite number of terms. Otherwise a sum of the form

$$\sum_{n=1}^{N} b_n (1 - 4\pi^2\alpha^2) \sin(2\pi n x) = 0 \tag{5.25}$$

remains after plugging it into the equation. Since the sines are linearly independent, the sum only vanishes when the coefficients b_n are all zero. In section 5.3 we aim to find such a infinite series for the two dimensional case.

5.3 Fourier Series with δ's in 2D

In two dimensions we write the Fourier series of an arbitrary function $f(x, y)$ on the square $[-\frac{1}{2}, \frac{1}{2}] \times [-\frac{1}{2}, \frac{1}{2}]$ in terms of exponentials

$$F[f](x, y) = \sum_{n,m=-\infty}^{\infty} C_{nm} e^{i\vec{k}\cdot\vec{x}}, \quad \vec{k} = 2\pi \begin{pmatrix} n \\ m \end{pmatrix}. \tag{5.26}$$

Once again the function is in general not periodic and so the Fourier series only agrees

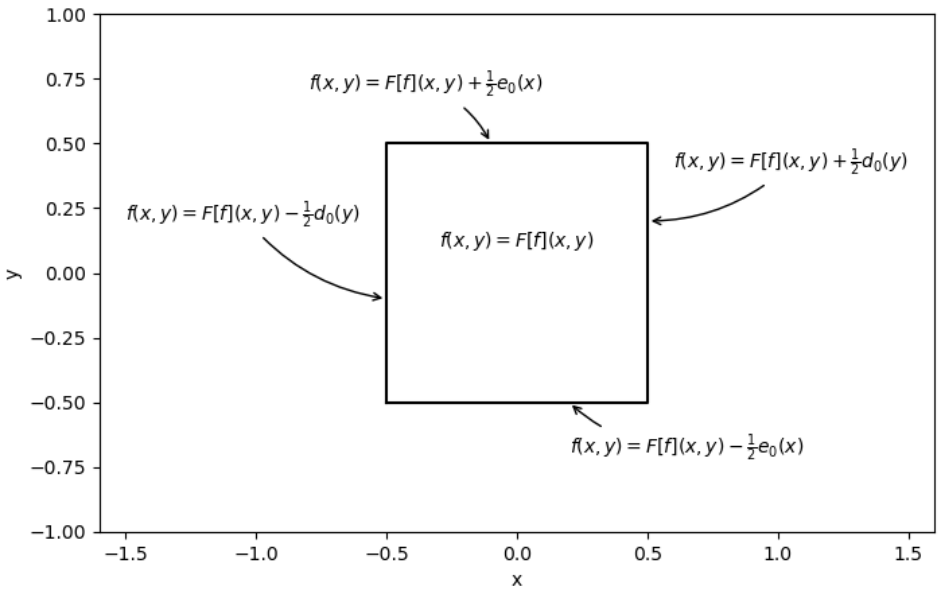

Figure 5.2: Relation between function at its Fourier series

with the function inside the square (see Figure 5.2). At the boundaries it takes the average of the left and right or top and bottom function values. The corners form a special case which will be described later. Instead of a constant describing the jump size there are now two jump functions, one along ∂P_x (denoted by d) and one along ∂P_y (denoted by e).

$$d_0(y) = f(\tfrac{1}{2}, y) - f(-\tfrac{1}{2}, y) \tag{5.27}$$
$$e_0(x) = f(x, \tfrac{1}{2}) - f(x, -\tfrac{1}{2}) \tag{5.28}$$

To get the correct Fourier series for the partial derivatives of f we need, similar to the 1D case, to add a Dirac δ-function to the partial derivative of the Fourier series. For $\partial_x f$ this means:

$$F[\partial_x f(x, y)] = \partial_x F[f(x, y)] + F[d_0(y)\delta(x - \tfrac{1}{2})] \tag{5.29}$$

The difference to the 1D case now is, that the jump is represented by a function, instead of a constant. To get back the correct values of the derivatives at the boundaries we again need jump functions:

$$d_x(y) = \partial_x f(\tfrac{1}{2}, y) - \partial_x f(-\tfrac{1}{2}, y) \tag{5.30}$$
$$e_x(x) = \partial_x f(x, \tfrac{1}{2}) - \partial_x f(x, -\tfrac{1}{2}) \tag{5.31}$$

The subscript denotes the derivative to which the jump function belongs, e.g. d_x for the jump in $\partial_x f$. The relation between the function values and the Fourier series is then given by

$$\partial_x f(x,y) = \begin{cases} F[\partial_x f(x,y)] & -\frac{1}{2} < x, y < \frac{1}{2} \\ F[\partial_x f(x,y)] \pm \frac{1}{2} d_x(y) & x = \pm\frac{1}{2}, -\frac{1}{2} < y < \frac{1}{2} \\ F[\partial_x f(x,y)] \pm \frac{1}{2} e_x(x) & y = \pm\frac{1}{2}, -\frac{1}{2} < x < \frac{1}{2}. \end{cases} \tag{5.32}$$

To get the second derivatives we treat the first derivative as the function f and use what we already know:

$$\begin{aligned} F[\partial_x^2 f(x,y)] &= \partial_x F[\partial_x f(x,y)] + F[d_x(y)\delta(x-\tfrac{1}{2})] \\ &= \partial_x \left(\partial_x F[f(x,y)] + F[d_0(y)\delta(x-\tfrac{1}{2})] \right) + F[d_x(y)\delta(x-\tfrac{1}{2})] \\ &= \partial_x^2 F[f(x,y)] + F[d_0(y)\delta'(x-\tfrac{1}{2})] + F[d_x(y)\delta(x-\tfrac{1}{2})] \end{aligned} \tag{5.33}$$

The second y-derivative looks very similar to the expression in the 1D case, but the mixed derivative is more interesting, because the second derivative now also acts on the jump function.

$$\begin{aligned} F[\partial_x \partial_y f(x,y)] &= \partial_x F[\partial_y f(x,y)] + F[d_y(y)\delta(x-\tfrac{1}{2})] \\ &= \partial_x \left(\partial_y F[f(x,y)] + F[e_0(x)\delta(y-\tfrac{1}{2})] \right) + F[d_y(y)\delta(x-\tfrac{1}{2})] \\ &= \partial_x \partial_y F[f(x,y)] + \partial_x F[e_0(x)] F[\delta(y-\tfrac{1}{2})] + F[d_y(y)\delta(x-\tfrac{1}{2})] \end{aligned} \tag{5.34}$$

But this has to be equivalent to the expression when taking the partial derivatives in the other order:

$$F[\partial_y \partial_x f] = \partial_y \partial_x F[f] + \partial_y F[d_0(y)] F[\delta(x-\tfrac{1}{2})] + F[e_x(x)\delta(y-\tfrac{1}{2})] \tag{5.35}$$

To see that these two expressions agree we have to investigate the jump functions further. Using the definitions we can see that there is a relation between the tangential derivatives along the edges and the jump function on these edges:

$$\partial_y d_0(y) = \partial_y \left[f(\tfrac{1}{2}, y) - f(-\tfrac{1}{2}, y) \right] = \partial_y f(\tfrac{1}{2}, y) - \partial_y f(-\tfrac{1}{2}, y) = d_y(y) \tag{5.36}$$

and similarly also

$$\partial_x e_0(x) = e_x(x). \tag{5.37}$$

For the normal derivatives there is no such relation, therefore d_x and e_y are completely new and independent functions. Now this relation can be used to find a relation between the Fourier series of the jump functions and their derivatives

$$F[d_y(x)] = \partial_y F[d_0(y)] + \left[d_0(\tfrac{1}{2}) - d_0(-\tfrac{1}{2}) \right] F[\delta(y-\tfrac{1}{2})] \tag{5.38}$$
$$F[e_x(x)] = \partial_x F[e_0(x)] + \left[e_0(\tfrac{1}{2}) - e_0(-\tfrac{1}{2}) \right] F[\delta(x-\tfrac{1}{2})]. \tag{5.39}$$

Next, using the definition of the jump function d_0, the constant Δ is defined as the jump in the jump functions:

$$\Delta := d_0(\tfrac{1}{2}) - d_0(-\tfrac{1}{2}) = f(\tfrac{1}{2},\tfrac{1}{2}) - f(-\tfrac{1}{2},\tfrac{1}{2}) - f(\tfrac{1}{2},-\tfrac{1}{2}) + f(-\tfrac{1}{2},-\tfrac{1}{2}) = e_0(\tfrac{1}{2}) - e_0(-\tfrac{1}{2}).$$

With the help of this the mixed derivatives get a nice and symmetric form:

$$F[\partial_x\partial_y f] = \partial_x\partial_y F[f] + \partial_x F[e_0(x)]F[\delta(y-\tfrac{1}{2})] + \partial_y F[d_0(y)]F[\delta(x-\tfrac{1}{2})] + \Delta\ F[\delta(x-\tfrac{1}{2})\delta(y-\tfrac{1}{2})]$$
$$F[\partial_y\partial_x f] = \partial_y\partial_x F[f] + \partial_y F[d_0(y)]F[\delta(x-\tfrac{1}{2})] + \partial_x F[e_0(x)]F[\delta(y-\tfrac{1}{2})] + \Delta\ F[\delta(x-\tfrac{1}{2})\delta(y-\tfrac{1}{2})]$$

The goal now is to use this to find a solution to the equation (3.14) with the boundary conditions (3.15) which are rewritten below for reference.

$$\varphi^i + \bar{c}_2^2\Delta\varphi^i + \bar{c}_3^2\partial^i\partial_k\varphi^k = 0.$$

$$\begin{aligned}(2\mu+\lambda)\partial_x\varphi^x|_{\partial P_x} + \lambda\partial_y\varphi^y|_{\partial P_x} &= -\mu L A_+\\ (2\mu+\lambda)\partial_y\varphi^y|_{\partial P_y} + \lambda\partial_x\varphi^x|_{\partial P_y} &= \mu L A_+\\ \partial_x\varphi^y|_{\partial P} + \partial_y\varphi^x|_{\partial P} &= -L A_\times\end{aligned}$$

The desired function has an x- and y-component and is now called φ instead of f. Therefore all Fourier-Coefficients and jump functions also get an index. It is useful to first look at the boundary conditions expressed in terms of the Fourier series. For instance the expression for σ_{xy} at $x = \pm\frac{1}{2}$ reads

$$F[\partial_x\varphi^y(\pm\tfrac{1}{2},y)] \pm \tfrac{1}{2}d_x^y(y) + F[\partial_y\varphi^x(\pm\tfrac{1}{2},y)] \pm \tfrac{1}{2}d_y^x(y) + A_\times = 0. \tag{5.40}$$

The Fourier series at $x = \frac{1}{2}$ has the same value as the one at $x = -\frac{1}{2}$ so when both cases are subtracted from one another what remains is the simple relation

$$d_x^y(y) + d_y^x(y) = 0 \tag{5.41}$$

Similar relations can be found when looking at σ_{xx} on ∂P_x, σ_{yy} on ∂P_y and σ_{xy} on ∂P_y respectively:

$$(2\mu+\lambda)d_x^x(y) + \lambda d_y^y(y) = 0 \tag{5.42}$$
$$\lambda e_x^x(x) + (2\mu+\lambda)e_y^y(x) = 0 \tag{5.43}$$
$$e_x^y(x) + e_y^x(x) = 0 \tag{5.44}$$

Using these, all equations can be expressed in terms of d_0^i and e_0^i only, e.g.

$$d_x^x = -\tfrac{\lambda}{2\mu+\lambda}d_y^y = -\tfrac{\lambda}{2\mu+\lambda}\partial_y d_0^y. \tag{5.45}$$

For the second x- and y-derivatives this means

$$F[\partial_x^2\varphi^x] = \partial_x^2 F[\varphi^x] + F[d_0^x(y)\delta'(x-\tfrac{1}{2})] - \tfrac{\lambda}{2\mu+\lambda}F[\delta(x-\tfrac{1}{2})]\left(\partial_y F[d_0^y(y)] + \Delta\ F[\delta(y-\tfrac{1}{2})]\right)$$
$$F[\partial_y^2\varphi^x] = \partial_y^2 F[\varphi^x] + F[e_0^x(y)\delta'(x-\tfrac{1}{2})] - \partial_x F[e_0^y(x)]F[\delta\left(x-\tfrac{1}{2}\right)] - \Delta\ F[\delta(x-\tfrac{1}{2})\delta(y-\tfrac{1}{2})]$$

Before plugging all this into equation (3.14), we rewrite it by grouping equal derivatives. For the x-component this leads to

$$\varphi^x + \bar{c}_1^2 \partial_x^2 \varphi^x + \bar{c}_2^2 \partial_y^2 \varphi^x + \bar{c}_3^2 \partial_x \partial_y \varphi^y = 0. \tag{5.46}$$

The Fourier series for each of the three derivatives includes one term containing the factor $F[\delta(x-\frac{1}{2})\delta(y-\frac{1}{2})]$. Looking only at their prefactors, one finds

$$\Delta\left(-c_1^2 \frac{\lambda}{2\mu+\lambda} - c_2^2 + c_3^2\right) = \Delta\left(-\frac{2\mu+\lambda}{\rho_0}\frac{\lambda}{2\mu+\lambda} - \frac{\mu}{\rho_0} + \frac{\lambda+\mu}{\rho_0}\right) = 0. \tag{5.47}$$

These terms now cancel each other out in the Fourier series of (5.46) and its Fourier series becomes

$$\begin{aligned} &F[\varphi^x] + \bar{c}_1^2 \left(\partial_x^2 F[\varphi^x] + F[d_0^x(y)\delta'(x-\tfrac{1}{2})] - \tfrac{\lambda}{2\mu+\lambda}\partial_y F[d_0^y(y)] F[\delta(x-\tfrac{1}{2})]\right) \\ &\quad + \bar{c}_2^2 \left(\partial_y^2 F[\varphi^x] + F[e_0^x(x)\delta'(y-\tfrac{1}{2})] - \partial_x F[e_0^y(x)] F[\delta\left(y-\tfrac{1}{2}\right)]\right) \\ &\quad + \bar{c}_3^2 \left(\partial_x \partial_y F[\varphi^y] + \partial_x F[e_0^y(x)] F[\delta(y-\tfrac{1}{2})] + \partial_y F[d_0^y(y)] F[\delta(x-\tfrac{1}{2})]\right) = 0. \end{aligned} \tag{5.48}$$

By combining equal terms this can be rewritten as

$$\begin{aligned} &F[\varphi^x] + \bar{c}_1^2 \left(\partial_x^2 F[\varphi^x] + F[d_0^x(y)\delta'(x-\tfrac{1}{2})]\right) + \tfrac{\lambda}{\rho_0 \omega^2 L^2}\partial_x F[e_0^y(x)] F[\delta(y-\tfrac{1}{2})] \\ &\quad + \bar{c}_3^2 \partial_x \partial_y F[\varphi^y] + \bar{c}_2^2 \left(\partial_y^2 F[\varphi^x] + F[e_0^x(x)\delta'(y-\tfrac{1}{2})] + \partial_y F[d_0^y(y)] F[\delta(x-\tfrac{1}{2})]\right) = 0. \end{aligned}$$

Following a similar derivation the y-component of the equation takes the form

$$\begin{aligned} &F[\varphi^y] + \bar{c}_2^2 \left(\partial_x^2 F[\varphi^y] + F[d_0^y(y)\delta'(x-\tfrac{1}{2})]\right) + \bar{c}_1^2 \left(\partial_y^2 F[\varphi^y] + F[e_0^y(x)\delta'(y-\tfrac{1}{2})]\right) \\ &\quad + \bar{c}_3^2 \partial_x \partial_y F[\varphi^x] + \bar{c}_2^2 \partial_x F[e_0^x(x)] F[\delta(y-\tfrac{1}{2})] + \tfrac{\lambda}{\rho_0 \omega^2 L^2}\partial_y F[d_0^x(y)] F[\delta(x-\tfrac{1}{2})] = 0. \end{aligned}$$

These can now be turned into equations for the Fourier coefficients C_{nm}^i of the function and the jumps $c_m(d_0^i)$ and $c_n(e_0^i)$. The Fourier series for $\delta(x-\frac{1}{2})$ and $\delta'(x-\frac{1}{2})$ are given by

$$F[\delta(x-\tfrac{1}{2})] = \sum_{n=-\infty}^{\infty} (-1)^n e^{i2\pi n x} \tag{5.49}$$

$$F[\delta'(x-\tfrac{1}{2})] = \sum_{n=-\infty}^{\infty} 2\pi i n (-1)^n e^{i2\pi n x}. \tag{5.50}$$

We also use that the Fourier series of a product is the product of the Fourier series and the relation $\frac{\lambda}{\rho\omega^2 L^2} = \bar{c}_1^2 - 2\bar{c}_2^2$ which can be easily checked by expanding c_1 and c_2 in terms of μ and λ.

$$\begin{aligned} &C_{nm}^x (1 - 4\pi^2(\bar{c}_1^2 n^2 + \bar{c}_2^2 m^2)) - C_{nm}^y 4\pi^2 nm\bar{c}_3^2 + 2i\pi[\bar{c}_1^2 c_m(d_0^x) n(-1)^n + \\ &\quad + \bar{c}_2^2 c_n(e_0^x) m(-1)^m + (\bar{c}_1^2 - 2\bar{c}_2^2) n c_n(e_0^y)(-1)^m + \bar{c}_2^2 m c_m(d_0^y)(-1)^n] = 0 \end{aligned} \tag{5.51}$$

$$\begin{aligned} &C^y_{nm}(1-4\pi^2(\bar{c}_2^2n^2+\bar{c}_1^2m^2))-C^x_{nm}4\pi^2nm\bar{c}_3^2+2i\pi[\bar{c}_2^2c_m(d_0^y)n(-1)^n+\\ &\quad+\bar{c}_1^2c_n(e_0^y)m(-1)^m+\bar{c}_2^2nc_n(e_0^x)(-1)^m+(\bar{c}_1^2-2\bar{c}_2^2)mc_m(d_0^x)(-1)^n]=0 \end{aligned} \tag{5.52}$$

Next come the boundary conditions. There the gravitational wave A_{ij} is also rewritten in terms of a (very simple) Fourier series:

$$A_{ij}=\sum_{m,n=-\infty}^{\infty}A_{ij}\delta_{n0}\delta_{m0}e^{i2\pi(nx+my)}. \tag{5.53}$$

If we set $x=\pm\frac{1}{2}$ the 2 dimensional Fourier series turns into a one-dimensional Fourier series with an extra factor $e^{\pm i2\pi\frac{n}{2}}=(-1)^n$. We then require the new Fourier Coefficients of this to vanish. $\sigma_{xx}(\pm\frac{1}{2},y)=0$ then leads to the expression

$$\sum_{n=-\infty}^{\infty}(\text{-}1)^n[c_1^2(2\pi inC^x_{nm}+c_m(d_0^x)(\text{-}1)^n)+(c_1^2-2c_2^2)(2\pi imC^y_{nm}+c_n(e_0^y)(\text{-}1)^m)]=\text{-}c_2^2LA_+\delta_{m0}.$$

Here the corrected expression for the derivative of a Fourier series has once again been used. From the condition $\sigma_{xy}(\pm\frac{1}{2},y)=0$ then follows

$$\sum_{n=-\infty}^{\infty}(-1)^n[2\pi imC^x_{nm}+c_n(e_0^x)(-1)^m+2\pi inC^y_{nm}+c_m(d_0^y)(-1)^n]=-LA_\times\delta_{m0}.$$

The other two boundary conditions $\sigma_{yy}(x,\pm\frac{1}{2})=0$ and $\sigma_{xy}(x,\pm\frac{1}{2})=0$ give similar conditions, except that now a sum over m remains, instead of one over n.

$$\sum_{m=-\infty}^{\infty}(\text{-}1)^m[(c_1^2-2c_2^2)(2\pi inC^x_{nm}+c_m(d_0^x)(\text{-}1)^n)+c_1^2(2\pi imC^y_{nm}+c_n(e_0^y)(\text{-}1)^m)]=c_2^2LA_+\delta_{m0}.$$

$$\sum_{m=-\infty}^{\infty}(-1)^m[2\pi imC^x_{nm}+c_n(e_0^x)(-1)^m+2\pi inC^y_{nm}+c_m(d_0^y)(-1)^n]=-LA_\times\delta_{m0}.$$

So we now have 6 relations (for each n and m) which contain the same information as the original BVP, but now expressed in Fourier Coefficients. These are summarized in the following box.

In terms of Fourier coefficients C^j_{nm} for the functions φ^j and $c_n(e_0^j),c_m(d_0^j)$ for the jump functions the BVP looks as follows:
PDE:

$$\begin{aligned} &C^x_{nm}(1-4\pi^2(\bar{c}_1^2n^2+\bar{c}_2^2m^2))-C^y_{nm}4\pi^2nm\bar{c}_3^2+2i\pi[\bar{c}_1^2c_m(d_0^x)n(-1)^n+\\ &\quad+\bar{c}_2^2c_n(e_0^x)m(-1)^m+(\bar{c}_1^2-2\bar{c}_2^2)nc_n(e_0^y)(-1)^m+\bar{c}_2^2mc_m(d_0^y)(-1)^n]=0\\ &C^y_{nm}(1-4\pi^2(\bar{c}_2^2n^2+\bar{c}_1^2m^2))-C^x_{nm}4\pi^2nm\bar{c}_3^2+2i\pi[\bar{c}_2^2c_m(d_0^y)n(-1)^n+\\ &\quad+\bar{c}_1^2c_n(e_0^y)m(-1)^m+\bar{c}_2^2nc_n(e_0^x)(-1)^m+(\bar{c}_1^2-2\bar{c}_2^2)mc_m(d_0^x)(-1)^n]=0 \end{aligned} \tag{5.54}$$

Boundary conditions:

$$\sum_{n=-\infty}^{\infty} (\text{-}1)^n[c_1^2(2\pi i n C_{nm}^x + c_m(d_0^x)(\text{-}1)^n) + (c_1^2 - 2c_2^2)(2\pi i m C_{nm}^y + c_n(e_0^y)(\text{-}1)^m)] = \text{-}c_2^2 L A_+ \delta_{m0}$$

$$\sum_{n=-\infty}^{\infty} (-1)^n[2\pi i m C_{nm}^x + c_n(e_0^x)(-1)^m + 2\pi i n C_{nm}^y + c_m(d_0^y)(-1)^n] = -L A_\times \delta_{m0}$$

$$\sum_{m=-\infty}^{\infty} (\text{-}1)^m[(c_1^2 - 2c_2^2)(2\pi i n C_{nm}^x + c_m(d_0^x)(\text{-}1)^n) + c_1^2(2\pi i m C_{nm}^y + c_n(e_0^y)(\text{-}1)^m)] = c_2^2 L A_+ \delta_{m0}$$

$$\sum_{m=-\infty}^{\infty} (-1)^m[2\pi i m C_{nm}^x + c_n(e_0^x)(-1)^m + 2\pi i n C_{nm}^y + c_m(d_0^y)(-1)^n] = -L A_\times \delta_{m0}$$

5.3.1 Values at the corners

At the corners of the square the Fourier series gives the average of the function values at the four corners:

$$F[f](\pm\tfrac{1}{2}, \pm\tfrac{1}{2}) = \tfrac{1}{4}\left(f(\tfrac{1}{2}, \tfrac{1}{2}) + f(\tfrac{1}{2}, -\tfrac{1}{2}) + f(-\tfrac{1}{2}, \tfrac{1}{2}) + f(-\tfrac{1}{2}, -\tfrac{1}{2})\right). \tag{5.55}$$

This can be motivated by first developing the x-dependence into a Fourier series while keeping y fixed. Then the Fourier coefficients are functions of y which again can be developed as a Fourier series. In each step the Fourier series at the border $\pm\frac{1}{2}$ takes the average of the two values. This leads to the average of the average which is the same as the average of the values at the 4 corners.
To get back the correct function values we have to add correction terms consisting of the jump functions d_0 and e_0 ,but here they are more complicated than at the edges:

$$f(\tfrac{s_x}{2}, \tfrac{s_y}{2}) = F[f](\tfrac{1}{2}, \tfrac{1}{2}) + \tfrac{3}{8}(s_x d_0(\tfrac{s_y}{2}) + s_y e_0(\tfrac{s_x}{2})) + \tfrac{1}{8}(s_x d_0(\tfrac{-s_y}{2}) + s_y e_0(\tfrac{-s_x}{2})) \tag{5.56}$$

where $s_x = \pm 1$,$s_y = \pm 1$ give the corner which is considered.

5.4 Motion in TT-coordinates

The six sets of equations written in the box at the end of section 5.3 describe the BVP. The first two equations can be solved for C_{nm}^x and C_{nm}^y in terms of the coefficients of the jump functions. Then the infinite sums in the boundary conditions can be truncated at some value M and the resulting linear system of $4 * (2 * M + 1)$ equations in the $4 * (2 * M + 1)$ variables $c_m(d_0^i)$ and $c_n(e_0^i)$ are solved on the computer. As the number of equations and variables is equal, we expect that a solution exists. Here we chose $M = 70$ to get a good compromise of accuracy of the solution and runtime. Once the jump coefficients are known, they can be used to calculate the Fourier coefficients of the solution and these can then be used to calculate the solutions themselves.

The solution obviously depends on the chosen material, represented by the speeds of sound c_1 and c_2 in the medium, and the gravitational wave frequency ω. The dimension

of the plate is chosen to be $L = 1m$ as we have shown in section 3.5 that all other cases can be obtained by a scaling argument.

As an exemplary case, we show here two solutions for a plate with wave-speeds $c_1 = 1950\frac{m}{s}, c_2 = 540\frac{m}{s}$ which could be made of polyethylene [9]. Once for purely plus-polarized wave $A_+ = 1, A_\times = 0$ and once for a purely cross-polarized wave $A_+ = 0, A_\times = 1$. Since the equations are linear, the solution for an arbitrary polarization can be constructed as a superposition of these two special cases (where the time-dependence of the cross polarization solution gets a phase shift, when its amplitude is complex). Keep in mind, that $\varphi^j(x, y)$ represents only the spatial part of the solution, to get the full solution one needs to multiply by $\cos(\omega t)$ so that $u^j(t, x, y) = \cos(\omega t)\varphi^j(x, y)$. Moreover these results are in TT-coordinates and hence don't directly describe the physical motion of the plate.

5.4.1 Purely plus-polarized GW

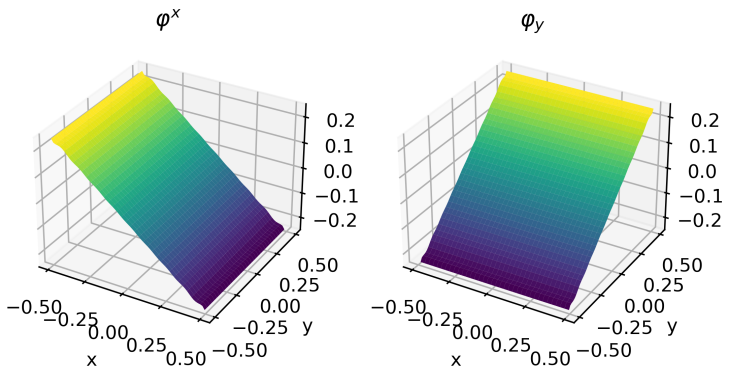

Figure 5.3: Surface plot of φ^x and φ^y for purely plus-polarized GW.

In the first representation, shown in Figure 5.3, the components of $\vec{\varphi}$ are plotted as a function of x and y. The linear behaviour dominates the solution, a fact which fits nicely with the low frequency limit in section 3.8. Figure 5.4 gives a better intuition of what happens to the plate. It is compressed in one direction, and stretched in the other. The farther the point is away from the origin, the larger the deformation, which is exactly the linear behaviour. But this is only the representation in TT-coordinates, so it doesn't show the actual physical behaviour, which is discussed in chapter 6.

The whole plate looks like it's uniformly stretched in one direction and compressed in the other. That looks very similar to the quadrupole motion of a ring of free particles under the influence of a GW. But actually it is the exact opposite motion, so that when we transform it to local Lorentz coordinates there is no motion, i.e. the plate prevents the motion.

The uniformity is explained by the following intuitive argument: The time it takes for elastic waves/information traveling at the speed of sound $c_2 = 540\frac{m}{s}$ or $c_1 > c_2$ through the plate is $t = \frac{L}{c_2} \approx 2ms$. On the other hand the period of the gravitational wave is $T = \frac{2\pi}{\omega} \approx 63ms$. So $t << T$, or if we consider c_1 instead of c_2 this means that the period

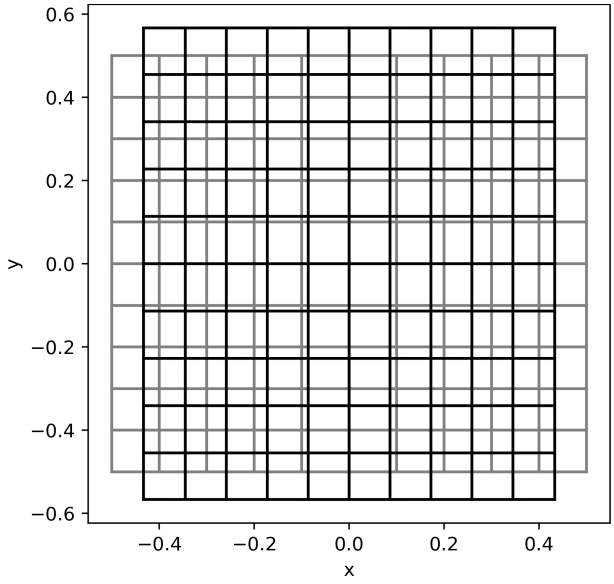

Figure 5.4: Deformation of the quadratic plate under a plus-polarized GW of frequency $\omega = 100\frac{1}{s}$. Grey lines represent the original plate, black lines the deformed plate. The Amplitude is scaled up for better visibility.

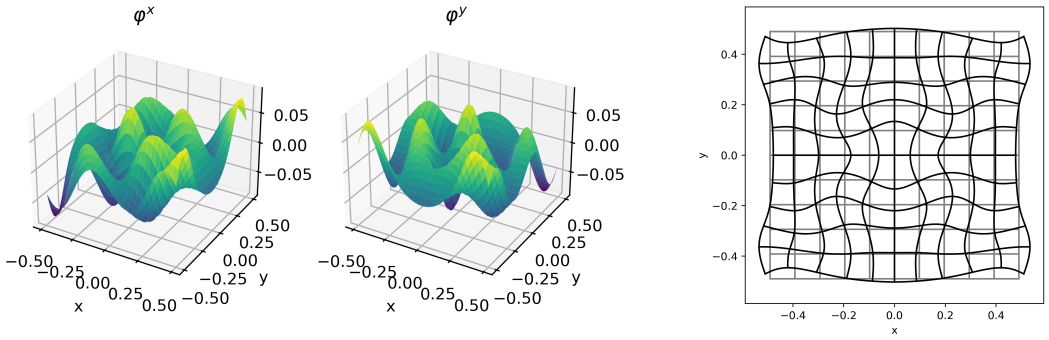

(a) surface plot

(b) grid plot

Figure 5.5: Plots for purely plus-polarized wave with $\omega = 10^4\frac{1}{s}$.

ratio ε from section 3.8 is small. Hence the spread of elastic waves/information in the plate is much faster than the change of the GW, which acts in TT-coordinates only on the boundary. Therefore the whole plate can react as one.

By this argument, that should no longer be the case for higher frequencies and indeed Figure 5.5 confirms this for $\omega = 10^4\frac{1}{s}$. Different parts of the plate move differently since changes have no longer enough time to propagate through the plate and 'equilibrate'.

One interesting thing to consider is, how the deformation, especially its amplitude, changes with the GW-frequency. To get a first impression we plot the maximum value

of $\vec{\varphi}$ relative to L as a function of ωL in Figure 5.6. One can see, that there are certain resonance frequencies where the deformation gets very large. At these resonances our model no longer makes sense as we haven't implemented any damping behaviour.

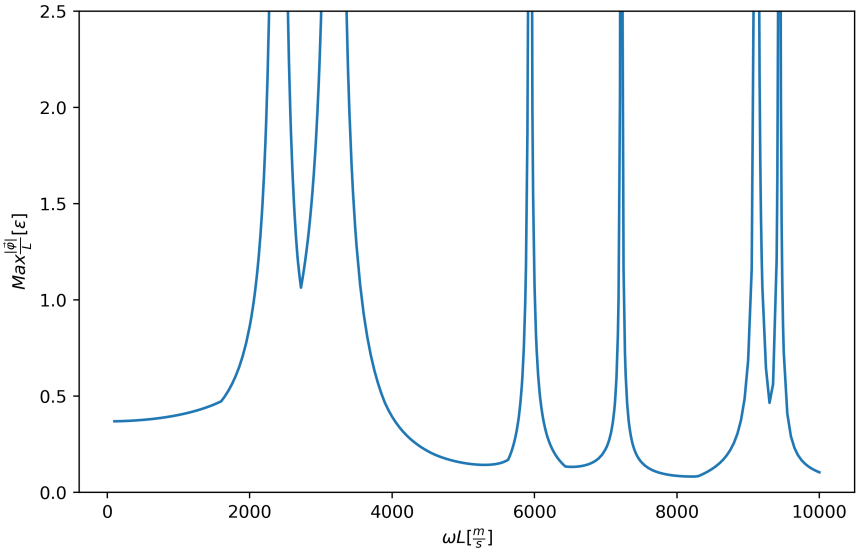

Figure 5.6: Max of $\vec{\varphi}$ relative to L in units of ϵ as a function of ωL.

5.4.2 Purely cross-polarized GW

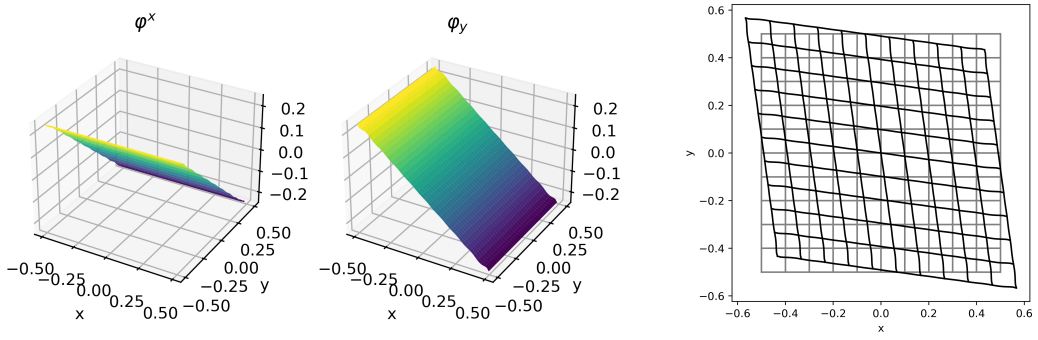

(a) Surface Plot

(b) Grid plot

Figure 5.7: Surface and Grid plot for a purely cross-polarized GW of frequency $\omega = 100\frac{1}{s}$.

At a first glance the result in Figure 5.7 looks very similar to the plus-polarized case except, that they are rotated by 90°. What this implies can be better seen in the grid plot. The stretching and compressing now happens along the diagonals, in contrast to along the axes as it was the case for the plus-polarized wave and is again the opposite motion of a ring of free particles.

Chapter 6

Physical Distances

In the last chapter we obtained a procedure to numerically solve the BVP describing the motion of an elastic quadratic plate under the influence of a gravitational wave. But this solution was obtained in TT-coordinates so it doesn't directly describe the behaviour of the plate. We start this chapter by introducing a coordinate transformation to local Lorentz coordinates and then discuss the results in more detail, before going on to calculate the signal, an interferometer mounted on the plate would measure, in the next chapter. Throughout this and the next chapter we assume that, except were explicitly stated otherwise, the plate has length $L = 1m$.

6.1 Coordinate Transformation to Local Lorentz Coordinates

We want to mount an interferometer on the plate to measure gravitational waves. To calculate the signal it would measure we need to calculate the physical path lengths of the two interferometer arms. This is done using local Lorentz coordinates [12], given by the transformation

$$\begin{aligned} \bar{x} &= x(1 - \tfrac{A_+}{2}\epsilon\cos(\omega t)) \\ \bar{y} &= y(1 + \tfrac{A_+}{2}\epsilon\cos(\omega t)) \end{aligned} \tag{6.1}$$

for the case of a purely plus-polarized GW ($A_+ = 1, A_\times = 0$). The coordinates with bar denote the TT-coordinates, the ones without a bar are Local Lorentz coordinates, i.e. physical distances are given by the difference in coordinates. For small ϵ, this transformation can be inverted:

$$\begin{aligned} x &= \frac{\bar{x}}{1 - \frac{A_+}{2}\epsilon\cos(\omega t)} \approx \bar{x}(1 + \tfrac{A_+}{2}\epsilon\cos(\omega t)) \\ y &= \frac{\bar{y}}{1 + \frac{A_+}{2}\epsilon\cos(\omega t)} \approx \bar{y}(1 - \tfrac{A_+}{2}\epsilon\cos(\omega t)). \end{aligned} \tag{6.2}$$

In matrix form this can be written as

$$\begin{pmatrix} x \\ y \end{pmatrix} = \begin{pmatrix} 1 + \frac{A_+}{2}\epsilon\cos(\omega t) & 0 \\ 0 & 1 - \frac{A_+}{2}\epsilon\cos(\omega t) \end{pmatrix} \begin{pmatrix} \bar{x} \\ \bar{y} \end{pmatrix}. \tag{6.3}$$

To get the transformation rule for the cross-polarization we employ a rotation of 45° in the x-y plane. The coordinates in the rotated frames are denoted by x', y' and $\bar{x}', \bar{y}'$ and related to the original coordinates by the transformation $\mathcal{R}$ via

$$\begin{pmatrix} x' \\ y' \end{pmatrix} = \mathcal{R} \begin{pmatrix} x \\ y \end{pmatrix} = \tfrac{1}{\sqrt{2}} \begin{pmatrix} 1 & 1 \\ -1 & 1 \end{pmatrix} \begin{pmatrix} x \\ y \end{pmatrix}. \tag{6.4}$$

Now notice, that a purely plus-polarized wave in the unprimed frame, turns into a purely cross-polarized wave in the primed frame:

$$\mathcal{R} \begin{pmatrix} 0 & A_\times \\ A_\times & 0 \end{pmatrix} \mathcal{R}^T = \begin{pmatrix} A_\times & 0 \\ 0 & -A_\times \end{pmatrix}. \tag{6.5}$$

So, to obtain the local Lorentz coordinates under a cross-polarized wave, we first rotate the coordinates, apply the transformation for the plus-polarized wave and then rotate them back.

$$\begin{aligned} \begin{pmatrix} x \\ y \end{pmatrix} &= \mathcal{R}^{-1} \begin{pmatrix} 1 + \frac{A_\times}{2}\epsilon\cos(\omega t) & 0 \\ 0 & 1 - \frac{A_\times}{2}\epsilon\cos(\omega t) \end{pmatrix} \mathcal{R} \begin{pmatrix} \bar{x} \\ \bar{y} \end{pmatrix} \\ &= \begin{pmatrix} 1 & \frac{A_\times}{2}\epsilon\cos(\omega t) \\ \frac{A_\times}{2}\epsilon\cos(\omega t) & 1 \end{pmatrix} \begin{pmatrix} \bar{x} \\ \bar{y} \end{pmatrix} \end{aligned}$$

So the Local Lorentz coordinates are given by

$$\begin{aligned} x &= \bar{x} + \bar{y}\tfrac{A_\times}{2}\epsilon\cos(\omega t) \\ y &= \bar{y} + \bar{x}\tfrac{A_\times}{2}\epsilon\cos(\omega t). \end{aligned} \tag{6.6}$$

Combining both cases gives the transformation for an arbitrary polarized wave:

$$\begin{aligned} x &= \bar{x} + \bar{x}\tfrac{A_+}{2}\epsilon\cos(\omega t) + \bar{y}\tfrac{A_\times}{2}\epsilon\cos(\omega t) \\ y &= \bar{y} - \bar{y}\tfrac{A_+}{2}\epsilon\cos(\omega t) + \bar{x}\tfrac{A_\times}{2}\epsilon\cos(\omega t). \end{aligned} \tag{6.7}$$

The TT-coordinates are related to the deformation by

$$\bar{x}^i = X^i + \epsilon u^i \tag{6.8}$$

where the upper case coordinates are the body coordinates $X^i = f^i$. Putting this all together and ignoring ϵ^2 terms we get

$$\begin{aligned} x &= X(1 + \tfrac{A_+}{2}\epsilon\cos(\omega t)) + Y\tfrac{A_\times}{2}\epsilon\cos(\omega t) + \epsilon u^x \\ y &= Y(1 - \tfrac{A_+}{2}\epsilon\cos(\omega t)) + X\tfrac{A_\times}{2}\epsilon\cos(\omega t) + \epsilon u^y. \end{aligned} \tag{6.9}$$

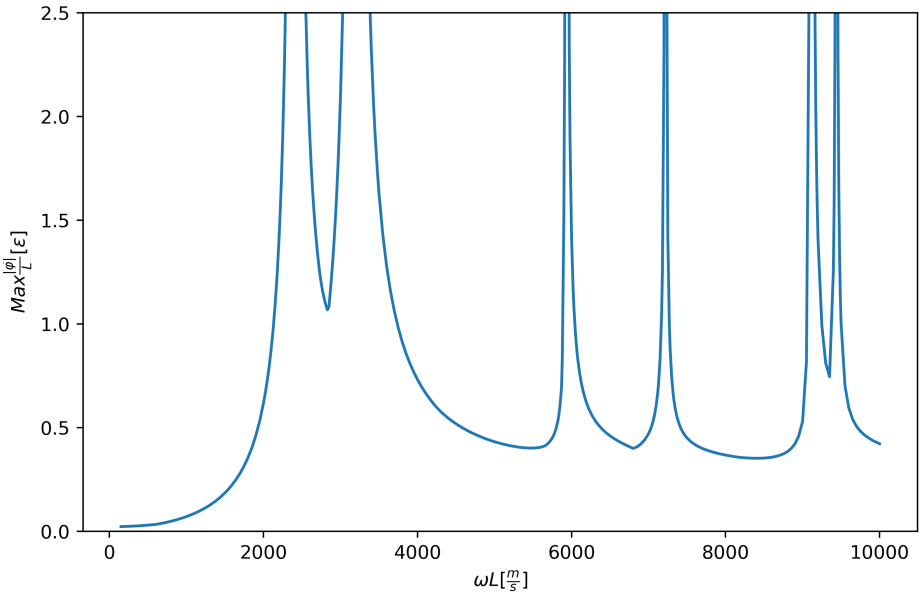

Figure 6.1: Maximum of the physical displacement field in units of ϵ as a function of ωL for the response to a purely plus-polarized GW.

6.2 Physical Displacement Field

We can use the coordinate transformation (6.9) to translate the displacement fields u^i or their spatial part φ^i into the physical displacement fields $\tilde{u}^i$ or $\tilde{\varphi}^i$.

$$\begin{aligned} \tilde{\varphi}^x &= \varphi^x + X\frac{A_+}{2} + Y\frac{A_\times}{2} \\ \tilde{\varphi}^y &= \varphi^y - Y\frac{A_+}{2} + X\frac{A_\times}{2} \end{aligned} \tag{6.10}$$

This is used to translate the results from section 5.4 where the plate has parameters $c_1 = 1950\frac{m}{s}$ and $c_2 = 540\frac{m}{s}$. First we investigate the response to a purely plus-polarized wave, then to a purely cross-polarized wave. All other cases can be constructed from these two.

6.2.1 Purely plus-polarized GW

For small ω, the solution φ^i is almost linear, such that the transformation cancels the result almost completely. Figure 6.1 confirms this by showing, that the maximum of the physical displacement field is very small for small ωL. This also fits nicely with the low frequency limit where we have $\varphi^x \approx -\frac{A_+}{2}x$ and $\varphi^y \approx \frac{A_+}{2}y$.

The resonances stay at the same frequencies as in the TT-gauge. The frequencies of the first four are $\omega_1 \approx 2400\frac{1}{s}$, $\omega_2 \approx 3200\frac{1}{s}$, $\omega_3 \approx 5940\frac{1}{s}$ and $\omega_4 \approx 7220\frac{1}{s}$. At the first resonance a few interesting things happen:

- The amplitude grows very large.

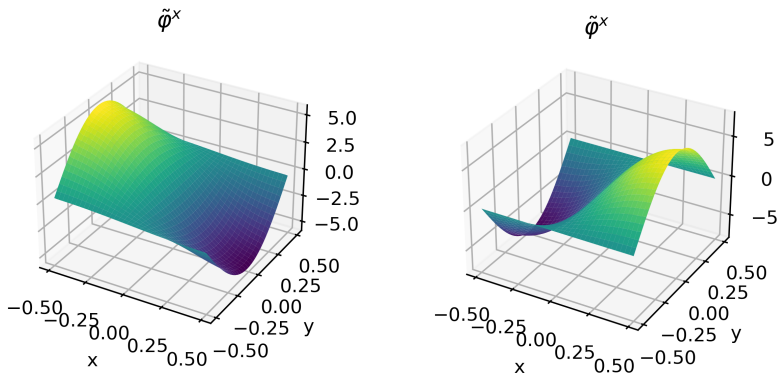

(a) $\omega = 2350$ (b) $\omega = 2450$

Figure 6.2: Surface plot of φ^x shortly before (a) and shortly after (b) the first resonance.

- The sign of the solution flips. This can be seen in Figure 6.2. Before the resonance (a) the solution is bulging upward near $x = -0.5$ after the resonance (b) $\tilde{\varphi}^x$ is bulging downward. This is related to the phase shift of forced oscillations relative to the driving force, cf. the damped driven oscillator in Appendix B. When there is no damping the phase shift happens jumps from 0 to π at the resonance, which manifests here as a minus sign.

- At the corners nodes appear, around which the plate rotates locally, but they themselves don't move. We call them rotation centers. This is in addition to the node at the center which is always present and due to the fact that the center of mass doesn't move. Figure 6.3 shows this behaviour at $\omega = 2700\frac{1}{s}$, so a bit after the resonance. The rotation centers can be seen as eddies which appear at the four corners and move inward.

The first Resonance looks like the $n = 1$ eigenmode from section 4.3.1. These have wave vectors $k_x = k_y = n\frac{\pi}{L}$. With the dispersion relation for s-waves $\omega = c_2|\vec{k}|$ we predict a eigenfrequency $L\omega_1 = 540\frac{m}{s}\sqrt{2}\frac{\pi}{1m} \approx 2399\frac{1}{s}$ for the first eigenmode. This agrees very well with the first Resonance frequency, which is what is to be expected in a model without damping. A damping term would shift the resonance frequencies, see 1D analogy in appendix B.

At the second resonance, 4 additional nodes appear, but this time at the middle of the four edges. Also, they are shear fixed points, similar to the node at the center, i.e. they are compressed along one direction and stretched along the other, while they themselves don't move. The sign flip again occurs and leads to the rotation centers changing direction. For this resonance we didn't find any eigenmode with the correct frequency or motion pattern, which is an indication that there are more eigenmodes than the ones we found in section 4.3.

What about the next eigenmode from section 4.3.1 with $n = 2$? We would expect to find it at the frequency $\omega \approx 4800\frac{1}{s}$, but there is no corresponding resonance in Figure

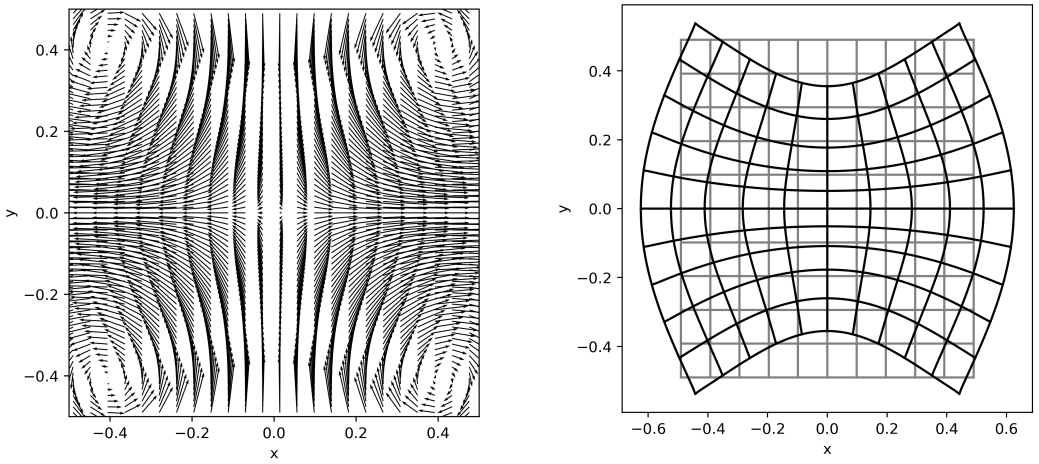

(a) Vector plot (b) Grid Plot

Figure 6.3: Vector plot (a) and grid plot (b) of the physical displacement field at $\omega = 2700\frac{1}{s}$ shortly after the first resonance near $\omega_1 \approx 2400\frac{1}{s}$.

6.1. To understand why it doesn't appear, we again look at a simpler analogy, this time a clamped string. All higher harmonics have nodes, i.e. points of the string which don't move. If we want to drive the string to oscillate at one of these harmonics, by applying a periodic force, we not only need to hit the right frequency, but also apply the force at the correct position. For example it is impossible to excite the 2nd harmonic, which has a node at the center, by applying the force in the middle. Applying this analogy to our plate, the force applied by the GW has to match the pattern of the eigenmode for it to be excitable. Looking at motion pattern of the $n = 2$ quadratic eigenmode we see that along the edges one half is bulging inward, the other outward. This is incompatible with the plus-polarized GW, which acts symmetric around the middle of the edges (think of free particles lying in a circle around the origin). Therefore this motion is incompatible with the GW and hence there exists no corresponding spike in the resonance curve.

Following this argument further, the next eigenmode with $n = 3$ is at $\omega = 7200\frac{1}{s}$ and indeed there is a corresponding spike in the resonance curve Figure 6.1. This suggests, that only the odd-numbered eigenmodes are compatible with the plus-polarized GW. The reason being that these are symmetric under reflections around the axes, as is the GW, but the even-numbered eigenmodes are not. Section 6.2.3 discusses the relation of excitability to the mass quadrupole moment and confirms this pattern.

What about the other Resonances in Figure 6.1, e.g. those at $\omega_2 \approx 3200\frac{1}{s}$ and $\omega_2 \approx 6000\frac{1}{s}$? They don't correspond to any of the known quadratic eigenmodes from section 4.3. They also don't appear to belong to one family of eigenmodes following a pattern $\omega_n = n\omega_0$. But maybe they are just the fundamental frequencies of two separate such series of eigenmodes.

The behaviour of the nodes with higher frequencies no longer follows a clear cut pattern. It seems like they vanish and reappear. But there is no longer any clear connection to

the resonances. See for example Figure 6.4, which shows the solution at $\omega L = 7000\frac{m}{s}$ in-between the third and fourth resonance. There don't appear to be any fixed-points but the whole middle part doesn't move much.

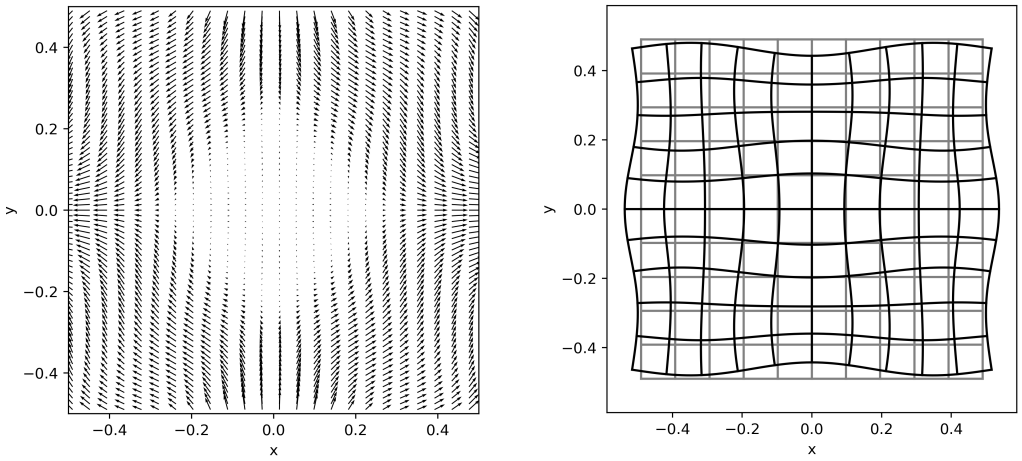

(a) Vector Plot (b) Grid plot

Figure 6.4: Vector plot (a) and Grid plot (b) of the physical displacement field for $\omega = 7000\frac{1}{s}$ and $L = 1$ in response to a purely plus-polarized GW.

6.2.2 Purely cross-polarized GW

For the case of a purely cross-polarized gravitational wave, the resonance curve is shown in Figure 6.5. The resonance frequencies for the shown peaks are now approximately $\omega_1 = 2150\frac{1}{s}, \omega_2 = 5050\frac{1}{s}, \omega_3 = 6950\frac{1}{s}$, $\omega_4 = 8400\frac{1}{s}$ and $\omega_5 = 9300\frac{1}{s}$. They are distinct from the ones for the plus-polarized wave. This is not surprising as we have already mentioned that the motion-pattern of the eigenmode, which can be excited has to fit to the 'force' applied by the GW. This if obviously the case for different eigenmodes, when the polarization is different. Moreover, none of the eigenmodes we found in section 4.3.1 belong to one of these frequencies.

In contrast to the plus-polarization, no nodes appear at the first resonance, see Figure 6.6 (a). The first four rotation centers appear near $\omega = 4000\frac{1}{s}$ at the middle of the edges as can be seen in 6.6 (b). So here there is no connection between the nodes and the resonance frequencies. Going to higher frequencies one can also see four shear-centers, which appear at the corners of the square formed by the four rotation-centers. While not visible in the vector plot for $\omega = 4000\frac{1}{s}$, they are clearly visible in the vector plot at the second resonance. A catalogue of the motion patterns of all resonances up to $\omega = 10000\frac{1}{s}$ for both polarizations can be found in Appendix A

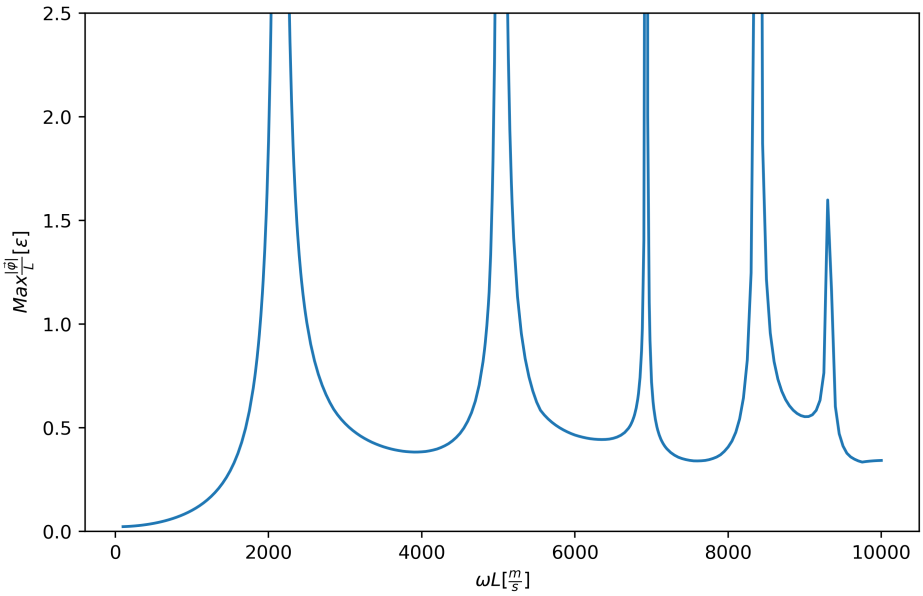

Figure 6.5: Maximum of the physical displacement field as a function of ωL for a cross-polarized GW.

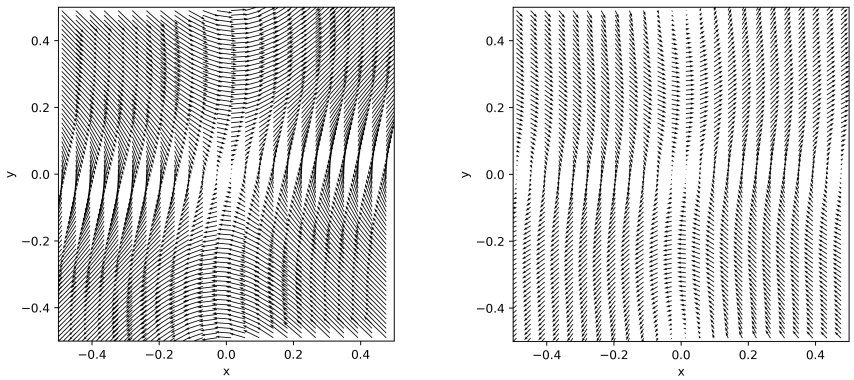

(a) $\omega = 2150\frac{1}{s}$ (b) $\omega = 4000\frac{1}{s}$

Figure 6.6: Vector plots of the physical displacement field at the first resonance (a) and in-between the first and the second (b). In (b) the appearance of rotation centers at the middle of the edges can be seen.

6.2.3 Relation to Quadrupole Moment

According to Einsteins famous quadrupole formula (see e.g. [5]) gravitational waves are related to the second time-derivative of the mass quadrupole moment. In electrodynamics a receiver needs a changing electric dipole moment to be sensitive to electromagnetic dipole radiation. In analogy one expects that a receiver needs a changing mass quadrupole moment to be sensitive to gravitational quadrupole radiation. The (traceless) quadrupole moment can be calculated by the integral

$$I_{ij}^T = \int d^3r \rho(\vec{r}) \left[r_i r_j - \tfrac{1}{3} r^2 \delta_{ij} \right] \tag{6.11}$$

where $\rho(\vec{r})$ is the mass density and the integral goes over the whole elastic body. This formula can be used to calculate the quadrupole moment of the eigenmodes from section 4.3.1. For the two dimensional plate the integral goes over the undisturbed square $[-\frac{1}{2}, \frac{1}{2}] \times [-\frac{1}{2}, \frac{1}{2}]$ but the positions are given by $r_i = x_i + \epsilon u_i$. The density is constant throughout the plate $\rho(\vec{x}) = \rho_0$. Ignoring terms of order $O(\epsilon^2)$ we first find an expression for r^2:

$$r^2 = (\vec{r} + \vec{u})^2 = x^2 + y^2 + 2\epsilon(xu^x + yu^y). \tag{6.12}$$

This can be used in formula (6.11), starting with the I_{11} component.

$$\begin{aligned} I_{11} &= \rho_0 \int_{-0.5}^{0.5} dxdy \left[x^2 + 2\epsilon x u^x - \tfrac{1}{3} r^2 \right] \\ &= \frac{\rho_0}{3} \int_{-0.5}^{0.5} dxdy \left[2x^2 - y^2 + 2\epsilon \cos(\omega t)(2x\varphi^x - y\varphi^y) \right] \\ &= \frac{\rho_0}{3} \left[\frac{1}{12} + 2\epsilon \cos(\omega t) \int_{-0.5}^{0.5} dxdy (2x\varphi^x - y\varphi^y) \right] \end{aligned} \tag{6.13}$$

The first term in the brackets is constant in time so that we are only interested in the second term. The integral can be evaluated separately for even and odd numbered eigenmodes.

- n even:

$$\begin{aligned} &= \int_{-0.5}^{0.5} dxdy \left[2x \cos(n\pi x) \sin(n\pi x) + y \sin(n\pi x) \cos(n\pi y) \right] \\ &= \int_{-0.5}^{0.5} 2x \cos(n\pi x) dx \int_{-0.5}^{0.5} \sin(n\pi y) dy + \int_{-0.5}^{0.5} \sin(n\pi x) dx \int_{-0.5}^{0.5} y \cos(n\pi y) dy = 0 \end{aligned}$$

  Each of these vanishes as they integrate an odd function over a symmetric interval.

- n odd:

$$
\begin{aligned}
&= -\int_{-0.5}^{0.5} dxdy\,[2x\sin(n\pi x)\cos(n\pi x) + y\cos(n\pi x)\sin(n\pi y)] \\
&= -2\int_{-0.5}^{0.5} x\sin(n\pi x)dx\int_{-0.5}^{0.5}\cos(n\pi y)dy - \int_{-0.5}^{0.5}\cos(n\pi x)dx\int_{-0.5}^{0.5} y\sin(n\pi y)dy \\
&= -6\frac{\sin(n\frac{\pi}{2})}{n^2\pi^2} = \frac{6(-1)^{\frac{n-1}{2}}}{n^2\pi^2} \neq 0
\end{aligned}
$$

Since this is the traceless quadrupole tensor, we can easily find the other diagonal component $I_{22} = -I_{11}$. Both of them are constant for even numbered eigenmodes. Only the odd numbered eigenmodes have a part which changes with time. This agrees with the results above, where we found that the gravitational wave only excites odd numbered eigenmodes.

Now we look at the other independent component $I_{12} = I_{21}$:

$$
\begin{aligned}
I_{12} &= \rho_0\int_{-0.5}^{0.5} dxdy\ (x+\epsilon u^x)(y+\epsilon u^y) \\
&= \rho_0\int_{-0.5}^{0.5} dxdy\ (xy + \epsilon(u^x y + x u^y)) \\
&= \rho_0\epsilon\cos(\omega t)\int_{-0.5}^{0.5}(\varphi^x y + x\varphi^y)
\end{aligned}
\tag{6.14}
$$

The integral for even and odd numbered cases are again considered separately:

- n even:

$$
\int_{-0.5}^{0.5}\cos(n\pi x)dx\int_{-0.5}^{0.5} y\sin(n\pi y)dy - \int_{-0.5}^{0.5} x\sin(n\pi x)dx\int_{-0.5}^{0.5}\cos(n\pi y)dy = 0
$$

- n odd:

$$
-\int_{-0.5}^{0.5}\sin(n\pi x)dx\int_{-0.5}^{0.5} y\cos(n\pi y)dy + \int_{-0.5}^{0.5} x\cos(n\pi x)dx\int_{-0.5}^{0.5}\sin(n\pi y)dy = 0
$$

So this component vanishes identically. As the quadrupole tensor has the same symmetries as the gravitational wave we expect the I_{11} component to be related to a plus-polarized GW and the I_{12} component to a cross-polarized GW. Therefore, this result nicely agrees with the fact that the plus-polarized wave can excite the odd-numbered eigenmodes (as they have a non-constant I_{11} component), but a cross-polarized wave can excite none of the eigenmodes since none have a changing I_{12} component.

Chapter 7

Interferometer

This chapter describes the setup of how an interferometer is placed on the plate. We assume, that the instruments are rigid and move as the plate, they are mounted on, does. Then we will find an expression for the signal of the interferometer and look at how this behaves for different gravitational wave frequencies. So far we have only looked at the resonances of the maximum of $\vec{\varphi}$. These do not necessarily correspond to the frequencies at which the interferometer gives the strongest signal, as it might be possible, that the deformations along the path of the laser cancel each other out.

7.1 Interferometer Setup and Assumptions

We consider a standard Michelson-Interferometer consisting of a laser, a beam-splitter, two mirrors and a detector. For the placement of beam-splitter and mirrors see Figure 7.1 and the explanation below. The light enters the apparatus from the left and divides into two at the beam splitter, moving along both orthogonal arms. At the mirrors the light is reflected back to the beam-splitter where it is recombined. Assuming that there is a difference between the time it takes the light to travel along both arms, the laser interferes with itself. This leads to a change in intensity which can be measured in the detector. In a more realistic setting, a Fabry-Pérot-Interferometer would be used, where the laser effectively bounces back and forth multiple times.

For simplicity it is assumed that the plate doesn't change while the light crosses the instrument. Is this a good assumption? The light takes about $T_l = \frac{2L}{c} \approx 10^{-7}s$ for a $15m$ large plate. The upper limit of frequencies of gravitational waves from known physical phenomena we want to detect is 10 kHz, which corresponds to a period of $T_{GW} = 10^{-4}s$. For this values their ratio is 10^{-3}, so that the assumption of a static plate during the photon flight is justified. This ratio stays constant as long as the product ωL is constant. Thus, for smaller plates, larger frequencies can be considered, and the other way around. Once the plate is large enough for the light to take more than half a gravitational wave period to cross, the deformations change their sign and the effects start to cancel each other out. This gives also an upper limit on the effective path length of an Fabry-Pérot-Interferometer.

We have three different periods or time intervals: The light-crossing time T_l, the gravitational wave period T_{GW} and the sound-crossing time $T_c = \frac{L}{c_1}$. Their ratios determine the behaviour of the plate. As long as the first is far smaller than the second

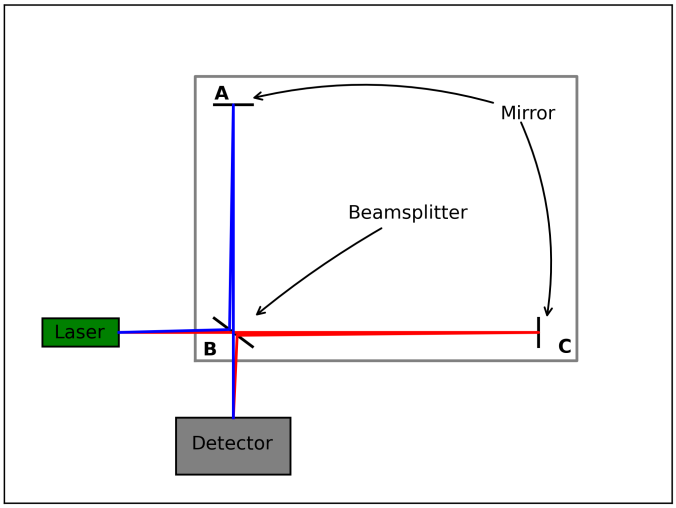

Figure 7.1: Sketch of a Interferometer on a plate consisting of a laser, a beamsplitter, two mirrors and a detector.

one, $T_l \ll T_{GW}$, the assumption of a stationary plate is valid. When the second one is also large compared to the third one $T_c \ll T_{GW}$, the low-frequency limit (see section 3.8) can be applied.

The positions of the mirrors $A = (-X_0, Y_0)$ and $C = (X_0, -Y_0)$ and the beam-splitter $B = (-X_0, -Y_0)$ (see Figure 7.1) in Local Lorentz coordinates are given by

$$\begin{aligned}
(x_A, y_A) &= \left(-X_0(1+\tfrac{h_+}{2}) + Y_0\tfrac{h_\times}{2} + \epsilon u^x|_A \ , Y_0(1-\tfrac{h_+}{2}) - X_0\tfrac{h_\times}{2} + \epsilon u^y|_A\right) \\
(x_B, y_B) &= \left(-X_0(1+\tfrac{h_+}{2}) - Y_0\tfrac{h_\times}{2} + \epsilon u^x|_B \ , -Y_0(1-\tfrac{h_+}{2}) - X_0\tfrac{h_\times}{2} + \epsilon u^y|_B\right) \\
(x_C, y_C) &= \left(X_0(1+\tfrac{h_+}{2}) - Y_0\tfrac{h_\times}{2} + \epsilon u^x|_C \ , -Y_0(1-\tfrac{h_+}{2}) + X_0\tfrac{h_\times}{2} + \epsilon u^y|_C\right)
\end{aligned} \tag{7.1}$$

where X_0 and Y_0 denote the coordinates of the instruments on the body manifold. Later $X_0 = Y_0 = 0.4L$ is chosen for the calculations. This is to avoid the error due to the finite number of terms in the Fourier series approximation. Looking at Figure 7.2 one can see this behaviour near the borders. The points $x = y = 0.4L$ are far enough from the border to still avoid this artifact. In an experimental setting one would probably set the instruments at the border to maximize the signal.

7.2 Calculation of Signal

In this section we calculate the phase difference between the laser going along the two different interferometer arms. The calculations are similar to those for the case of free mirrors, found for example in [12] or [10] . We start with the case of pure plus-polarization,

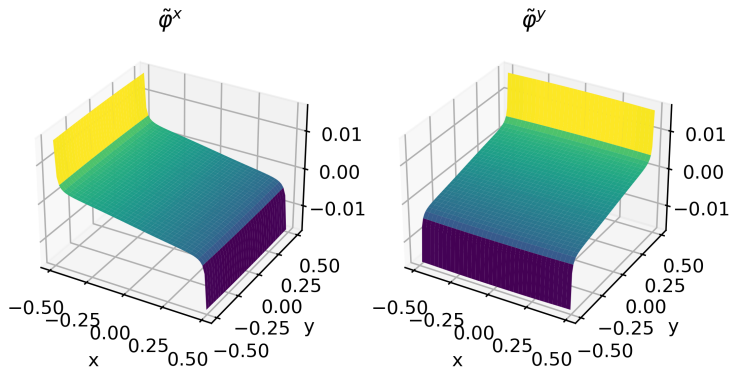

Figure 7.2: Surface plot of φ^x and φ^y for purely cross-polarized GW.

$A_+ = 1, A_\times = 0$. Looking at the metric in the local Lorentz frame as given in [12]

$$g_{\mu\nu} = \eta_{\mu\nu} - \frac{2}{c^2}\begin{pmatrix} \Phi & 0 & 0 & \Phi \\ 0 & 0 & 0 & 0 \\ 0 & 0 & 0 & 0 \\ \Phi & 0 & 0 & \Phi \end{pmatrix} \tag{7.2}$$

with Φ given by

$$\Phi = -\frac{1}{4}\ddot{h}(t)\left(x^2 - y^2\right) = \frac{\epsilon\omega^2}{4}\cos(\omega t)\left(x^2 - y^2\right). \tag{7.3}$$

one can see, that the g_{00} component is different from the flat-space metric. As it is dependent on the position on the plate, clocks run at different rates depending on where they are. Combining this with the motion of the mirrors there are two effects which change the time it takes light to travel along the two interferometer arms:

- A difference in time elapsed because one path is longer than the other.
- A difference due to clocks running at different speeds along both paths, and hence the light traveling at different coordinate speeds.

We calculate the elapsed time along null geodesics (which are still straight lines) taken by the photons. First we look at the photon moving along the lower interferometer arm from point B to C. For the four-velocity of the photons u^μ we have

$$0 = g_{\mu\nu}u^\mu u^\nu = (\eta_{tt} - \tfrac{2}{c^2}\Phi)(u^t)^2 + \eta_{xx}(u^x)^2 = -(1 + \tfrac{\epsilon\omega^2}{2c^2}\cos(\omega t)\left(x^2 - y^2\right))(u^t)^2 + (u^x)^2.$$

Using $u^t = \frac{dt}{d\lambda}$ and $u^x = \frac{dx}{d\lambda}$ for a path parameterized by λ this can be rearranged to an expression for the coordinate speed of light

$$\frac{dx}{dt} = \frac{u^x}{u^t} = \sqrt{1 + \tfrac{\epsilon\omega^2}{2c^2}\cos(\omega t)\left(x^2 - y^2\right)} \approx 1 + \tfrac{\epsilon\omega^2}{4c^2}\cos(\omega t)\left(x^2 - y^2\right). \tag{7.4}$$

We again use the assumption, that the plate is stationary during one light crossing, i.e. the cosine is approximately constant and we take it to be 1. This results in the maximum possible amplitude of the effect. To obtain the result for other times, one would need to bring this factor back. Then one can rearrange the terms into a form one can easily integrate along the path.

$$cdt = \left(1 + \tfrac{\epsilon\omega^2}{4c^2}\cos(\omega t)\left(x^2 - y^2\right)\right)^{-1} dx \approx \left(1 - \tfrac{\epsilon\omega^2}{4c^2}\cos(\omega t)\left(x^2 - y^2\right)\right) dx \tag{7.5}$$

The path along which we integrate goes from $x_B = -0.4L + \epsilon\tilde{\varphi}^x(-0.4L, -0.4L)$ to $x_C = 0.4L + \epsilon\tilde{\varphi}^x(0.4L, -0.4L)$ and $y = -0.4L$.

$$c\Delta t_{BC} = \int_{x_B}^{x_C} dx \left(1 - \tfrac{\epsilon\omega^2}{4c^2}\left(x^2 - y^2\right)\right) \tag{7.6}$$

$$= x_C - x_B - \tfrac{\epsilon\omega^2}{4c^2}\left(\tfrac{x_C^3 - x_B^3}{3} - y^2(x_C - x_B)\right) \tag{7.7}$$

$$= 0.8L + \epsilon\left[\tilde{\varphi}^x(0.4L, -0.4L) - \tilde{\varphi}^x(-0.4L, -0.4L)\right] - \epsilon\tfrac{\omega^2}{4c^2}(0.4L)^3(\tfrac{2}{3} - 2) \tag{7.8}$$

The first term is the time it would take the laser to cross the path without any GW. The second term is due to the motion of the mirrors and the last term is the correction due to the different rates at which time passes.

Now this is only for the trip from the beam-splitter to the mirror. To consider the return path, we have to integrate from C to B and, since we go along the path in the other direction, also change dx to $-dx$. Thus, instead of doing the integral, we can interchange the limits of integration and have again the same expression as above, so that the total elapsed time is

$$c\Delta t_{BCB} = 1.6L + 2\epsilon\left[\tilde{\varphi}^x(0.4L, -0.4L) - \tilde{\varphi}^x(-0.4L, -0.4L)\right] + \epsilon 2\tfrac{\omega^2}{3c^2}(0.4L)^3. \tag{7.9}$$

Next the elapsed time along the other interferometer arm is needed. We can arrive at the result by interchanging x and y, which changes the component of $\tilde{\varphi}^i$ and flips the sign in the $(x^2 - y^2)$ term so that we arrive at

$$c\Delta t_{BAB} = 1.6L + 2\epsilon\left[\tilde{\varphi}^y(-0.4L, 0.4L) - \tilde{\varphi}^y(-0.4L, -0.4L)\right] - \epsilon\tfrac{2\omega^2}{3c^2}(0.4L)^3. \tag{7.10}$$

The difference in the two elapsed times is what generates the phase difference and comes out as

$$c\Delta t = \Delta t_{BAB} - \Delta t_{BCB} = \Delta l - \epsilon\tfrac{4\omega^2}{3c^2}(0.4L)^3 \tag{7.11}$$

where Δl is the difference in path lengths given by

$$\Delta l = 2\epsilon\cos(\omega t)(\tilde{\varphi}^y|_A - \tilde{\varphi}^y|_B - \tilde{\varphi}^x|_C + \tilde{\varphi}^x|_B). \tag{7.12}$$

The two effects are additive and can be considered separately. Is the second effect relevant? We will later see, that Δl is of magnitude 1ϵ. The correction term is proportional to $\frac{\omega^2}{c^2}L^3 \approx 10^{-9}L^3$ for $\omega = 10000\frac{1}{s}$. Δl on the other hand is proportional to $\tilde{\varphi}^i$, which scales linearly with L. So for them to be of the same magnitude $10^{-9}L^2$ would need to be

approximately 1. That is the case if the plate would be more than 30 kilometers long. So for realistic plate sizes the time-effect is not relevant. This agrees with the statement in the conclusion of [10] where this effect was said to be much smaller than the other effect (though there the mirrors where considered to be free).

Thus the relevant part of the signal results from the difference in lengths along the two interferometer arms l_1 and l_2: $\Delta l = 2(l_1 - l_2)$. The factor 2 is due to the laser going back and forth across the lengths. The two lengths can now be easily calculated for the case of general polarizations:

$$\begin{aligned} l_1 &= \sqrt{(x_A - x_B)^2 + (y_A - y_B)^2} \\ &= y_A - y_B + O(\epsilon^2) = Y_0(2 - h_+) + \epsilon(u^y|_A - u^y|_B) \\ l_2 &= x_C - x_B = X_0(2 + h_+) + \epsilon(u^x|_C - u^x|_B) \end{aligned} \tag{7.13}$$

Then the difference of the length of the laser paths is given by

$$\Delta l = 2l_1 - 2l_2 = 4(Y_0 - X_0) - 2h_+(Y_0 + X_0) + 2\epsilon(u^y|_A - u^y|_B - u^x|_C + u^x|_B). \tag{7.14}$$

The first term vanishes since $X_0 = Y_0$. Inserting the expressions for the gravitational wave and separating off the time dependence of the displacement u^i it turns back into equation 7.12. Looking more closely at this , we notice that a purely cross-polarized wave has no effect. To see this, first note that the last term vanishes because $A_+ = 0$. In the other terms we use the symmetry for a cross-polarized GW 3.44:

$$\Delta l \propto \varphi^y|_A - \varphi^y|_B - \varphi^x|_C + \varphi^x|_B \tag{7.15}$$

$$= \varphi^y(-X_0, Y_0) - \varphi^y(-X_0, -Y_0) - \varphi^x(X_0, -Y_0) + \varphi^x(-X_0, -Y_0) \tag{7.16}$$

$$= \varphi^y(-X_0, Y_0) - \varphi^y(-X_0, -Y_0) - \varphi^y(-Y_0, X_0) + \varphi^y(-Y_0, -X_0) = 0. \tag{7.17}$$

In the last equality $X_0 = Y_0$ was used. Looking at one of the pictures of the result this is not too surprising. The displacement is symmetric across the diagonal, so that both arms of the interferometer undergo the same change and hence there is no difference in path lengths. In fact both path lengths stay constant.

7.3 Results

From the discussion above we conclude, that only the plus-polarized wave gives a signal, so we look at a purely plus-polarized wave. To look at a concrete example, we choose again $c_1 = 1950\frac{m}{s}$ and $c_2 = 540\frac{m}{s}$.

The resulting difference in path lengths for different frequencies are shown in Figure 7.3. Also, for comparison, the resulting signal for an interferometer with freely suspended mirrors (like LIGO, $\tilde{\varphi}^i = 0$) of the same size is plotted. One can see, that there are long ranges (for instance from $\omega L = 3000\frac{m}{s}$ to almost $6000\frac{m}{s}$) where the signal from the interferometer on the plate is larger. So this is not only the case near the resonances.

Keeping the scaling argument from section 3.5 in mind we can choose the size of the plate L so that the frequency range, where known interesting phenomena happen coincides

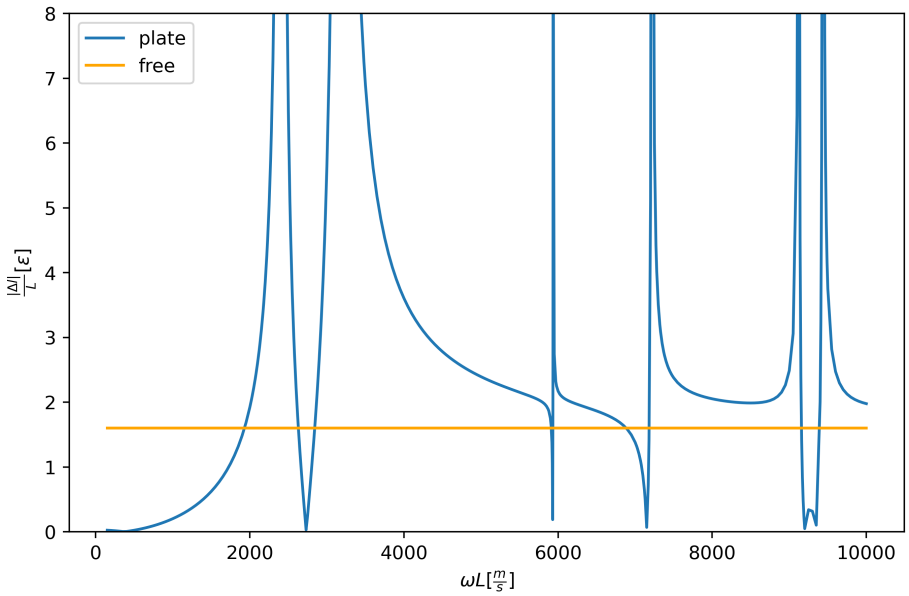

Figure 7.3: Difference in path lengths Δl in units of ϵ for the interferometer on the plate and the freely suspended mirrors.

with the range where the signal is largest. Say for instance an interesting event happens at a frequency of $\omega = 400\frac{1}{s}$. Then we could choose a plate of length $L = 10m$ to shift the region in Figure 7.3 near $\omega L = 4000\frac{m}{s}$ to the frequency we are interested in. In addition, the signal scales linearly with the size of the plate so that we also get a 10 times stronger signal.

For small gravitational wave frequencies ω the signal goes to zero. This fits nicely with the fact that the physical displacement field also goes to zero for small ω. Physically the explanation for this is, that the oscillations of the wave are slow enough for the material in the plate to resist deformation. There is enough time for the elastic waves to spread throughout the body and the atoms can realign themselves. When the frequencies of the GW is larger, and hence the period smaller this is no longer the case. The signal starts to increase noticeable at approximately $\omega = 1000\frac{1}{s}$ which corresponds to a period $T = \frac{2\pi}{\omega} = 6ms$. Comparing this to the time a s-wave needs to cross the plate $\tau = \frac{1}{c_2} = 2ms$ one sees that this is a considerable fraction of the period of the GW, or in other words, the period ration becomes almost one.

In section 3.8 we found an approximate polynomial solution for the case of small period ratio $\varepsilon = \frac{\omega L}{c_1}$ and pure plus-polarization. This can be used to explore the small frequency case (small compared to $\frac{c_1}{L}$). We first need to convert it to local Lorentz coordinates using (6.10):

$$\tilde{\varphi}^x = \frac{L}{48} A_+ \varepsilon^2 \frac{c_1^2}{c_2^2} \frac{c_1^2}{c_3^2} \left[-\frac{3}{2} x \left(1 - \frac{c_2^2}{c_1^2} \right) + 3 \left(1 - 2\frac{c_2^2}{c_1^2} \right) xy^2 + x^3 \right]. \tag{7.18}$$

Note, that this is of order ε^2 and hence very small. This confirms that the signal here

will also be very small. First we rewrite the expression for the path length difference (7.12) using the symmetry for the pure plus-polarization ($A_+ = 1$) and then insert the polynomial solution.

$$\begin{aligned}
\Delta l &= 2\epsilon\cos(\omega t)\left[\tilde{\varphi}^y(-X_0,Y_0) - \tilde{\varphi}^y(-X_0,-Y_0) - \tilde{\varphi}^x(X_0,-Y_0) + \tilde{\varphi}^x(-X_0,-Y_0)\right] \\
&= 2\epsilon\cos(\omega t)\left[-\tilde{\varphi}^x(Y_0,-X_0) + \tilde{\varphi}^x(-Y_0,-X_0) - \tilde{\varphi}^x(X_0,-Y_0) + \tilde{\varphi}^x(-X_0,-Y_0)\right] \\
&= 4\epsilon\cos(\omega t)\left[\tilde{\varphi}^x(-Y_0,-X_0) - \tilde{\varphi}^x(X_0,-Y_0)\right] \\
&= \frac{L}{12}\varepsilon^2\frac{c_1^4}{c_2^2c_3^2}\epsilon\cos(\omega t)\left[\frac{3}{2}(Y_0+X_0)\left(1-\frac{c_2^2}{c_1^2}\right) - 3\left(1-2\frac{c_2^2}{c_1^2}\right)(Y_0X_0^2 + X_0Y_0^2) - (Y_0^3+X_0^3)\right] \\
&= \epsilon L^3\cos(\omega t)\omega^2 2.03\times 10^{-7}
\end{aligned}$$

The approximation is valid up to at most $\omega = 100\frac{1}{s}$ and if we insert this value, we find $\Delta l = \epsilon\cos(\omega t)2.03\times 10^{-3}$. This confirms that the signal indeed almost vanishes for low frequencies. Figure 7.4 shows a plot of the signal for the polynomial solution and the numerical approach. It can be seen, that the two curves start to diverge at approximately $\omega L = 800$, which is to be expected since the low frequency limit no longer applies there. Also, for very small frequencies the agreement is not perfect. This is because the numerical approach becomes ill-conditioned. Overall, the two curves become closer, if the series in the numerical approach are truncated at larger values M.

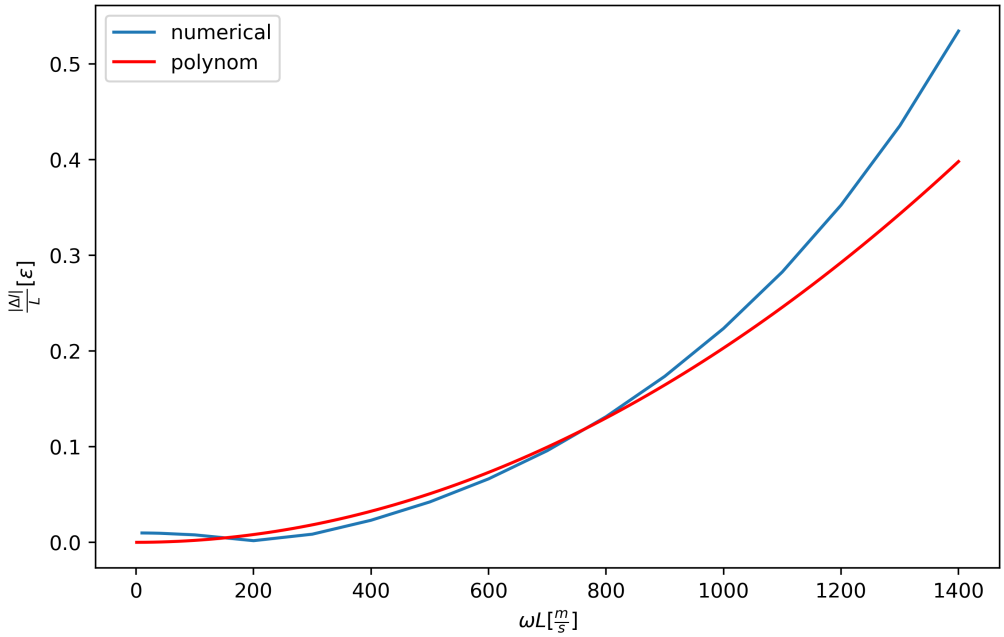

Figure 7.4: Comparison of polynomial solution in the low frequency limit and numerical solution from the corrected spectral method.

Chapter 8

Conclusion

In this work we were able to find a numerical solution describing the behaviour of a quadratic elastic plate under the influence of a gravitational wave. This was done by developing a spectral approach which deals with the derivatives of Fourier series of non-periodic functions. Correction terms were introduced to get a relation between the derivative of the Fourier series and the Fourier series of the derivative of the function. For low frequency limit a polynomial solution was found and used to check the validity of the numerical approach.

This solution was then used to calculate the signal a laser interferometer placed on this plate would see. It was discovered, that for broad frequency ranges, the signal is larger than the one a interferometer consisting of freely suspended mirrors and of the same size, would measure. Of course, the advantage of interferometers with free mirrors, like LIGO, is that they can use kilometer-long tunnels to get a larger signal. Plates are restricted to far smaller sizes. But it is still an interesting and surprising effect. One would intuitively expect, that the material would oppose the motion of the mirrors. And since the effect of the GW is weak there should be almost no signal. It turns out, that this is only true for low gravitational wave frequencies.

The behaviour of the plate is determined by two period-ratios: First, the ratio of the time it takes light to cross the plate and the gravitational wave period. As long, as this is small, the plate can be assumed to be stationary during the light crossing. If this gets too large, the signal gets weaker. Second, the ratio of the time it takes sound waves to cross the plate to the gravitational wave period. This ratio is called ε and when it is small, the low frequency solution can be used.

The signal is especially large near certain resonance frequencies. Looking at the motion pattern of the plate near the resonances, we discovered that some of them corresponds to the eigenmode solutions from section 4.3.1. The amplitude of the signal is of the order of $\epsilon L \approx 10^{-20} L$. This can be improved by using longer (effective) path lengths, i.e. either a Fabry-Pérot-Interferometer to bounce the laser back and forth multiple times, or make the plate larger. Though there are limits to these improvements, as the effects will start to cancel once the plate undergoes more than half of its oscillation during the light-crossing. This result has to be compared to the wavelength of the laser which is of order $10^{-7} m$. As this is far larger, the phase difference and hence the interference effect will be very small.

8.1 Outlook

During the work on this thesis a lot of points which require further investigation were discovered:

- It would be interesting to investigate the convergence behaviour of the series representing the boundary conditions in box 5.3. How fast does the error decrease, when increasing M, the limit in the sums? One starting point could be to solve the problem for different M and look at how the resonance frequencies change. For instance, the first resonance in the plus-polarization corresponds to the first eigenmode which has a frequency $\omega L = 2399\frac{m}{s}$. If the problem is solved with $M = 40$,$M = 70$ and $M = 100$ the resonance appears at $\omega L = 2410\frac{m}{s}$, $\omega L = 2406\frac{m}{s}$ and $\omega L = 2404\frac{m}{s}$ respectively. So the numerical solution appears to approach the correct value, though not very fast.

- The resulting deformations of the plate are very small, of the order of $10^{-20}m$. To examine how realistic it is to ever detect such small changes, one should compare it to thermal noise and seismic disturbances of the plate.

- One could investigate the computational complexity of using the delta corrected spectral method developed in this thesis and compare it to other numerical approaches. For instance, would it be faster to solve the BVP directly using a finite-difference scheme? Though it is not straightforward to implement the boundary conditions in that case. Another approach might be to use the Finite-Elements method.

- The model used in this work doesn't consider any damping behaviour. We expect, that a few things would change if this is done. The amplitude at the resonances should stay finite and the resonance-frequencies should be shifted. In general the signal would probably be smaller. In the literature one approach, called structural damping, is to express the material parameters in terms of Young's Modulus E and then let it be complex $\bar{E} = E(1 + i\eta)$ where η represents the damping.

- In this work, the solution was only discussed for one set of material parameter, i.e. wave speeds. For different materials, the resonances would appear at different frequencies. As the ratio of the wave speeds changes, some of the eigenmodes will change order, as they scale differently. The s-wave eigenmodes for instance have eigenfrequencies proportional only to c_2, while others will depend on a combination of c_1 and c_2. It might also be possible that not all eigenmodes will be available for all materials.

- Here only the steady-state solution of the plate under the influence of a continuous plane gravitational wave was considered. In reality one would have a plate at rest, which is then set into motion when it is hit by a GW-pulse. Depending on the duration of the pulse and the damping, this behaviour will settle down to the steady-state solution.

Bibliography

[1] R. Beig and B. G. Schmidt. Relativistic elasticity. *Classical and Quantum Gravity*, 20(5):889–904, feb 2003.

[2] S. Broda. *Comparison of two different formalisms for relativistic elasticity theory.* Faculty of Physics, University of Vienna, 2008.

[3] S. M. Carroll. *Spacetime and Geometry: An Introduction to General Relativity.* Cambridge University Press, 2019.

[4] J. Cervantes-Cota, S. Galindo-Uribarri, and G. Smoot. A brief history of gravitational waves. *Universe*, 2(3):22, Sep 2016.

[5] P. T. Chruściel. *Elements of general relativity.* Compact textbooks in mathematics. Springer International Publishing Imprint: Birkhäuser, Cham, 1st ed. 2019. edition, 2019.

[6] V. Girault. *Finite element methods for Navier-Stokes equations : theory and algorithms.* Springer series in computational mathematics ; 5. Springer, Berlin [u.a.], [extended vers. of prev. text, 1979]. edition, 1986.

[7] M. Hudelist. *Relativistic Theory of Elastic Bodies in the Presence of Gravitational Waves.* Faculty of Physics, University of Vienna, 2021.

[8] L. D. Landau. *Lehrbuch der theoretischen Physik. 7, Elastizitätstheorie / L. D. Landau ; E. M. Lifschitz. In dt. Sprache hrsg. von Hans-Georg Schöpf.* Harri Deutsch, Frankfurt am Main, 7., unveränd. aufl.. edition, 1991.

[9] D. R. Lide. *CRC handbook of chemistry and physics*, volume 85. CRC press, 2004.

[10] A. Melissinos and A. Das. The response of laser interferometers to a gravitational wave. *American Journal of Physics*, 78(11):1160–1164, 2010.

[11] C. W. Misner. *Gravitation.* Princeton University Press, Princeton Oxford, first princeton university press edition. edition, 2017.

[12] M. Rakhmanov. Response of test masses to gravitational waves in the local lorentz gauge. *Phys. Rev. D*, 71:084003, Apr 2005.

[13] M. Wernig-Pichler. Relativistic elastodynamics. *Institute for theoretical physics, University of Vienna*, 2006.

Appendix A

Motion Pattern Catalogue

For reference a catalogue of motion patterns/grid plots at all eigenfrequencies and resonance-frequencies up to $\omega L = 10000\frac{m}{s}$ is included in this appendix.

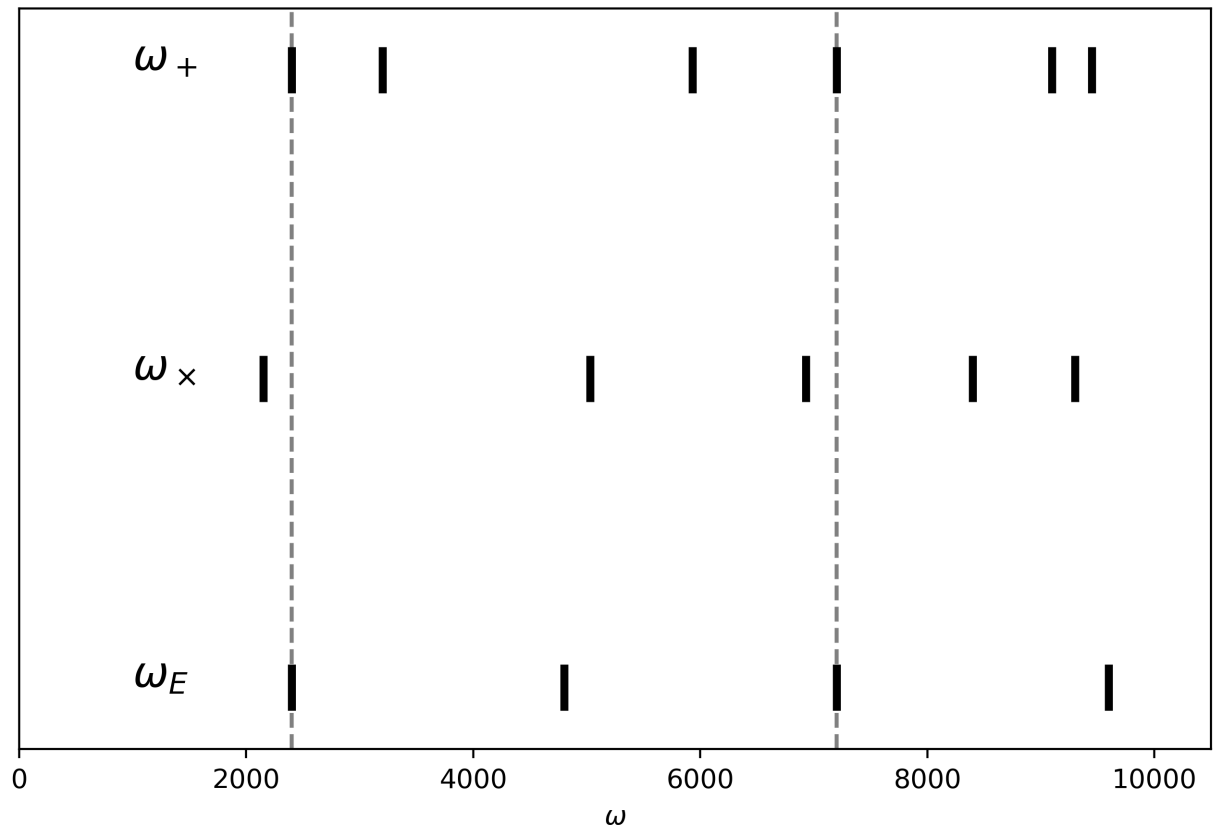

Figure A.1: Comparison of resonance frequencies of the two polarizations and eigenfrequencies.

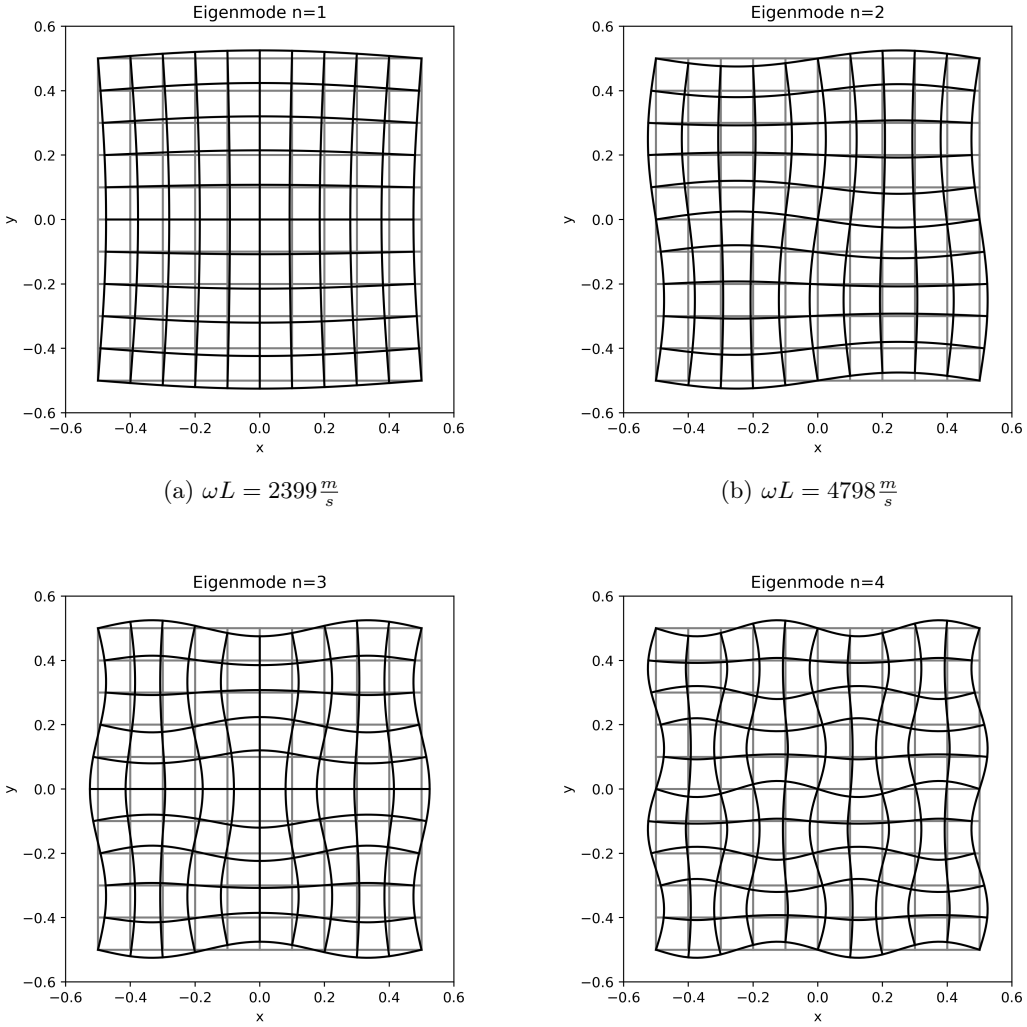

(a) $\omega L = 2399 \frac{m}{s}$

(b) $\omega L = 4798 \frac{m}{s}$

(c) $\omega L = 7197 \frac{m}{s}$

(d) $\omega L = 9597 \frac{m}{s}$

Figure A.2: Grid plot of the first four eigenmodes with given frequencies.

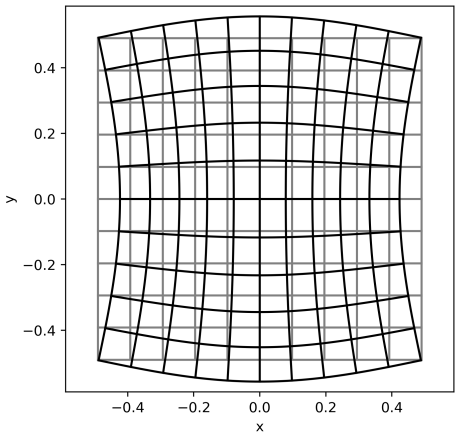

(a) $\omega L = 2406 \frac{m}{s}$

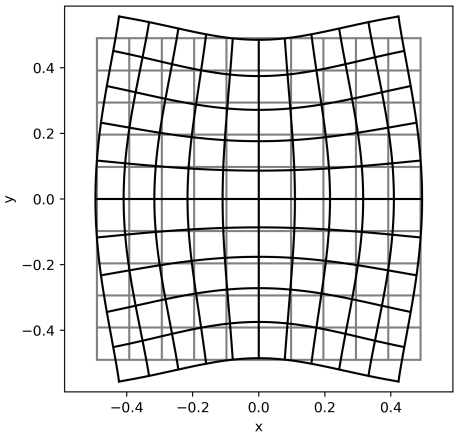

(b) $\omega L = 3192 \frac{m}{s}$

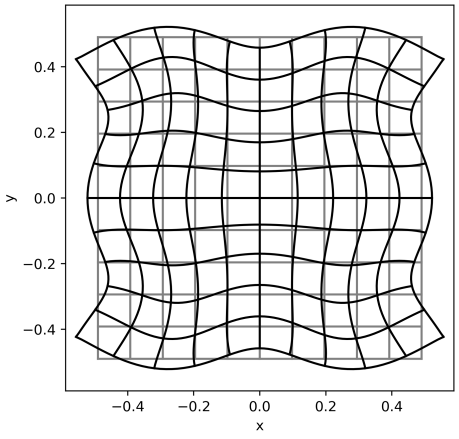

(c) $\omega L = 5936 \frac{m}{s}$

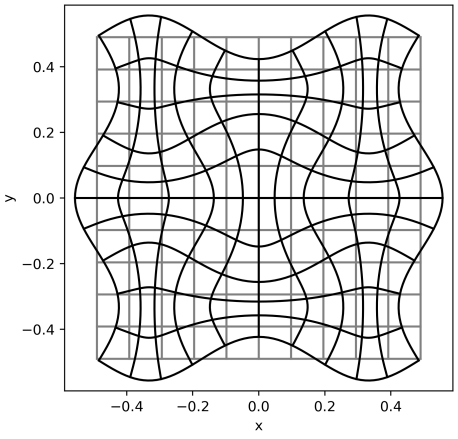

(d) $\omega L = 7218 \frac{m}{s}$

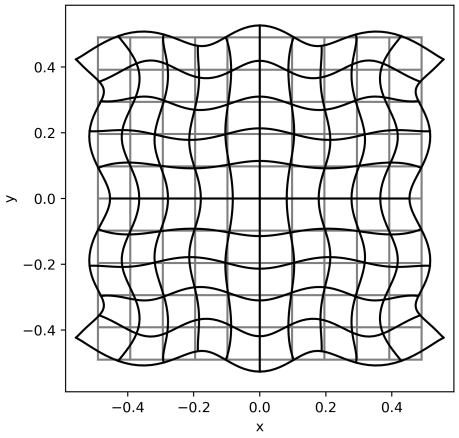

(e) $\omega L = 9122 \frac{m}{s}$

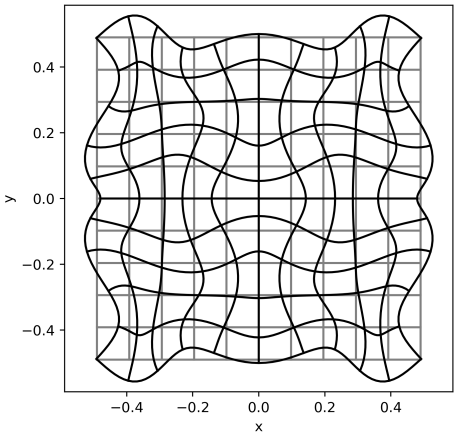

(f) $\omega L = 9438 \frac{m}{s}$

Figure A.3: Grid plot of the first six resonances for a plus-polarized gravitational wave.

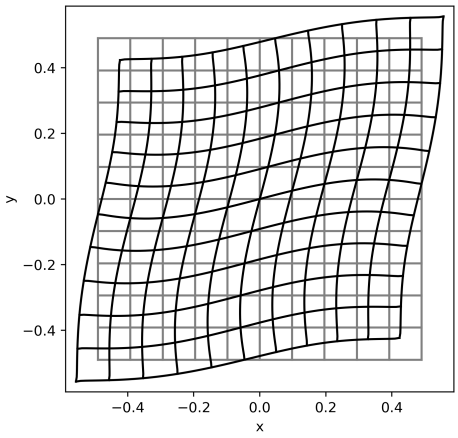

(a) $\omega L = 2150 \frac{m}{s}$

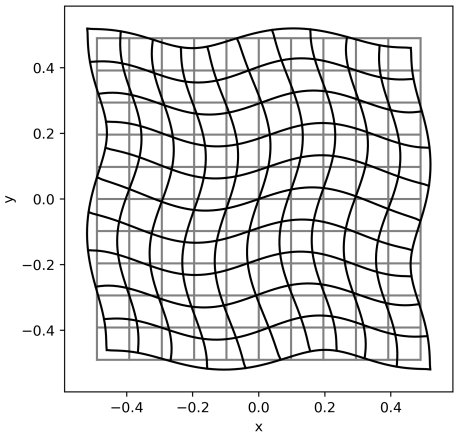

(b) $\omega L = 5030 \frac{m}{s}$

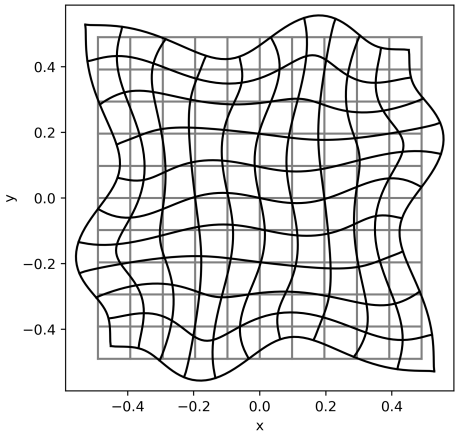

(c) $\omega L = 6930 \frac{m}{s}$

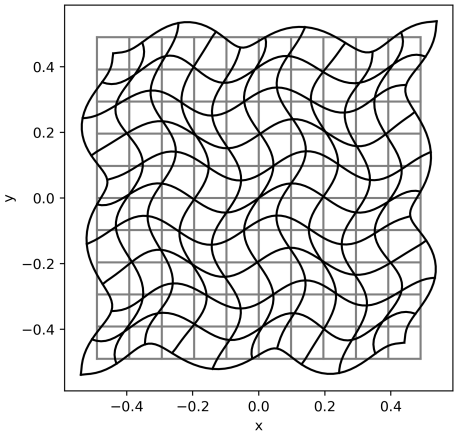

(d) $\omega L = 8400 \frac{m}{s}$

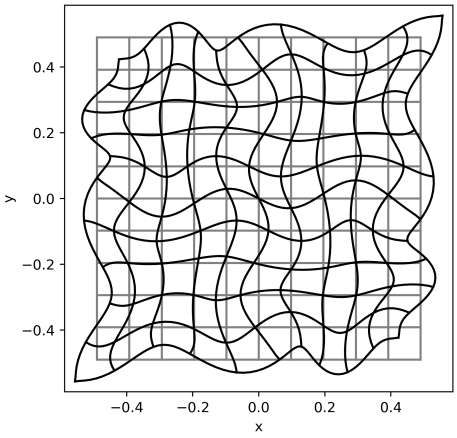

(e) $\omega L = 9300 \frac{m}{s}$

Figure A.4: Grid plot of the first five resonances for a cross-polarized gravitational wave.

Appendix B

Damped Driven Oscillator

The equation governing a damped driven oscillator in the unknown x is

$$m\ddot{x} + b\dot{x} + kx = F_0 m \cos(\omega t) \tag{B.1}$$

where m represents the mass, b describes the damping, k is the spring constant and F_0 the amplitude per unit mass of the driving force. For simplicity we divide by the mass m and introduce the resonance frequency of the undamped oscillator $\omega_0^2 = \frac{k}{m}$ and the damping factor $\gamma = \frac{b}{m}$.

$$\ddot{x} + \gamma\dot{x} + \omega_0^2 x = F_0 \cos(\omega t) \tag{B.2}$$

We make the ansatz

$$x = Ae^{i\omega t} \tag{B.3}$$

for the steady-state solution with complex amplitude A and at the end take the real part. Moreover the driving force is also rewritten as $F_0 e^{i\omega t}$. Inserting this into the equation and canceling the exponential factor we find

$$A\left(-\omega^2 + i\omega\gamma + \omega_0^2\right) = F_0. \tag{B.4}$$

This can be rearranged to an expression for A:

$$A = \frac{F_0}{\omega_0^2 - \omega^2 + i\omega\gamma} = F_0 \frac{\omega_0^2 - \omega^2 - i\omega\gamma}{(\omega_0^2 - \omega^2)^2 + \gamma^2\omega^2}. \tag{B.5}$$

From that expression the magnitude $|A|$ and phase φ of the complex amplitude A can be calculated.

$$\begin{aligned} |A| &= \frac{F_0}{\sqrt{(\omega_0^2 - \omega^2)^2 + \gamma^2\omega^2}} \\ \tan(\varphi) &= -\frac{\omega\gamma}{(\omega_0^2 - \omega^2)} \end{aligned}$$

The final solution then looks like

$$x(t) = \frac{F_0 \cos(\omega t + \varphi)}{\sqrt{(\omega_0^2 - \omega^2)^2 + \gamma^2\omega^2}}. \tag{B.6}$$

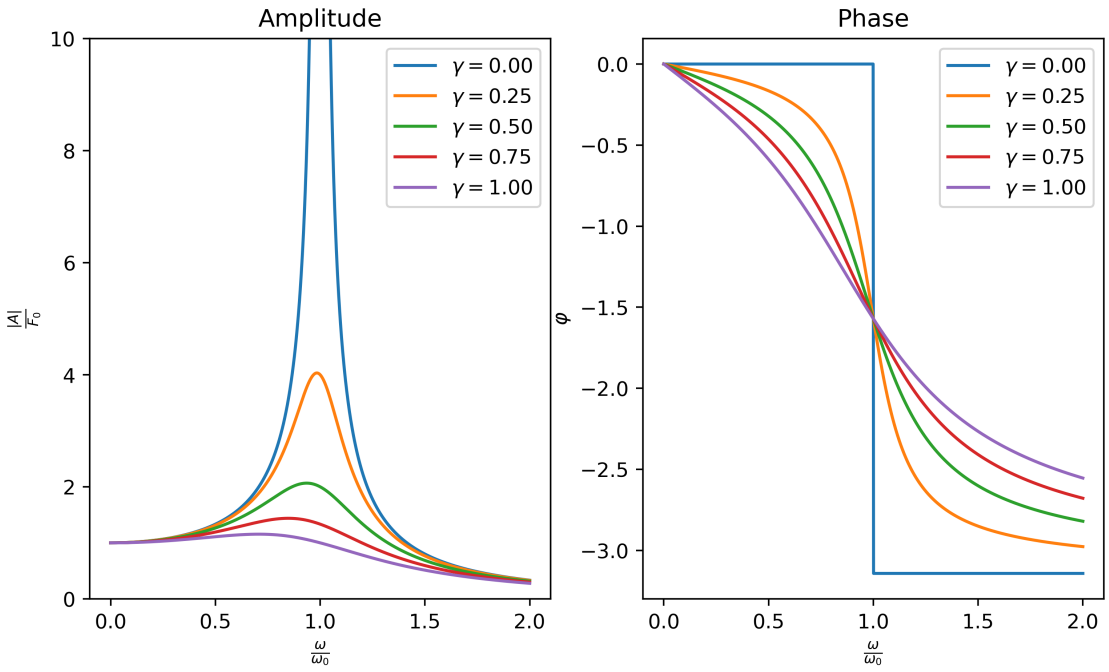

Figure B.1: Amplitude and phase-shift of a damped driven oscillator for different values of damping γ.

The amplitude and phase-shift are plotted below for different values of ω. The amplitude becomes very large near the resonance frequency and has its maximum at

$$\omega_r = \sqrt{\omega_0^2 - \frac{\gamma^2}{2}}. \tag{B.7}$$

The larger the damping, the smaller the maximum amplitude. Once we reach $\gamma = 1(\omega_0)$ the peak vanishes completely. For small frequencies the amplitude always corresponds to the amplitude of the driving force, for very large frequencies the amplitude vanishes.

The phase shift vanishes for small frequencies, i.e. the oscillator moves in sync with the driving force. Then it increases in absolute value until it reaches $\frac{\pi}{2}$ at $\omega = \omega_0$. For very high frequencies it approaches $\varphi = \pi$. The smaller the damping, the steeper the curve. For the case of no damping, it turns into a step function, which corresponds to a sign-flip at $\omega = \omega_0$.